

CHARACTERIZING SOFTBALL BAT MODIFICATIONS AND THEIR RESULTING
PERFORMANCE EFFECTS

By

CURTIS MATTHEW CRUZ

A thesis submitted in partial fulfillment of
the requirements for the degree of

MASTER OF SCIENCE IN MECHANICAL ENGINEERING

WASHINGTON STATE UNIVERSITY
Department of Mechanical and Materials Engineering

May 2005

To the Faculty of Washington State University:

The members of the Committee appointed to examine the thesis of
Curtis Matthew Cruz find it satisfactory and recommend that it be accepted.

Chair

ACKNOWLEDGEMENTS

None of my accomplishments over the course of my schooling would have been possible if it were not for the wonderful people in my life. I would first like to thank my amazing wife Cammie, who in addition to working three jobs and volunteering much of her time has still found time to support all of my endeavors as a graduate student. Through my own 40+ hour work weeks and stressful days she has always found the right things to say and helped me to remember the things that are most important in life.

The rest of my family's support and guidance through the years is also greatly appreciated. My ever-supportive parents have been truly exceptional role models, and my sister's courage and conviction is an inspiration to me every day.

My success at WSU has also been a function of the people I have been fortunate enough to work with and learn from. For all of the time and effort he has put forth on my behalf, and the opportunities he has provided me with, I will be forever thankful to Dr. Lloyd Smith. More than anything, I will always value the friendship that we have developed.

For all of their companionship and help through the years I also need to thank my fellow Bat Rats. Aaron and Joey, I cannot imagine a more fun and entertaining work environment than the one you guys helped create. In the coming years I am sure I'll forget all about the work I did at WSU, but I will never forget the good times we had. Eric, if the Bat Lab were a pie it would be cherry. I've enjoyed the last semester and am confident the lab will continue to excel under your watch.

Janet Danforth deserves as big a thank you as anybody. I flooded her desk with purchase orders for two years and her diligence allowed the lab to grow into what it is today.

Charlena Grimes has been a huge help through my six year career at WSU. As an advisor and a friend, she has always been there for anything I have needed. The WSU machine shop has also been a big help with my schooling. Without them, our many projects could not have been as successful as they were.

I also need to thank everybody else that has helped to distract me from my schooling. Matt, Brian, Phil, and many others have provided an escape from the monotony of schoolwork.

Last, but definitely not least, I need to thank Dr. Daniel Russell and Dr. Alan Nathan for their technical assistance through my research. The many conversations regarding the physics of softball have been both entertaining and enlightening. Finally, the ASA is acknowledged for their financial support of my work. If it were not for their desire to better the game of softball none of this work would be possible.

CHARACTERIZING SOFTBALL BAT MODIFICATIONS AND THEIR
RESULTING PERFORMANCE EFFECTS

Abstract

by Curtis Matthew Cruz, M.S.
Washington State University
May 2005

Chair: Lloyd V. Smith

In recent years the procedure for measuring the performance of softball bats, and the metric used in these measurements have seen significant changes. Due partially to these changes, it has become increasingly common for players to modify stock bats with the purpose of improving their performance. This work examines the most common bat alteration methods in terms of their effects on performance as well as their effect on bats' physical properties such as barrel stiffness and vibration characteristics. In addition, a study investigating the effect that weight distribution has on performance and bat characteristics was conducted.

Numerical simulations describing three different bat constructions were also performed with the goal of verifying experimentally obtained values and predicting the effect various bat weight distributions would have on bat characteristics.

All of the bat modification methods were studied by measuring performance levels and physical characteristics before and after the bats had been modified. All of the bat alterations were found to improve bat performance. The most effective alteration method improved performance an average of 6.6%, while the least effective method resulted in performance gains of 2.6%. Barrel stiffness and vibration characteristics were

found to be sensitive to the bat alterations, although neither was sensitive enough to quantify the performance changes. Bat performance was also found to be a function of the number of bat-ball impacts the bat has undergone. After 500 impacts the performance level of multiple-wall aluminum and composite bats improved 4.2%.

Varying the weight distribution of stock bats was shown to have a considerable effect on the location of maximum performance along the length of the bat barrel. Those same weighting variations had some effect on the bats' measured physical characteristics. These measured properties correlated favorably with numerical simulation, including a description of a multiple-wall bat.

TABLE OF CONTENTS

ACKNOWLEDGEMENTS.....	iii
Abstract.....	v
TABLE OF CONTENTS.....	vii
CHAPTER ONE	
INTRODUCTION	1
REFERENCES	5
CHAPTER TWO	
LITERATURE REVIEW	6
2.1 General Trends in Bat Performance.....	6
2.2 Direct Measurements of Bat Performance.....	13
2.3 Comparison of Bat Performance Tests and Metrics	18
2.4 Indirect Performance Metrics	21
2.4.1 Modal Analysis	21
2.4.2 Barrel Compression	29
2.4.3 Contact Time.....	33
2.5 Bat Doctoring.....	34
2.5.1 Weighting.....	35
2.5.2 Shaving	38
2.5.3 Natural Break In.....	41
2.5.4 Accelerated Break In.....	41
2.5.5 Bat Painting.....	45
2.6 Bat Models.....	45
2.7 Summary	47
REFERENCES	48
CHAPTER THREE	
BAT MODIFICATIONS	51
3.1 Bat Doctoring Study	51
3.2 Results.....	56
3.2.1 Structural group - shaved bats.....	56
3.2.2 Structural group - ABI bats.....	61

3.2.3	Naturally Broken In Group	66
3.2.4	Weighting group	69
3.2.5	Painted group	71
3.3	Discussion	76
	REFERENCES	80
CHAPTER FOUR		
	BAT WEIGHT DISTRIBUTIONS.....	81
4.1	Weighting Study	81
4.2	Results.....	85
4.2.1	Wood bat.....	86
4.2.2	Single wall aluminum bat	87
4.2.3	Multiple-wall aluminum bat	88
4.2.4	Multiple-wall composite bat	89
4.3	Discussion	90
	REFERENCES	98
CHAPTER FIVE		
	COMPUTER MODELING	99
5.1	Modeling Methods.....	99
5.2	Convergence study.....	102
5.3.1	Bat models	107
5.3.2	Solid wood bat	112
5.3.3	Single wall aluminum	114
5.3.4	Multiple-wall aluminum	115
5.4	Summary	116
	REFERENCES	118
CHAPTER SIX		
	SUMMARY	119
6.1	Review	119
6.2	Bat modifications	119
6.3	Weighting study	119
6.4	Computer modeling	120

6.5 Future work	120
APPENDIX ONE	
Apparatus	122
APPENDIX TWO	
Standard Bat Data and Plots	125
APPENDIX THREE	
Flowchart describing doctored bat testing procedure	127
APPENDIX FOUR	
Flowchart describing NBI bat testing procedure	128
APPENDIX FIVE	
Doctoring Study Data	129
APPENDIX SIX	
Doctoring Study: Weighted bat data.....	132
APPENDIX SEVEN	
Weighting Study Data.....	133
APPENDIX EIGHT	
Bat Profiles (all profiles in inches) used for numerical modeling	137
Model information used in numerical simulations	140
Detailed information used for multiple-wall aluminum bat model	141

LIST OF TABLES

Table 3.1 – List of all bats included in the bat doctoring study.....	52
Table 3.2 – Performance Rankings Based on Indirect and Direct Performance Measures	65
Table 5.1 – Measured and simulated vibrational characteristics of a solid wood bat	113
Table 5.2 – Measured and simulated physical characteristics of a solid wood bat	113
Table 5.3 – Measured and simulated vibrational characteristics of a weighted solid wood bat.....	113
Table 5.4 – Measured and simulated physical characteristics of a weighted solid wood bat	113
Table 5.5 – Measured and simulated vibrational characteristics of a single wall aluminum bat.....	114
Table 5.6 – Measured and simulated physical characteristics of a single wall aluminum bat.....	114
Table 5.7 – Measured and simulated vibrational characteristics of a weighted single wall aluminum bat	115
Table 5.8 – Measured and simulated physical characteristics of a weighted single wall aluminum bat	115
Table 5.9 – Measured and simulated vibrational characteristics of a multiple-wall aluminum bat	116
Table 5.10 – Measured and simulated physical characteristics of a multiple-wall aluminum bat	116
Table A2.1 – Standard bat barrel compression and modal analysis data.....	125

LIST OF FIGURES

Figure 2.1a – Schematic of bat-ball collision	8
Figure 2.1b – Solid aluminum barrel-ball collision	9
Figure 2.2 – Schematic of relevant bat regions.....	9
Figure 2.3 – Coordinate system definition.....	14
Figure 2.4 – Balance Point Schematic	15
Figure 2.5 – MOI Stand Schematic.....	16
Figure 2.6 – Modal Analysis Schematic.....	24
Figure 2.7 – Waterfall plot showing the 1st two flexural frequencies and mode shapes of a softball bat.....	25
Figure 2.8 – Bending Modes of a Softball Bat	28
Figure 2.9 – Hoop Modes of a Softball Bat	29
Figure 2.10 – Single-wall Plate.....	30
Figure 2.11 – Multiple-wall Plate	32
Figure 2.12 – Prototype pendulum bat tester	34
Figure 2.13 – Cross section of handle portion of softball bats	36
Figure 2.14 – Setup for turning down the outside diameter of a bat	39
Figure 2.15 – Setup for boring down the inside diameter of a bat.....	40
Figure 2.16 – Picture of a Ball Hammer and Rubber Mallet	42
Figure 2.17a – Composite Bat in a Vise	43
Figure 2.17b – Composite Bat Compressed in a Vise	44
Figure 3.1 – Batting cage used for NBI bat group.....	56
Figure 3.2 – MOI Changes due to Shaving.....	57
Figure 3.3 – Flexural Frequency Changes due to Shaving	58
Figure 3.4 – First Resonant Hoop Frequency Changes due to Shaving	59
Figure 3.5 – Barrel Stiffness Changes due to Shaving	60
Figure 3.6 – Performance Changes due to Shaving.....	60
Figure 3.7 – MOI changes due to ABI processes	61
Figure 3.8 – Flexural Frequency Changes due to ABI Processes.....	62
Figure 3.9 – First Resonant Hoop Frequency Changes due to ABI Processes	62
Figure 3.10 – Barrel Stiffness Changes due to ABI Processes.....	63

Figure 3.11 – Performance Changes due to ABI processes.....	64
Figure 3.12 – Visible Damage Resulting from BCT Treatment.....	64
Figure 3.13 – Flexural frequency trends due to natural break in methods	66
Figure 3.14 – BBS trends due to natural break in methods	68
Figure 3.15 – Barrel stiffness trends due to natural break in methods	68
Figure 3.16 – Hoop frequency trends due to natural break in methods	69
Figure 3.17 – Method of Increasing MOI of Weight Group.....	70
Figure 3.18 – Performance Changes due to End Loading	71
Figure 3.19 – Barrel Stiffness Comparison Before and After Painting	72
Figure 3.20 – Ultra Converted to Velocit-e II.....	73
Figure 3.21 – Ultra Converted to Velocit-e II (knobs)	73
Figure 3.22 – Ultra converted to Velocit-e II (end caps).....	73
Figure 3.23 – Ultra II Converted to Freak	74
Figure 3.24 – Ultra II Converted to Freak (knobs)	74
Figure 3.25 – Ultra Ii converted to Freak (end caps).....	74
Figure 3.26 – Ultra II Converted to Freak 98	75
Figure 3.27 – Ultra II Converted to Freak 98 (knobs)	75
Figure 3.28 – Ultra II converted to Freak 98 (end caps).....	75
Figure 3.29 – Effectiveness of Various Doctoring Methods	76
Figure 3.30 – Hoop frequencies plotted against bat performance	78
Figure 3.31 – Barrel stiffnesses plotted against bat performance.....	78
Figure 4.1 – Schematic of bat impact and weight addition locations	82
Figure 4.2 – MOI Study weight addition example 1	83
Figure 4.3 – MOI Study weight addition example 2	83
Figure 4.4 – MOI Study weight addition example 3	84
Figure 4.5 – MOI Study weight addition example 4	84
Figure 4.6 – MOI Study weight addition example 5	85
Figure 4.7 – BBCOR as a function of weight location – wood bat	87
Figure 4.8 – BBCOR as a function of weight location – single wall aluminum bat	88
Figure 4.9 – BBCOR as a function of weight location – multiple-wall aluminum bat	89
Figure 4.10 – BBCOR as a function of weight location – multiple-wall composite bat ..	90

Figure 4.11 – Waterfall plot of single wall aluminum: no weight.....	92
Figure 4.12 – Waterfall plot of single wall aluminum: weight at 17” location	92
Figure 4.13 – Waterfall plot of multiple-wall composite: no weight	93
Figure 4.3 – Waterfall plot of multiple-wall composite: weight at 17” location.....	93
Figure 4.15 – High speed video capture of bat-ball impact.....	96
Figure 4.16 – Discretized softball bat	96
Figure 5.1 – Flexural frequency convergence due to longitudinal element variations...	103
Figure 5.2 – Hoop frequency convergence due to longitudinal element variations	103
Figure 5.3 – Flexural frequency convergence due to circumferential element variations	104
Figure 5.4 – Hoop frequency convergence due to circumferential element variations ..	105
Figure 5.5 – Flexural frequency convergence due to through the thickness element variations.....	106
Figure 5.6 – Hoop frequency convergence due to through the thickness element variations.....	106
Figure 5.7 – Wood bat model	108
Figure 5.8 – Sectioned view of wood bat model	109
Figure 5.9 – Single wall aluminum bat model.....	109
Figure 5.10 – Sectioned view of single wall aluminum bat model.....	110
Figure 5.11 – Views of knob used on aluminum bat models.....	110
Figure 5.12 – Multiple-wall aluminum bat model	111
Figure 5.13 – Sectioned view of multiple-wall aluminum bat model.....	111
Figure 5.14 – Close-up of sectioned view of multiple-wall aluminum bat model	112
Figure A1.1 – Ball cannon, Breach plate, and Air tank accumulator	123
Figure A1.2 – Ball cannon loading procedure	123
Figure A1.3 – Arrestor plate, Light curtains, and bat in position for impact.....	124
Figure A2.1 – Standard bat barrel compression trend	125
Figure A2.2 – Standard bat modal analysis trends	126

CHAPTER ONE

- INTRODUCTION -

The game of softball was created in 1887 by George Hancock, who used a tied-up boxing glove as a ball and a broomstick as a bat [1.1]. As softball grew in popularity and participation levels increased on a national scale, organizations were founded with the purpose of standardizing the rules of the game and organizing consistent and fair competition. The first of these organizations was the Amateur Softball Association of America (ASA), which was founded in 1933, and named the National Governing Body of Softball by the United States Olympic Committee in 1978 [1.2].

While a tied up boxing glove was a sufficient ball for use in the first game of softball, it was quickly replaced by a ball that resembled a modern-day baseball. The most common construction consisted of three layers; a core, a wrap, and a cover. The cores were made from either a mixture of cork and rubber, or Kapok (a cork substitute made from natural fibers). The cores were then wrapped with yarn and covered with cowhide, horsehide, or a synthetic material [1.1]. Balls of this construction were not especially durable, as they often deformed when the cores softened with repeated impacts. Despite this drawback, this style of ball was used for nearly a century before alternative, polyurethane-based, or “poly-core” balls were introduced.

The first poly-core balls were produced in 1972 – they were constructed of a polyurethane-based core and had leather or synthetic covers [1.3]. When first introduced, the durability and liveliness of poly-core balls were significantly higher than those of traditional balls. As a result, standards were implemented to measure the liveliness and hardness of the balls. A restriction on the ball liveliness was developed in the early

1980's, while a restriction on the ball hardness was not developed until the late 1990's [1.4, 1.5]. Poly-core balls have almost completely replaced traditional balls, and there are currently many combinations of softball hardness and liveliness that are acceptable for play in the major softball associations.

A few years prior to the introduction of poly-core balls, another major equipment change took place. In 1970, aluminum softball bats were produced [1.3], which marked the first alternative to wood bats. Originally, the aluminum bats were in demand because they offered superior durability compared to wood bats. As technology improved, more exotic aluminum alloys were used to manufacture bats, and by the mid to late 1980's aluminum bats were performing at a higher level than any bats ever produced. Around this same time, manufacturers began experimenting with bats made from composite materials, such as graphite and fiberglass, although these bats were not highly regarded because they did not perform as well as the best aluminum bats [1.6]. By 1994, both titanium and multiple-walled aluminum bats were in production [1.6]. The performance of these bats was significantly higher than even the highest performing single-walled aluminum bats of the time.

The major national softball organizations believed in order to maintain an acceptable level of safety and a competitive balance in their game,^{*} standards needed to be put in place so that the performance of bats could be controlled. A bat test was soon developed, and it was adopted by the American Society of Testing and Materials (ASTM). By 2000, the most prominent national softball organizations required all of the bats used in their leagues to conform to their prescribed standards (as measured by the

^{*} The ASA felt that an average player should not be able to hit the ball out of a field with fences set at 300 feet from home plate [1.2].

new ASTM bat test). Nearly all of the bats that had been in production were able to be certified using these standards. Titanium bats, however, exceeded the standards and were banned from use by most associations.

The new performance limitations did not significantly limit the creativity of manufacturers, and bats continued to evolve as technology improved. The use of composite materials increased as companies developed high-performing metal/composite hybrids and full composite designs. In addition, existing multiple-walled bat designs were improved upon and this style of bat grew in popularity as multiple manufacturers put them into production. By 2004, the National Governing body of Softball had again become concerned with the level of safety and competitive balance of the game of softball. Based on an improved bat testing procedure and a desire to maintain the character of softball, the ASA lowered the performance limit on the bats that it would certify. The reduction in allowable performance resulted in the banning of previously-certified bats and much controversy.

While there were many reactions to the ASA's revised performance limit, one unanticipated consequence was a dramatic increase in the number of modified bats* used in recreational leagues and tournament play. In order to understand why the use of modified bats increased, it is useful to understand the advantages and disadvantages of high performing and modified bats. In general, a bat's performance and durability work against each other – as performance goes up, durability goes down, and vice versa.

Prior to 2004, the highest performing bats were optimized for performance and suffered from marginal durability. Modifying these bats resulted in a small performance

* The term "modified bat" refers to any stock bat that has been modified with the purpose of improving its performance. Bat modifications will be discussed in detail in the following chapter.

increase and a significant decrease in durability. Consequently, the majority of people that modified bats competed only in the highest levels of softball, where nearly all teams were sponsored and used similar high-performing equipment. Therefore, the small performance advantage gained by modifying a bat outweighed the decrease in durability because sponsors usually provided the teams with equipment. In contrast, players in recreational softball leagues were usually not willing to spend the time, money, and effort to continually replace a bat for only minimal gains in performance.

After the lower performance limit was introduced in 2004, the highest performing ASA approved bats were no longer optimized for performance. As a result, the top performing bats did not suffer from marginal durability. Now, for the first time, modifying a top performing bat resulted in a significant performance increase and only a moderate decrease in durability. Subsequently, many recreational softball players are willing to spend the time, money, and effort to occasionally replace a bat for significant performance increases.

With the use of modified bats on the rise, understanding the effects that various modifications have on bats and how modified bats can be detected have become important issues surrounding the game of softball. This study considers the methods used to modify bats and their effects on bat performance and physical characteristics. In addition to the investigation of modified bats, stock bats are also evaluated in order to determine how their performance and physical characteristics change with normal use. Finally, bat performance and physical characteristics were modeled using Finite Element Analysis (FEA) and the results were compared to experimental measurements.

REFERENCES

- 1.1 Sullivan, G. The Complete Guide to Softball. Fleet Publishing Corporation, New York. 1965.
- 1.2 ASA Certified Equipment. 1/30/2005.
http://www.softball.org/about/pdf/ASA_Bat_Ball_Certification_Program_Overview.pdf
- 1.3 Worth Innovation Timeline. 1/30/2005.
<http://www.worthsports.com/aboutworth/timeline.html>
- 1.4 McKeown, Kelly. Amateur Softball Association. *Private communication*. February, 2005.
- 1.5 Laws, Tony. Amateur Softball Association. *Private communication*. February, 2005.
- 1.6 Chauvin, Dewey. Easton Sports. *Private communication*. February, 2005.

CHAPTER TWO

- LITERATURE REVIEW -

2.1 General Trends in Bat Performance

In 2003, the ASA funded a study whose purpose was to determine how the performance of softball bats had evolved since the introduction of non-wood bats. The study included samples of bats from the six predominant eras of bat design – wood, standard grade aluminum, aerospace grade aluminum, multiple-wall aerospace grade aluminum, titanium, and composite. The study, which has come to be known as the Era Study, showed that in the span of nearly 30 years, revolutions in bat construction had led to a performance increase of 17% over traditional wood bats [2.1].

In recent history, researchers have conducted investigations in order to understand the factors that affect bat performance. One of the first of these studies was carried out by Naruo and Sato [2.2] who measured the coefficient of restitution (COR) between a ball and 12 different tubes. They found that the COR was dependent on both the flexural stiffness and circumferential stiffness of the tubes. Specifically, the COR rose with increasing bending stiffness and decreasing circumferential stiffness. Naruo and Sato confirmed that this same trend occurred in softball bats when they compared the COR and stiffness characteristics of bats made from wood, aluminum, composite, and titanium*.

Brooks, Knowles, and Mather [2.3] found a similar result when they investigated the COR of balls bouncing off of thin plates made from various materials. In a numerical analysis they observed that under certain conditions the contact time between the ball and

* Nauro and Sato used modal analysis (which will be described herein) to determine the relative stiffness between their tubes and bats.

the plate matched the time required for the plate to deflect and return to its original position. Under these conditions the COR increased because some of the vibrational energy in the plate was returned to the ball. The investigators referred to this type of impact as an *isoharmonic impact*, and they speculated that plates made from composite materials could be “tuned” to achieve an optimum COR.

Nishikawa [2.4] furthered the understanding of how bending and circumferential stiffness affected bat performance when his numerical model of a bat and ball collision identified values at which bending and circumferential stiffness produced a maximum COR. From his work, Nishikawa concluded that bending stiffness was not significant to performance because the flexural deflection cannot fully develop during the contact time, while the circumferential stiffness is significant because the area around the impact undergoes a full cycle of circumferential deflection*.

Russell [2.5], who ranked bat stiffness using modal analysis like Naruo and Sato, evaluated the Era Study bats and confirmed the trend that lower circumferential stiffness correlated with higher bat performance. Russell’s work also included using a simple mass-spring system to model the bat ball collision. With this model, Russell, like Nishikawa, found an optimum circumferential stiffness that would provide the most efficient bat ball collision.

A rigorous analysis of the bat ball collision has been conducted by Nathan, Russell, and Smith [2.6]. In their investigation, the collision was modeled using a mass-spring system similar to the one used in [2.5]. In their model, both the bat and ball were represented with a mass and a spring. In a simulation of an impact using a lower performing bat and a typical ball, the model showed that the spring representing the ball

* Nishikawa determined relative stiffness of his bats by comparing force vs. deflection values

compressed much more than the spring representing the bat. This results in a significant loss of energy because the ball spring behaves inelastically – which prevents all of the energy stored in the ball to be utilized in the collision. By holding the mass and spring constant (representing the ball) fixed, and varying the mass and spring constant of the bat, the effect of circumferential stiffness on performance was characterized. The model showed that the largest COR occurred when the bat spring compressed more than the ball spring – in which case the bat's stored energy can be utilized in the collision because the bat behaves elastically. This process is analogous to the physics of a trampoline, as a result, when a bat exhibits this behavior it is referred to as the *trampoline effect*. Figures 2.1a,b show a schematic of the bat-ball collisions and associated deflections between a solid bat and ball and a hollow bat and ball, and pictures of the impact area between a ball and a solid aluminum barrel section.

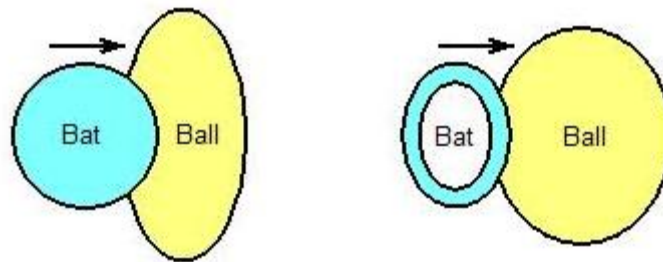


Figure 2.1a – Schematic of bat-ball collision



Figure 2.1b – Solid aluminum barrel-ball collision

Other commonly studied bat performance parameters are weight and its distribution. Before discussing these parameters it is useful to explicitly define the terms that will be used to describe specific portions of a bat. Figure 2.2 shows the regions of interest of the bat in this research.

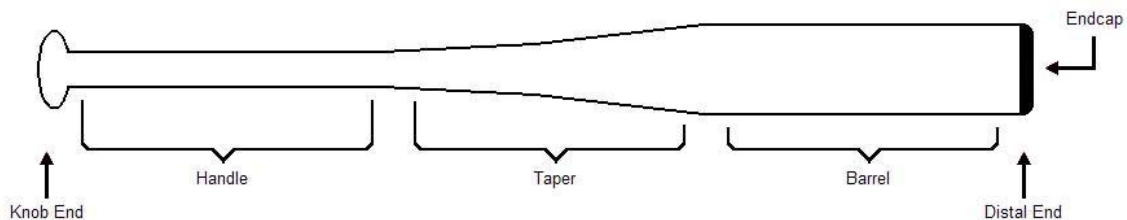


Figure 2.2 – Schematic of relevant bat regions

There are no strict definitions for the weighting (also known as *loading*), but bats are generally classified as either balanced or endloaded. Balanced bats have their mass

centers located closer to the knob of the bat than endloaded bats, which have their mass centers located closer to the distal end of the bat.

Noble and Eck [2.7] investigated the effect loading has on performance by adding weight to three similar bats. The additional weight was distributed uniquely for each bat, and results showed that adding weight to either the knob or distal ends of the bats increased performance. This result, as well as the observation that adding weight to the handle portion of a bat is the most effective loading strategy, will be examined in the current study.

House [2.8] stated that heavier bats are more effective than lighter bats because for a given swing speed a higher momentum is achieved and can be transferred to the ball. Adair [2.9] reached a similar conclusion in his book. Using a hollowed out (corked) bat as an example, he said a lighter bat should decrease performance because less energy can be transferred to the ball. Adair also touches on how adjusting the weight of a bat will affect more than collision efficiency, stating that a player's swing speed is not independent of bat loading.

Most other examinations of bat weight and weight distribution focus on how bat loading helps or hinders a player's ability to achieve a maximum swing speed. This is seen as an important idea because a faster swing is believed to increase batted ball speed. Bahill [2.10, 2.11] has completed two studies investigating this topic. Bahill examined the effect that a bat's weight has on the speed at which it can be swung by individual players. The study did not control moments of inertia (MOI) between the various weighted bats, but the bats did maintain similar centers of mass. Results showed that each player had an ideal bat weight that would optimize swing speed. Lighter bats were

generally swung faster than heavy bats; and in plots showing the decline in swing speed versus bat weight, the curves seemed to be approaching a nominal swing speed.

In [2.11], Bahill studied the effect of MOI on swing speeds. In the study, players swung four bats with a wide range of MOI. Results showed that, in general, players' swing speeds decreased linearly with increasing MOI. Bahill concluded that most players would benefit from swinging bats that are more endloaded than most bats currently in production.

In a study investigating the swing speeds of wood and aluminum baseball bats, Nichols, Elliot, Miller, and Koh [2.12] found that the aluminum bats were swung faster than wood bats. The average linear velocity of the distal end of the wood bats was 5.6% slower than the average linear velocity of the distal end of the aluminum bats. The differences in swing speed were determined to be a result of the MOI difference between the bats, as the wood bat's MOI was 22% higher than that of the aluminum bat.

Fliesig, Zheng, Stodden, and Andrews [2.13] evaluated the effect varying MOI has on the swing speed of both baseball and softball players in a study that consisted of 34 individuals. All of the test subjects competed at the collegiate level of their respective sport (baseball and fastpitch softball), and it was found that both baseball and softball swing speeds increased linearly with decreased MOI.

The relationship between bat mass properties (bat weight and MOI) and swing speed have been characterized in detail for both slowpitch and fastpitch softball players by Smith [2.14, 2.15]. In the slowpitch field study,^{*} players from all skill levels competing in the ASA National Championship Series hit with two different groups of bats. One set

^{*} A field study is conducted under conditions that simulate actual playing conditions as closely as possible by allowing test subjects to hit pitched balls on a standard outdoor softball field.

of bats had varying weight (24-31oz in 2oz increments) and constant MOI, while the second group of bats had constant weights and varying MOI (7,000-11,000 $oz \cdot in^2$ in 2,000 $oz \cdot in^2$ increments). It was found that for the range of bats tested, swing speed was independent of bat weight and dependent on MOI according to

$$V_{actual} = V_{nominal} \left(\frac{9,000oz \cdot in^2}{I} \right)^{1/4}, \quad (2.1)$$

where V_{actual} (*mph*) is the linear swing speed at the impact location normalized for bat inertia, $V_{nominal}$ (*mph*) is the nominal swing speed at the impact location, and I is the inertia of the bat ($oz \cdot in^2$) about a pivot point six inches from the knob end of the bat.

In Smith's [2.15] second field study, 31 female fastpitch softball players with skill levels ranging from high school to members of the 2004 Olympic Gold Medal winning USA Softball team hit with two groups of bats. The first set of bats had varying weight (22-28oz in 3oz increments) and constant MOI, and the second group of bats had constant weight and varying MOI (7,000-9,000 $oz \cdot in^2$ in 1,000 $oz \cdot in^2$ increments). This study produced similar results to its predecessor in that swing speed was dependent on MOI, but the swing speed of the fastpitch players was also found to be slightly dependent on bat weight. The dependence on MOI and weight were described by

$$V_{actual} = V_{nominal} \left(\frac{8,000oz \cdot in^2}{I} \right)^{.1}, \quad (2.2)$$

and

$$V_{actual} = V_{nominal} \left(\frac{25oz}{m} \right)^{.065} \quad (2.3)$$

where m is the weight of the bat (*oz*).

A salient feature of Smith’s field studies is evidence that in addition to swing speed being dependent on bat weight and/or MOI, it is also dependent on the style of game which is being played. While this result is nominally interesting in itself, it becomes more significant when one begins to analyze bats for the purpose of regulating their performance.

2.2 Direct Measurements of Bat Performance

Until now, the focus of this chapter has been to outline the general trends in bat performance – these general trends, however, are insufficient for determining absolute bat performance. For this, a more complete analysis is necessary.

Momentum is conserved in the bat–ball collision. The three largest regulating agencies, the ASA, the United States Specialty Sports Association (USSSA), and the National Collegiate Athletic Association (NCAA), use a momentum balance to compute bat performance. Each of these organizations uses a different bat performance metric and standard that will be discussed in more detail in the following section. The ASA uses a test described by ASTM F 2219-02 [2.16] in which a softball traveling at 110 *mph* impacts a stationary bat. The USSSA test follows the procedure outlined in ASTM F 1890-02 [2.17], which is similar to the procedure used by the ASA, except a 60 *mph* impact is used. In the test used by the NCAA to certify baseball bats, a ball traveling at 70 *mph* impacts a bat traveling at 66 *mph*. The momentum balance for the bat-ball collision has the form

$$(mv_i Q) + I_p \omega_i = mv_r Q + I_p \omega_r, \quad (2.4)$$

where m is the ball mass (*oz*), v_i is the inbound ball speed (*in/s*), v_r is the ball rebound speed (*in/s*), and Q is the impact location on the barrel measured from the pivot point

(in)* of the bat, ω_i is the initial bat rotational speed (rad/s), ω_r is the post impact rotational speed (rad/s), and I_p is the bat MOI ($oz \cdot in^2$). The sign convention to be used in equation 2.4 is defined with the help of figure 2.3. Positive is the left to right direction, and right to left is negative.

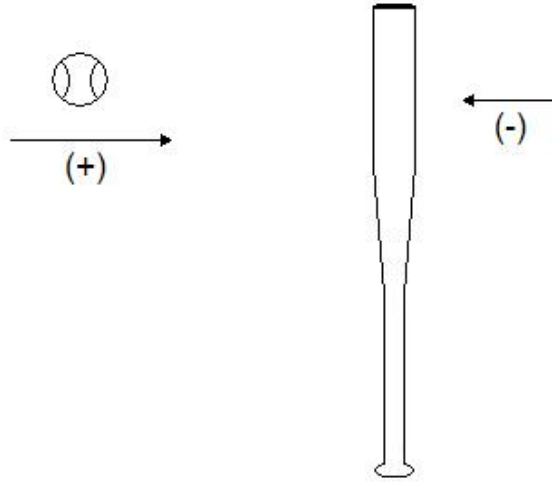


Figure 1.3 - Coordinate system definition

The bat MOI is measured from the pivot point and is calculated from a form of the dynamic equilibrium of a physical pendulum,

$$I_p = \left(\frac{(\eta)^2 g W_i a}{4\pi^2} \right), \quad (2.5)$$

in which case g is the gravitational acceleration (in/s^2), W_i is the total weight of the bat (oz), and a is the distance from the bat's balance point (BP) to the pivot point (in), given by

* The pivot point is 6.0 inches from the knob end of the bat in all testing standards. Therefore, a ball that impacts the barrel 27.0 inches from the knob end of the bat would have $Q = 21.0$ inches. All other references to a bat's pivot point in this paper refer to a location 6.0 inches from the knob end of the bat.

$$a = BP - 6.0. \quad (2.6)$$

The BP, also known as center of mass, is the point along the length of the bat where it would balance on a knife edge. To measure the BP, a bat is placed on a balance point stand, as shown in figure 2.4, and the weight at the 6.0 inch location (W_6) and the 24.0 inch location (W_{24}) are recorded. The balance point is then calculated from the equation

$$BP = \left(\frac{6W_6 + 24W_{24}}{W_t} \right). \quad (2.7)$$

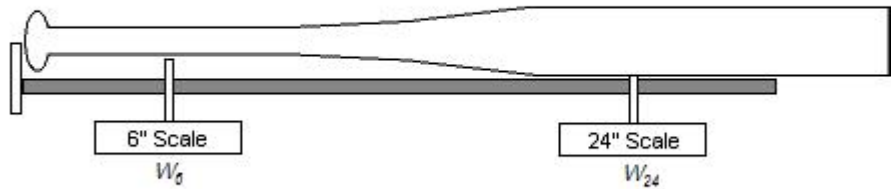


Figure 2.4 – Balance Point Schematic

The period η is found by measuring the time for a bat to swing through ten cycles in a pendulum, as shown in figure 2.5. The pivot point of the pendulum is 6.0 inches from the knob end of the bat.

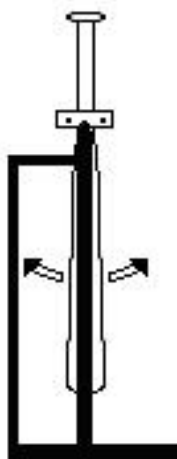


Figure 2.5 – MOI Stand Schematic

Assuming that the inbound speed of the ball and the initial bat speed are known, equation 2.3 has two unknowns, v_r and ω_r . Regulating agencies must determine which of these unknown values to measure. The ASA and NCAA choose to measure v_r and solve for ω_r , while the USSSA chooses to do the opposite. The methods should be equivalent, but in practice measuring the ball rebound speed can be more repeatable than measuring the bat recoil speed due to the fact that bat recoil speed can be affected by vibrations in the bat and any resistance to bat motion caused by the fixture used to grip the bat. The remaining calculations will be carried out assuming ball rebound speed is measured and bat recoil speed is solved for by rearranging equation 2.4 to

$$\omega_r = \frac{(v_i + v_r)mQ}{I_p} + \omega_i. \quad (2.8)$$

The Bat-Ball Coefficient of Restitution (BBCOR), or e_{BB} , is defined as the ratio of the outgoing to incoming relative speeds of the bat and ball,

$$e_{BB} = \frac{v_r + \omega_r Q}{v_i + \omega_i Q}. \quad (2.9)$$

Combining (2.8) and (2.9), and assuming an initially stationary bat ($\omega_i = 0$) yields

$$e_{BB} = \frac{v_r}{v_i} + \frac{mQ^2}{v_i I_p} (v_i + v_r). \quad (2.10)$$

The performance standard used by the USSSA is the Bat Performance Factor (BPF). It is defined as the ratio of e_{BB} to the measured coefficient of restitution (COR) of the ball, e .

The ball COR e is the ratio of the rebound to inbound speed of a ball impacting a rigid wall at 60 *mph* and is tested according to ASTM F 1887-02 [2.18]. The ball COR is calculated from the equation

$$e = \frac{v_r}{v_i}. \quad (2.11)$$

The USSSA performance metric is written as

$$BPF = \frac{e_{BB}}{e}. \quad (2.12)$$

Both the ASA and NCAA performance metrics require further numerical manipulations. Specifically, two dimensionless parameters, the bat recoil factor (r) and the bat-ball collision efficiency (e_a) are necessary. The bat recoil factor depends only on the inertial properties of the bat and ball [2.19] and is given by

$$r = \frac{m_n Q^2}{I_p}, \quad (2.13)$$

where m_n is the nominal ball weight (*oz*).

The collision efficiency is a model-independent relationship that can be derived using conservation laws [2.19], and is defined as

$$e_a = \left(\frac{e_{BB} - r}{1 + r} \right). \quad (2.14)$$

Further inspection of equation 2.14 illustrates that e_a is a maximum when the bat recoil factor is a minimum. From an energy standpoint, when equation 2.13 is small, less energy is transferred to the bat and more is transferred to the ball. As the bat inertia increases, $r \rightarrow 0$ and $e_a \rightarrow e_{BB}$.

The NCAA performance metric, the Ball Exit Speed Ratio (BESR), is based on the bat-ball collision efficiency and is written as

$$BESR = e_a + \frac{1}{2}. \quad (2.15)$$

The performance metric used by the ASA, Batted Ball Speed (BBS), is based on the bat-ball collision efficiency and also accounts for the pitch and swing speed of a player.

It is written as

$$BBS = (ve_a) + V(1 + e_a), \quad (2.16)$$

where v is the pitch speed and V is the bat swing speed at the impact location. The ASA assumes a pitch speed of 25 mph , and uses a special form of equation 2.1 to calculate swing speed. By accounting for the impact location and using the average swing speed found in [2.14], equation 2.1 becomes

$$V = 85 \left(\frac{Q + 8.5}{30.5} \right) \left(\frac{9000}{I_p} \right)^{\frac{1}{4}}. \quad (2.17)$$

Since the BBS performance metric describes bat performance in terms speed, it is easy to relate it to yet another tangible metric—hit distance. Using projectile motion equations and accounting for air resistance on a ball in flight, a one mile an hour change in batted ball speed can be shown to alter a ball's flight by 7.5 ft.

2.3 Comparison of Bat Performance Tests and Metrics

Bat performance can be measured using three different test procedures and two different data collection methods. The data collection methods (measuring either ball rebound or bat recoil speed and solving for the other) have been discussed in section 2.2.1, but the various testing procedures have not been specifically addressed. In test method one, a moving ball impacts an initially stationary bat, in method two, a swinging bat impacts an initially stationary ball, and in method three, a moving ball impacts a swinging bat. Each of these methods should provide identical performance ratings, but in practice, the test results and their repeatability can be affected by the test fixtures and the difficulty in performing each test.

Test methods one and two are simpler than test method three due to the fact that test method three requires a device to propel a ball and swing a bat, and must accurately control the timing between the two. Although the complexity of methods one and two are similar, method two is not used by any regulating associations to measure bat performance. Method one is used to measure BBS and BPF, while method three is utilized by the certified BESR test.

While the measurement of BBS and BPF use the same test method, they are dramatically different in three aspects. The BBS test protocol [2.16] requires a ball traveling at 110 *mph* to impact an initially stationary bat and measure the rebound speed of the ball. In addition, the bat is impacted in one half inch increments along the barrel portion of the bat in order to experimentally find the maximum BBS location.* The BPF test [2.17] is different because it requires a ball traveling at 60 *mph* to impact an initially stationary bat and measure the recoil speed of the bat. Furthermore, the bat is only

* This procedure is known as “scanning” a bat.

impacted at one predetermined location, its center of percussion (COP), which may or may not be near the maximum BPF location on the bat. A bat's COP can be found using

$$COP = \frac{I_p}{Md}, \quad (2.18)$$

where M is the total mass of the bat and d is the distance from the BP to the pivot point.

The test for BESR [2.20] requires a ball traveling at 70 mph to impact a bat whose linear velocity at a point measured 6 inches in from the distal end of the bat is 66 mph . In order to balance the momentum equation, ball rebound speed is measured, and the post-impact bat speed is calculated. In this test, the barrel of the bat is scanned in order to find the location which produces the maximum BESR value.

Smith [2.21] has investigated these performance standards in a study in which the effects of each of their distinct procedures and assumptions was discussed. It was found that the BPF tends to underestimate performance because it is performed at speeds that are inconsistent with game conditions and because it is measured at a predetermined location that does not consistently coincide with the location on the bat that would produce a maximum BPF value. Testing the bat using a 60 mph impact does not provide an effective performance metric because the trampoline effect is less dramatic at lower speeds due to the fact that the lower impact forces of the slower impact do not provide enough energy to flex the walls of bats as they are in games. Also, by testing at the COP of a bat, often times the maximum BPF of the bat is not measured. In recent years, manufacturers have taken advantage of this metric by altering the weight distributions of their bats in order to manipulate the COP location, and ensure that their bats would not exceed the 1.20 BPF limit.

The BESR performance metric has been shown to underestimate the performance of relatively low MOI bats. This occurs because the BESR test protocol requires all bats to be tested at the same swing speed. As a result, two bats of different MOI that test at the same level on the BESR scale can have very different on-field performances due to the fact that the lower MOI bat can be swung at a faster rate.

Based on these observations, Smith made recommendations for a performance test that better described conditions seen in play. The BBS metric was developed taking these recommendations into account, and as a result, it yields results closer to those seen in play. Appendix 1 describes the test setup used for the BBS scan.

2.4 Indirect Performance Metrics

In other organized sports that utilize striking implements, such as golf and cricket, rules are in place that limit the performance of the striking implements. One key difference between the golf and softball tests is that the United States Golf Association (USGA) test is not based on a direct measure of performance [2.22]. Instead, it measures characteristics of golf club heads that are known to correlate with performance. Similarly, softball bats have measurable characteristics that often correlate with bat performance. They will be discussed in the following sections.

2.4.1 Modal Analysis

While the vibration patterns of an excited structure may seem to be random, they are in fact very predictable. All structural objects have tendencies to vibrate at specific frequencies (natural or resonant frequencies) with associated deformation patterns, or mode shapes. Modal analysis can be thought of as the study of an object's dynamic characteristics, or its frequency, damping, and mode shapes.

In order to determine the dynamic characteristics of a structure, first the stimulus and the structure's response to that stimulus need to be measured and recorded. One acceptable method of stimulation is to apply a sinusoidal force to the structure, such that the frequency and the peak force of the loading cycle are fixed. By changing the frequency of the loading cycle and recording the structure's response with an accelerometer, it can be seen that the amplitude of the measured response varies as the frequency of the loading cycle changes. This trend can be seen by plotting the response in the time domain.

The previous observation becomes more useful when the data is transformed to the frequency domain using the Fast Fourier Transform (FFT), and calculating a Frequency Response Function (FRF)[2.23]. An FRF is defined as the ratio of the response signal to the stimulus signal under steady state conditions,

$$FRF = \frac{FFT\ Output}{FFT\ Input}. \quad (2.19)$$

When its magnitude is plotted versus frequency, peaks can be seen at each of the structure's resonant frequencies. The FRF can also be defined for a single degree of freedom system,

$$x(t) = m\ddot{y} + c\dot{y} + ky, \quad (2.20)$$

as

$$H(\omega) = \frac{1}{k} \frac{1}{1 - \left(\frac{\omega}{\omega_n}\right)^2 + i2\xi\left(\frac{\omega}{\omega_n}\right)}, \quad (2.21)$$

where ω is the frequency, ω_n is the natural frequency, and ξ is the critical damping factor [2.24].

In order to determine the second vibration characteristic, damping, equation 2.21 must be solved for the critical damping factor, at which point damping rate, σ_n can be found from

$$\sigma_n = \sqrt{\frac{\omega_n^2 \xi^2}{1 - \xi^2}}. \quad (2.22)$$

The final vibration characteristic, mode shape, can be found by evaluating the imaginary components of multiple FRF's. Before this process is fully examined, it will be useful to describe the modal analysis procedure in more detail.

It was stated before that one method of exciting a structure was to apply a constant sinusoidal load (this is also known as a shaker test); another acceptable method of stimulating a structure is to impact it with another object, usually an impact hammer.* The latter of these methods was used to obtain vibration data in this research, and further discussion of modal analysis refers to this method of testing. Until now, modal analysis has only been described in terms of a single measurement, but a complete analysis which defines mode shapes (or deflection patterns) in addition to frequency and damping of a structure, requires multiple measurements. Using a bat as an example, if an accelerometer was attached to the underside of the distal end of the bat, and the bat was impacted opposite the accelerometer, as shown in figure 2.6, the FRF generated from the collected data would describe the frequency and damping characteristics of the entire bat, but would only describe the deflection of one point on the bat due to a specific impact.

* An impact hammer is a device used for impact modal analysis testing. It utilizes an accelerometer to measure the input into the system.

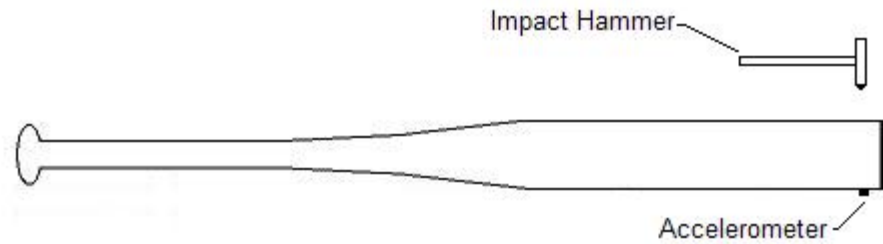


Figure 2.6 – Modal Analysis Schematic

In order to obtain the mode shape data describing the entire bat, more measurements are necessary. Two methods may be used to acquire the additional data. The first option, a roving response test, consists of moving the accelerometer along the length of the bat in small increments while continuing to impact the bat in the same location. The other method that can be used, and was used in this research, is called a roving impact test. It consists of leaving the accelerometer fixed in one location and impacting the bat at small increments along its length.

As they are derived from a Fourier Transform, FRF's are composed of real and imaginary components, and the mode shape data is carried by the imaginary components [2.5]. If the imaginary portions of the FRF's (obtained from a complete roving impact test on a bat) are plotted in a waterfall plot, a trace of the peak magnitudes at each natural frequency will show the mode shape corresponding to that frequency. Figure 2.7 shows an example of this.

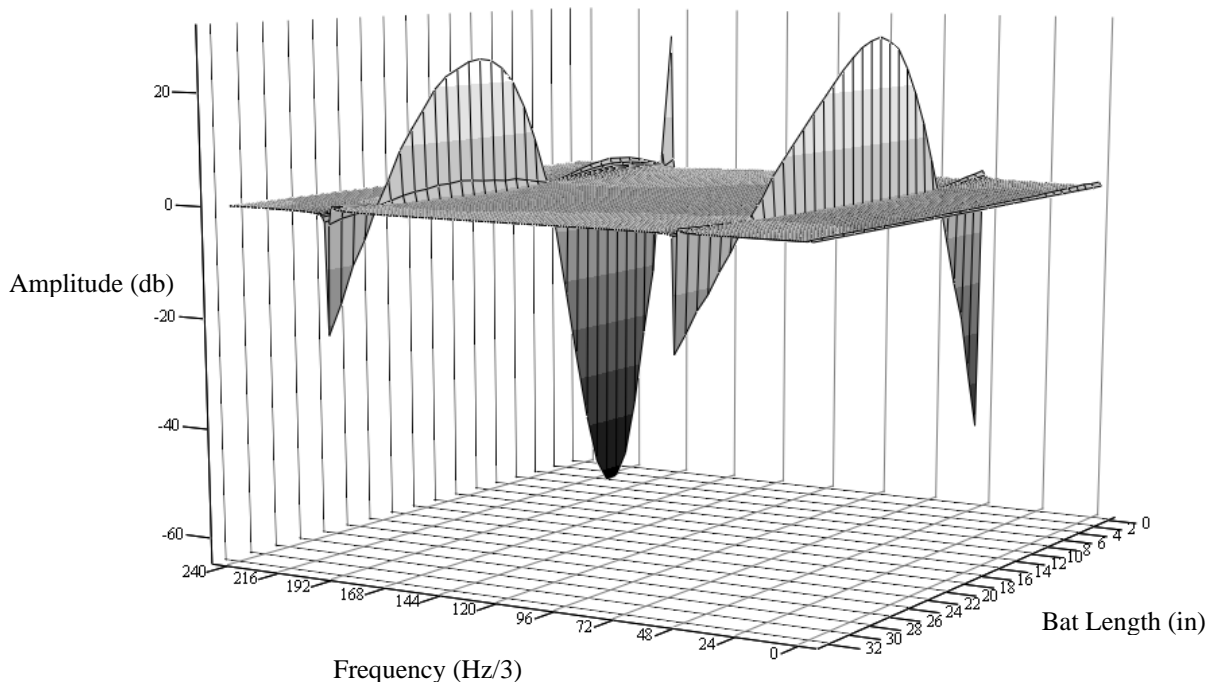


Figure 2.7 – Waterfall plot showing the 1st two flexural frequencies and mode shapes of a softball bat

The range of frequency information collected in a modal analysis depends on the equipment used to make the measurements. For example, when impacting a structure with a relatively stiff impact hammer tip, a higher range of frequencies will be excited than when using a less stiff hammer tip. The excited frequency ranges are dependent on the impact tip because a stiffer tip will result in a shorter contact time and thus higher frequency content. In the testing done for this work, a moderately stiff hammer tip* was used because the usual frequencies of interest when investigating bats are relatively low (less than 3000 *Hz*).

The boundary conditions imposed on a structure whose vibrational characteristics are being measured are of prime importance because the boundary conditions can influence

* The impact tip was made from Delrin; ideal for exciting frequencies up to 2.5 KHz [2.25].

the dynamic characteristics of the structure. As a result, modal testing is often conducted utilizing a setup that approximates service conditions. A free-free setup was used in this research. The validity of free-free boundary conditions describing in service bat constraints seen during the bat-ball collision will be touched on in more detail in Chapter Four.

An important step in assuring that the measured dynamic characteristics accurately describe a structure is to compute the coherence of the FRF. The coherence is an indication of how much of the structure's response is due to the input as opposed to external noise. Coherence is found from

$$C = \frac{PO_p}{MO_p}, \quad (2.23)$$

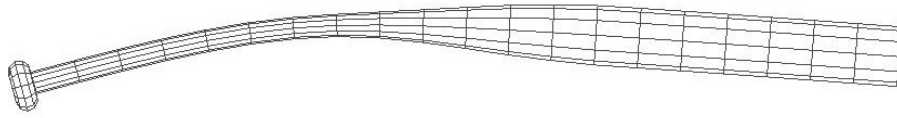
where PO_p is the predicted output power function and MO_p , is the measured output power function. The PO_p is based on a previous FRF measurement according to

$$PO_p = I_p * FRF \quad (2.24)$$

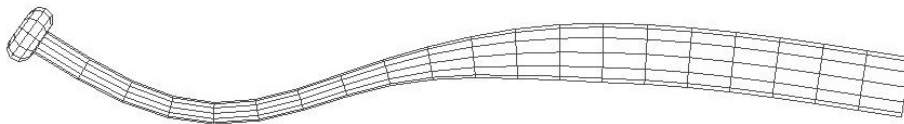
where I_p is the measured input power spectrum and FRF is the frequency response function obtained from the previous measurement.* It follows that in order to calculate coherence, a minimum of two measurements must be made. Coherence values are found as a function of frequency and can range from zero to one. A value of one implies that the measured frequency information matches the predicted information and is therefore acceptable. Since FRF's are unique for each combination of accelerometer placement and impact location, coherence cannot be used to compare data from multiple impact locations of a roving impact test.

* For further information regarding input and output power spectrums, and other details of modal analysis that are beyond the scope of this paper the reader is referred to [2.24], [2.26], and [2.27].

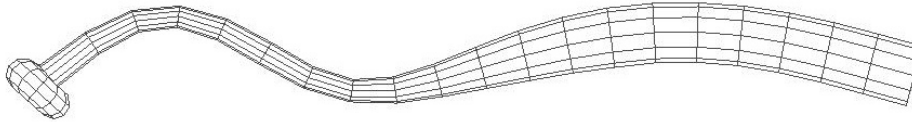
The vibration patterns of all bats are similar in that they exhibit flexural bending modes. The first four flexural bending mode shapes are shown in figure 2.8. In addition to the flexural bending frequencies which generally occur between 100 – 1800 Hz, hollow bats also exhibit hoop modes. These modes are responsible for the “ping” sound generated by aluminum bats, and they usually occur between 1000 and 2500 Hz. Figure 2.9 shows the general shape of the first two hoop modes. These modes are also the modes used to rank bats in order of stiffness as mentioned in section 2.1. Russell [2.28] has shown that hollow wood bats can demonstrate hoop modes. Because hoop mode frequencies are exponentially dependent on wall thickness, these hoop modes occur far above the normally observed range.



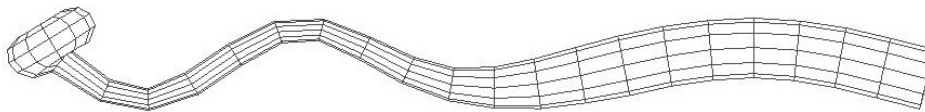
First Bending Mode



Second Bending Mode

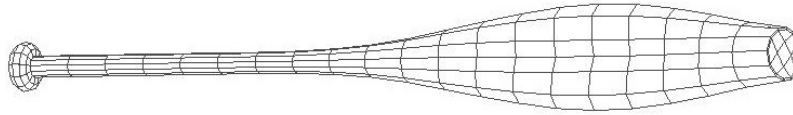


Third Bending Mode

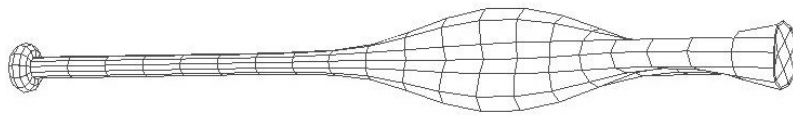


Fourth Bending Mode

Figure 2.8 - Bending Modes of a Softball Bat



First Hoop Mode



Second Hoop Mode

Figure 2.9 - Hoop Modes of a Softball Bat

2.4.2 Barrel Compression

Barrel compression describes a test in which a point on the barrel portion of a hollow bat is compressed 0.070 inches between two steel cylindrical surfaces with radii equal to that of a 12 inch circumference softball. By recording the peak force necessary to compress the bat, all bats can be rated by either the peak load at a maximum deflection or a force per deflection stiffness value. A stiffness scale (lb/in) normalizes small variations in peak deflection and was used in this work.

The concept of using a barrel compression measurement to determine a bat's performance stems from the general trend that softer barrel walls result in higher performing bats. Compression tests show that standard grade single wall aluminum bats have stiffness values on the order of, 9700 *lb/in*, newer single wall bats have stiffness

values on the order of 8700 *lb/in*, and the newest multi-wall aluminum and composite bats can have stiffness ratings in the range of 6500 *lb/in*. To show how changing the physical construction of a bat (by using different materials, thinner walls, or using multiple walls) is beneficial, it is useful to step through the basic physics behind the stiffness calculations.

The first step in this analysis is to simplify the system by evaluating the stiffness of a flat plate, rather than a cylindrical surface. In figure 2.10, such a plate is pictured, where *t* is the plate thickness, *L* is the length of the plate, *P* is the applied load due to the impact of a ball, and *y* is the deflection of the plate.

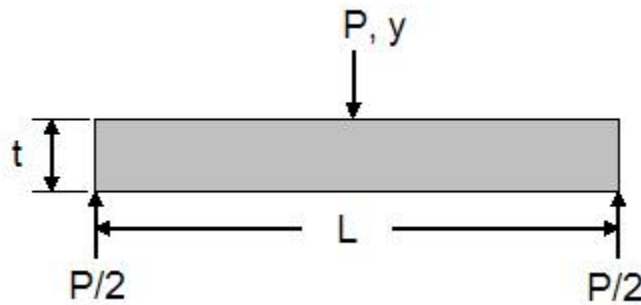


Figure 2.10 – Single-wall Plate

With the load acting at the midpoint of the plate, the maximum deflection and stress in the plate will occur at *L/2*, and can be readily obtained [2.29]. The equation describing the plate deflection is

$$y = \frac{PL^3}{48EI}, \quad (2.25)$$

where *E* is the modulus of elasticity, and *I* is inertia. Remembering

$$I = \frac{bh^3}{12}, \quad (2.26)$$

where b is the length of the plate and h is the height of the plate, the equation describing the deflection of the plate equation 2.25 becomes

$$y = \frac{PL^2}{4Et^3}. \quad (2.27)$$

Looking at the plate and ball system from an energy standpoint, conservation can be written as

$$\frac{1}{2}mv^2 = \frac{1}{2}ky^2, \quad (2.28)$$

where m is the mass of the ball, v is the ball's velocity, and $k = \frac{P}{y}$ is the spring constant.

Combining equations 2.28 and 2.27 and solving for y , one obtains

$$y = \frac{mv^2}{P}. \quad (2.29)$$

The stress in the plate is given by

$$\sigma = \frac{Mc}{I}, \quad (2.30)$$

where σ is stress, M is the moment acting on the plate, and c is the vertical distance from the centroid of the plate to the location of interest. Inspection of figure 2.10, shows that the moment in the plate is caused by the force $P/2$ acting over a distance $L/2$, and that the distance c that corresponds to a maximum stress is half of the plate thickness. Thus, equation 2.30 can be rewritten as

$$\sigma = \frac{3P}{2t^2}. \quad (2.31)$$

Combining equations 2.27, 2.29, and 2.31, stress can be written as

$$\sigma = \frac{3Lv}{bt^2} \sqrt{Ebm \frac{t^3}{L^3}}. \quad (2.32)$$

Consider the same geometry, but made from two plates of thickness $t/2$ as shown in figure 2.11. Deflection is now given as

$$y = \frac{PL^2}{Et^3} \cdot \quad (2.33)$$

Repeating the manipulations employed for the solid plate, stress for the two plate system is found as

$$\sigma = \frac{3Lv}{bt^2} \sqrt{Ebm \frac{t^3}{L^3}} \cdot \quad (2.34)$$

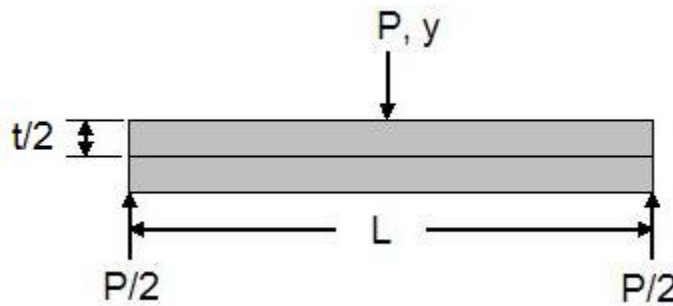


Figure 2.11 – Multiple-wall Plate

Comparing the deflections and stresses from a ball impact in the plates it becomes apparent that the multi-wall plate sees the same maximum stress as the single-wall, but undergoes four times more deflection. As a result of the increased deflection, a greater trampoline effect should occur. Further inspection of these equations shows that the most effective method of improving the trampoline effect in a bat is to decrease the thickness of its walls. It is also apparent that increasing the impact force or trampoline length, or decreasing the material's stiffness could improve the trampoline effect, although at a much lesser degree than altering wall thickness due to the fact that wall thickness has a cubed effect on the equation. Nathan, Russell, and Smith [2.6] have shown that there is a

finite limit at which barrel stiffness becomes so low that the trampoline effect is decreased because the barrel walls cannot spring back in an efficient manner.

2.4.3 Contact Time

As mentioned before, the USGA uses an indirect performance measure to determine whether or not a golf club head exceeds performance standards. The test is based on a byproduct of the trampoline effect – contact duration. In theory, the time in which an infinitely stiff ball is in contact with the object it is striking should directly correlate to the amount of deflection the striking implement is undergoing. In the case of a hollow object such as a bat or golf club head, this deflection is the trampoline effect.

Russell [2.30] has developed a working prototype, shown in figure 2.12, that measures the contact time between softball bats and objects of higher stiffness values. His work shows a trend that longer contact times are associated with higher performing bats, although significant inconsistencies occur. Contact time was not an aim of this study; it has been included here to provide a more complete overview of existing indirect performance metrics.



Figure 2.12 - Prototype pendulum bat tester

2.5 Bat Doctoring

The competitive nature of sport inevitably drives any athlete to seek a means of gaining an advantage over his/her opponent. In most cases, this desire to outperform the competition motivates softball players to train harder to improve their skills and utilize the best available approved equipment. An increasing number of players, however, have turned to using altered, and therefore unapproved, equipment in order to gain an advantage. The process of modifying bats is known as bat doctoring, and for this research a doctored bat will be defined as any bat whose physical characteristics and/or properties have been intentionally and unnaturally altered or modified for the purpose of improving performance.

By modifying approved softball bats, players can expect to gain significant performance increases. A variety of methods are currently used in order to enhance performance, though some are more successful than others. These bat modification methods can be broken down into four categories, each of which will be discussed in the following sections. Using modified bats in regulated games is against the rules and may be punishable by suspension from play. Nearly all modification methods are performed with such care that evidence of the modification cannot be found even under extensive scrutiny.

Some of the bat modification methods require significant machine shop experience; as a result, players without experience using these tools pay others to modify their bats for them. People that accept money in trade for bat modifications have come to be known as bat doctors. There are roughly ten well known bat doctors across the United States and Canada that modify dozens of bats each week. Additionally, there are numerous “regional” bat doctors that modify bats on a smaller scale. Finally, there are even more individuals that modify their own bats. Below the four methods currently employed to doctor a bat are discussed.

2.5.1 Weighting

Weighting, which is also known as loading, encompasses adding weight to, or removing it from a bat. The weight can be altered in any bat, from wood bats to the newest composite bats. Loading has little effect on the durability of hollow bats, but removing weight from wood bats can weaken them.

2.5.1.1 Knob Loading

Knob loading is a procedure in which the weight located in the handle region of a bat is adjusted. As shown in figure 2.13, many manufacturers fasten metal rods or weighted rings into the knob of their bats in order to achieve a desired mass center. It has become popular to remove these rods and rings because players believe that it improves the performance of the bats. This belief stems from the fact that in the summer of 2002, bats that were found to exceed the then-current performance limit could be “re-certified” by retesting the bats after they had metal rods or rings inserted in their knobs. As a result of the re-weighting, most bats conformed to the standard, but as discussed before, a major effect of re-weighting bats is to shift the COP location, which in turn allowed the bats to be tested at a location that did not coincide with the maximum performance location on the bat. In many players’ minds, it followed that the bats would perform at a higher level if one were to “undo” what was done to make the bat conform to the performance limit.

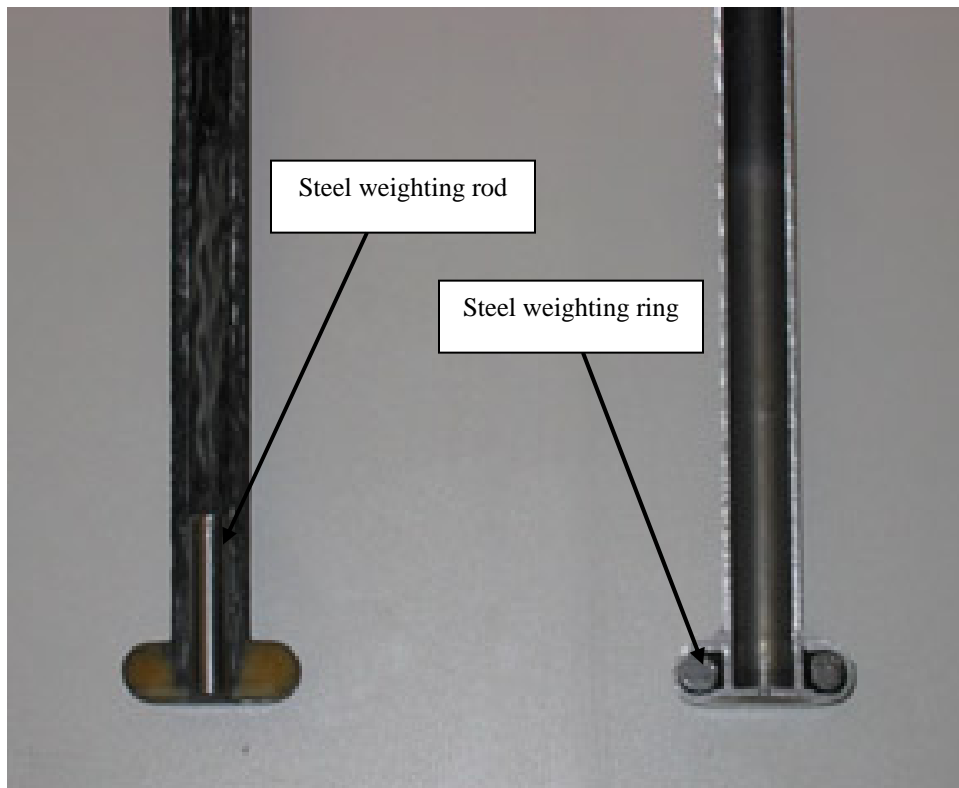


Figure 2.13 – Cross section of handle portion of softball bats

Removing the metal rods from most bats is a simple task that requires the use of a tool called an “easyout.” Removing the weighted rings is more difficult and requires removing the entire knob from a bat. Bat knobs are usually removed by cutting them from the handle. In the case of composite bats, replacing a knob is done by gluing it back to the handle. Replacing knobs on metal bats is more difficult, but can be accomplished by welding. As a result, aluminum knobs are usually not removed from their handles except by experienced bat doctors.

It is uncommon for players to have additional weight added to the handle region of their bats—although it can be accomplished by removing the knob and replacing it after adding weight to it or to the inside of the handle of the bat.

2.5.1.2 End Loading

End loading is a procedure in which the weight located in the distal end of the bat, usually in the end cap, is modified. The most common method of end loading is to add weight to the end cap. A major effect of adding weight to the distal end of a bat is to increase its MOI, while removing weight lowers the MOI. Both end loading methods are primarily done as a result of personal preference, although some believe, and this research suggests, that adding weight to the distal end of the bat improves performance.

Weight can be added to the distal end of a hollow bat by removing the bat knob and pouring a liquid urethane down the inside of the bat and allowing it to solidify at the distal end, but the most common method of end loading bats requires removing the end cap, which can be done in a number of ways. The easiest technique for removing an end cap is to simply pry it off with a screw driver or knife – this process is often facilitated by first heating up the end cap. Many Bat Doctors have manufactured their own molds so

that they can replicate stock end caps and therefore not put forth the time and effort often necessary to remove end caps without leaving signs of modification such as markings from screwdrivers.

2.5.2 Shaving

Shaving, also known as wall thinning, is a process in which a bat's stock wall thickness is reduced. All bats can be shaved, and in all cases durability is sacrificed. There are two types of shaving that can be performed on bats, handle shaving and barrel shaving, the latter of which is far more common than the former.

2.5.2.1 Handle Shaving

Handle shaving consists of thinning the walls in the handle region of a bat. It is accomplished by removing material from either the inside or outside diameter of a bat. The purpose of handle shaving is to improve the flexibility of the bat so that it can bend and whip back into place as it is swung, much like a golf club does. Even though shaving the outside diameter of the handle region of a bat increases the likelihood that the bat will be identified as modified, it can still be done because the shaved region can often be concealed by the bat's grip.

A bat that whips into position as it makes contact with a ball can benefit players because it would increase the effective swing speed by an amount proportional to the magnitude the bat flexes. The effective swing speed would then become the summation of the swing speed generated by the player plus the swing speed generated as the strain energy in the bat is converted into kinetic energy immediately before impact.

2.5.2.2 Barrel Shaving

Barrel shaving was the first bat alteration method which resulted in significant performance increases. All styles of bats can be barrel shaved, although the most commonly worked on bats are multiple-wall aluminum and composite bats. Some bat doctors use cylinder hones in an attempt to thin walls, but the most successful bat doctors fix bats in lathes and remove material via turning or boring processes - figures 2.14 and 2.15 show examples of these processes. Using a cylinder hone to shave bat barrels is less effective than boring because honing is not considered a material removal process, instead it is usually used as a finishing process

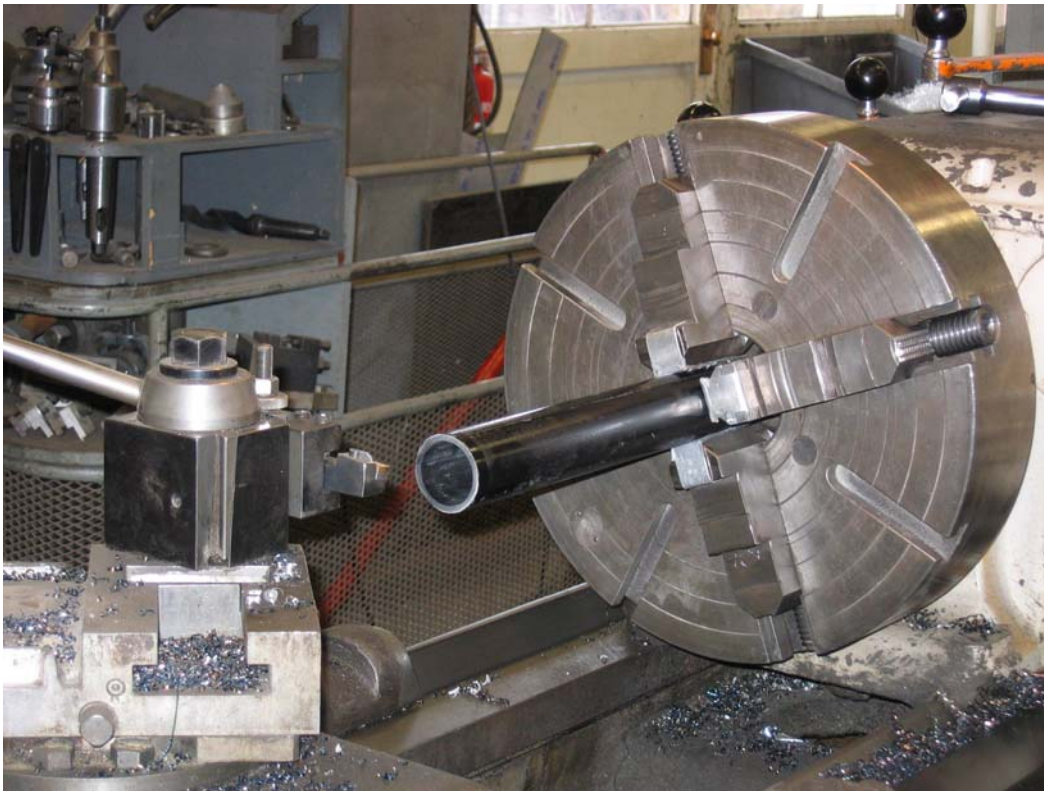


Figure 2.14 - Setup for turning down the outside diameter of a bat



Figure 2.15 - Setup for boring down the inside diameter of a bat

Single-wall bats are shaved by removing material from the inside diameter of the bat, while shaving multiple-wall aluminum bats can be accomplished by removing material from the inside or outside diameter of the interior walls, and/or removing material from the inside diameter of the outermost wall. In the case of multiple-wall aluminum bats whose walls fit together tightly, the shells can be separated using a mechanical or hydraulic press.

The magnitude of performance increase due to barrel shaving is related to how much material is removed. In general, the more material that is removed, the higher the performance will be, and the lower the durability will be. It is common to reduce wall thicknesses by about 0.010 *in* when shaving aluminum bats, and about 0.020 *in* when shaving composite bats. Due to the fact that a composite bat's barrel compliance is a

function of ply orientation and wall thickness, removing the same amount of material from two different composite bats can have drastically different effects on barrel compliance. This is in contrast to most aluminum bats whose barrel stiffness is a simple function of wall thickness.

2.5.3 Natural Break In

Among softball players it is a well known fact that the performances of the highest performing bats actually improve as the bats are used. This process is known as breaking-in a bat. The many methods used to break-in bats can be classified as natural (NBI) or accelerated break-in (ABI) procedures. Natural break-in includes using the bats in their intended manner, hitting pitched balls and hitting balls off of a batting tee, while accelerated methods include using “unnatural” methods to break-in their bats. The actual performance increases due to naturally broken-in bats have been quantified in this research.

2.5.4 Accelerated Break In

Accelerated Break In (ABI) techniques are processes which do not change the physical characteristics, such as wall thickness or weight distribution, of a bat. Instead they focus on altering the physical properties of a bat by inducing damage in the barrel portion of a bat by applying heat and or pressure to the walls. ABI techniques are exclusively performed on composite bats because aluminum bats experience extensive denting due to the applied pressure.

At least three of the well known bat doctors have developed there own ABI processes. The details of these techniques are not well known due to the competitive and

secretive nature of bat doctoring^{*}, but many other ABI processes can be performed by players with minimal technical expertise. The ABI techniques often used by players modifying their own bats are called, hammering and vising.

Hammering is a process in which the barrel portion of a bat is impacted with either a ball hammer or mallet as shown in figure 2.16. Players employing this method are careful to impact along the length of the barrel portion of their bats, making sure to turn the bat evenly such that the bat is broken-in in a uniform manner.



Figure 2.16 - Picture of a Ball Hammer and Rubber Mallet

Vising describes a process in which the barrel portion of a bat is circumferentially compressed in a standard shop vise, as shown in figure 2.17. Bats are generally compressed from their 2.25 inch diameter down to about a 1.75 inch diameter, although some bats can be compressed past a 1.50 inch diameter if a player is not worried about

^{*} These processes are known as Rolling, Advanced Composite Treatment, and Bat Compression Technique.

sacrificing durability. Similar to the Hammering process, a complete vising procedure will include rotating the bat between successive compressions in order to break-in the bat in a uniform manner.

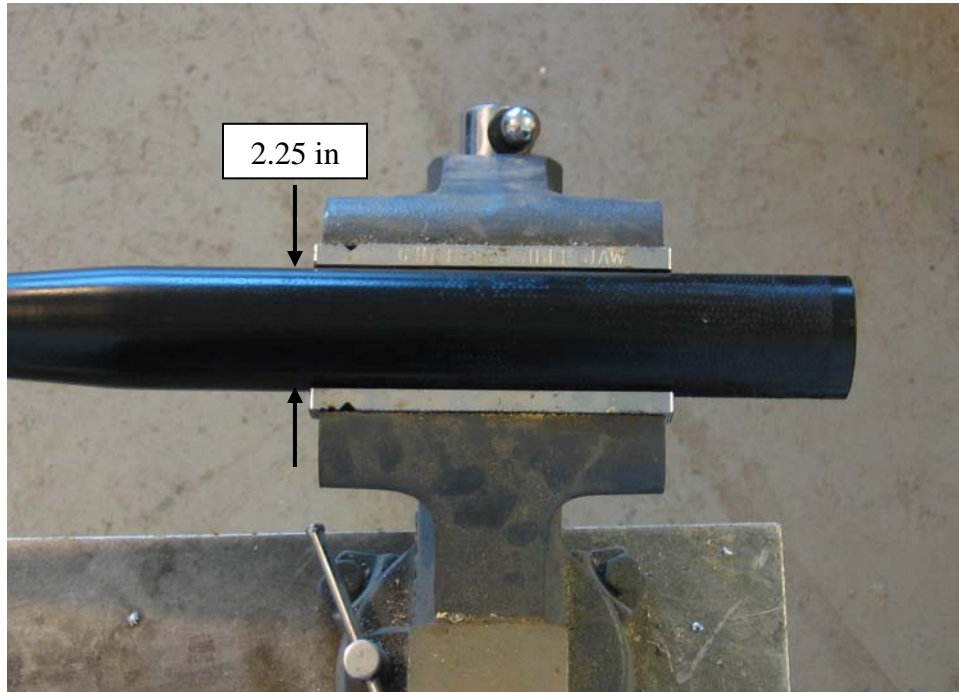


Figure 2.17a - Composite Bat in a Vise

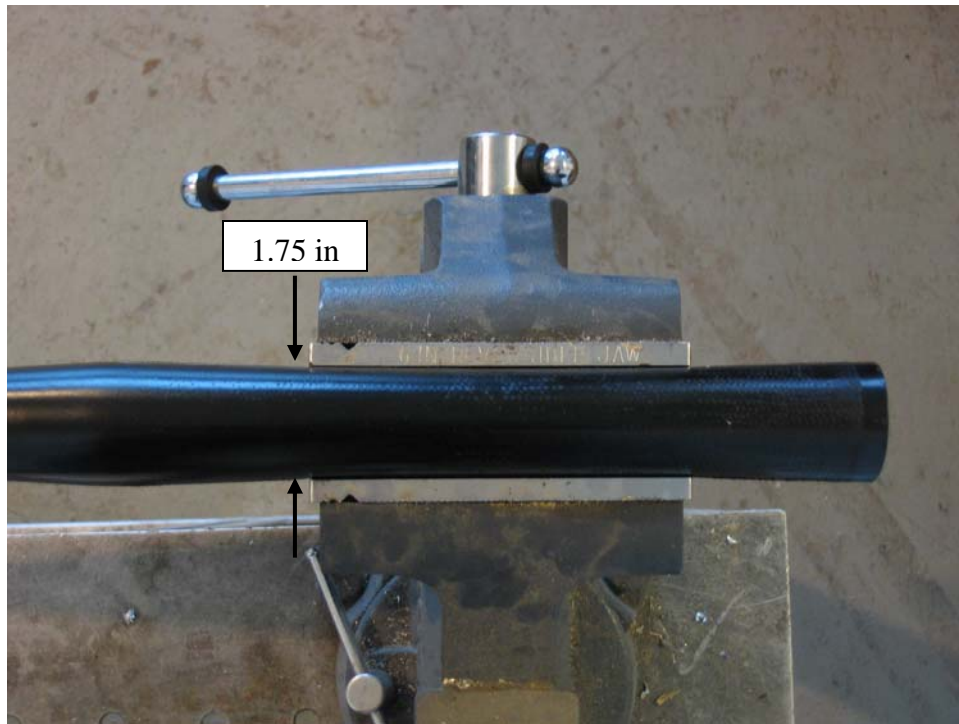


Figure 2.17b - Composite Bat Compressed in a Vise

Bats that have undergone ABI processes experience decreased durability and improved performance that are both proportional to the severity of the ABI process. The more severe the process, the more performance will increase and the lower durability will be.

Proponents of ABI processes claim they should not be considered doctoring methods because they are equivalent to hitting thousands of balls with a particular bat. In this study, bats that have undergone ABI treatments are considered to be doctored because the bats' physical properties have been unnaturally altered in an attempt to improve the bats' performance. The claim that ABI processes are equivalent to NBI processes has been investigated in this study. Due to the fact that hammering bats induces bat stresses less than those generated when a player actually hits a ball, the effects of hammering have not been studied in this research.

2.5.5 Bat Painting

Bat painting describes the process of painting a bat whose performance exceeds certification standards to look like a certified bat. This is done so that high performing, uncertified bats, such as titanium bats, can be used in leagues which would normally not allow them.

The procedure for painting a bat includes removing its stock graphics, and replacing them with replications of graphics that can be found on certified bats. The major difficulties in painting bats are dampening the characteristic “ping” noise made by titanium bats, finding a paint that can stand up to the extreme flexing the barrel walls experience, and using the best graphic reproductions. If these issues are not properly addressed, painted bats can be easily identified. As a result, most players do not paint their own bats; they have them done by one of three well known bat painters in the United States.

2.6 Bat Models

The ability to compare direct and indirect performance measurements to computer simulations is useful to verify that measured results follow logical trends. In addition, computer modeling is both practical and useful for analyzing difficult to measure events, such as the bat-ball collision. Herein, computer modeling will be used to verify modal analysis measurements of various bat constructions and to study the effects of bat altering on indirect performance characteristics.

To date, a relatively small number of articles describing FE modeling of bats have been published. Smith [2.31] modeled the bat and ball collision of a wood and a single wall aluminum bat, paying close attention to the stress levels generated in the bat as a

result of the collision and the post-impact rebound speed of the ball. In his work, Smith used 8-node solid elements to represent the wood bat and 4-node shell elements to represent the aluminum bat. The stress levels and ball rebound speeds predicted in numerical simulations were consistent with experimentally measured values.

In a more recent publication, Nicholls [2.32] modeled the bat ball collision and focused her analysis on post-impact ball velocity. In her work, Nicholls also modeled a wood and a single wall aluminum bat; both of the bats were modeled using 8-node solid elements. Results of Nicholls' numerical simulation also agreed well with experimental data.

Another finite element model investigating the bat ball collision has been developed by Mustone [2.33]. As in the previously described studies, Mustone also modeled a wood and a single wall aluminum bat. Mustone used 8-node solid elements in his wood bat model, and 4-node shell elements in the aluminum bat model. Prior to his investigation of the bat ball collision, Mustone calibrated his bat models by conducting an eigenvalue analysis on them and comparing the results to measured values obtained using modal analysis techniques. In this analysis, only the frequencies of the first two flexural bending mode shapes are reported for both bat models, and all numerical results are within 8% of experimentally measured frequency values. In addition to achieving a strong correlation between simulated and measured dynamic bat properties, bat performance data from Mustone's impact model also correlated well with measured performance values.

Irvine [2.34] has conducted research in which the vibrational response of a wood and a single wall aluminum bat have been modeled with finite element software. In his

model, the wood bat was modeled using 8-node solid elements and the aluminum bat was modeled using a combination of shell and solid elements. In addition to reporting the natural flexural frequencies of both bats, Irvine also reported the hoop mode frequencies of the aluminum bat. Though the values obtained in his numerical simulation seem reasonable, their accuracy of cannot be commented on because no comparison with measured vibration data was provided.

2.7 Summary

The focus of this chapter has been to review the current research relevant to baseball and softball bats. In doing so, bat testing methods and performance metrics have been examined and compared. Indirect performance characteristics have also been defined and reviewed with an emphasis on their relation to performance trends. Computer modeling of bats has been investigated and was found to correlate well with measured characteristics. Finally, the most common bat doctoring methods have been defined and discussed.

In the following chapters the previous topics will be expanded upon utilizing techniques such as performance testing, barrel compression, modal analysis, and computer modeling. Extensive studies regarding bat doctoring efficiency and the bat-ball collision have been carried out and will be reviewed, and a computer model will be used to verify the results.

REFERENCES

- 2.1 Smith, L. V., *Why ASTM F2219?* SGMA Annual Meeting, Dallas, TX. October 2, 2003.
- 2.2 Naruo, T., and F. Sato. *Performance of baseball bats*. Proceedings of 5th Japan International Society of Advanced Material Processes. Engineering Symposium, (1997): 1311-1316.
- 2.3 Brooks, R., S. Knowles, and J.S.B. Mather. *Design and construction of a high performance composite cricket bat*. Proceedings of ICCM-11. Gold Coast, Australia. July 1997.
- 2.4 Nishiwaki, T. *Designing of CFRP baseball bats*. SAMPE Journal. 38.2 (March/April 2002) : 80-82.
- 2.5 Russell, D. *Indirect performance measures*. Proceedings from Bat Ball 102. Pullman, WA. June 29-30, 2004.
- 2.6 Nathan, A., D. Russell, and L. Smith. *The physics of the trampoline effect in baseball and softball bats*. Proceedings of ISEA 2005. Davis, CA. September 2004.
- 2.7 Noble, L., and J. Eck. *Effects of selected softball bat loading strategies in impulse reaction impulse*. Medicine and Science in Sports and Exercise. 18.1 (1986) : 50-58.
- 2.8 House, G. *Chapter 10: Baseball and softball bats*. Sports and Fitness Equipment Design. Ed. E. Kreighbaum. Human Kinetics Publishers, 1995. ISBN: 087322695X.
- 2.9 Adair, R. The Physics of Baseball. Third Edition. Perennial: New York. 2002. ISBN: 0060084367.
- 2.10 Bahill, T., and W. Karnavas. *The ideal baseball bat*. New Scientist. April, 6 1991 : 26-31.
- 2.11 Bahill, T. *The ideal moment of inertia for a baseball or softball bat*. IEEE Transactions on Systems, Man, and Cybernetics-Part A: Systems and Humans. 34.2 (March 2004) : 197-204.
- 2.12 Nicholls, R., et al. *Bat kinematics in baseball: implications for ball exit velocity and player safety*. Journal of Applied Biomechanics. Vol. 19 (2003) : 283-294.

- 2.13 Fleisig, G., et al. *Relationship between bat mass properties and bat velocity*. Sports Engineering. Vol. 5 (2002) : 1-8.
- 2.14 Smith, L. V., J. Broker, A. Nathan. *A Study of Softball Player Swing Speed*. Sports Dynamics Discovery and Application. Melbourne, Australia (2003): 12-17.
- 2.15 Smith, L. V. *Oklahoma Fastpitch Softball Field Study*. NCAA Softball Rules Committee. November 18, 2004.
- 2.16 ASTM F2219-02e1. *Standard test methods for measuring high speed bat performance factor*. West Conshohocken, Pa. 2003.
- 2.17 ASTM F 1890-02. *Standard test method for measuring softball bat performance factor*. West Conshohocken, Pa. 2003.
- 2.18 F 1887-02. *Standard test method for measuring the coefficient of restitution of baseballs and softballs*. West Conshohocken, Pa. 2003.
- 2.19 Nathan, A. *Characterizing the performance of baseball bats*. American Journal of Physics. Vol. 71 (2002) : 134-143.
- 2.20 NCAA News Release. *NCAA provisional standard for testing baseball bat performance*. September 27, 1999.
- 2.21 Smith, L. *Evaluating baseball bat performance*. Sports Engineering. Vol. 4 (2001) : 205-214.
- 2.22 *Procedure for measuring the flexibility of a golf clubhead*. Revision 1.0 December 1, 2003. <http://www.usga.org>
- 2.23 Avitabile, P. *Experimental modal analysis – a simple non-mathematical presentation*. Sound and Vibration, February 2001.
- 2.24 Thomson, W. Theory of Vibration with Applications. Second Edition. Prentice-Hall: New Jersey. 1981. ISBN: 0139145230.
- 2.25 PCB Model 086C02 Spec Sheet. March, 8 2005. <http://www.pcb.com>
- 2.26 Smith, D. Vibration Measurement and Analysis. Butterworth and Co.: New York. 1989. ISBN: 0408041013.
- 2.27 Harris, C., ed. Shock and Vibration Handbook. Fourth Edition. McGraw Hill: New York. 1996. ISBN: 0070269203.
- 2.28 Russell, D. Kettering University. *Private communication*. March, 2005.

- 2.29 Craig, R. Mechanics of Materials. Second Edition. John Wiley and Sons: New York. 2001.
- 2.30 Russell, D. *Indirect Performance Measures*. Presentation at Bat-Ball 102 symposium. Pullman, WA. 2004.
- 2.31 Smith, L. V., Shenoy, M., Axtell, J.T. *Simulated composite baseball bat impacts using numerical and experimental techniques*. Abstract Proceedings of the Society for Experimental Mechanics. Spring Conference 2000. Orlando, FL.
- 2.32 Nichols, R. *Mathematical modeling of bat-ball impact in baseball*. Diss. University of Western Australia. 2003.
- 2.33 Mustone, T., J. Sherwood. *Using LS-DYNA to develop a baseball bat performance and design tool*. Proceedings of 6th international LS-DYNA Users Conference. Detroit, MI. April 2000.
- 2.34 Irvine, T. *Baseball bat sound and vibration*. Vibration data newsletter. December 2001. www.vibrationdata.com/Newsletters/December2001_NL.pdf

CHAPTER THREE

- BAT MODIFICATIONS -

3.1 Bat Doctoring Study

With the advent of a bat testing procedure that accurately ranks bats closely to their on-field performance and the implementation of a reduced performance limit, many softball players have turned to using altered bats in order to gain an advantage over their opponents. The bat alteration methods most commonly used include wall shaving, weighting, and various ABI techniques.

In this study, which will be referred to as the Doctoring Study, direct and indirect performance measurements were conducted on altered bats in order to determine the effect of the alterations. In addition, NBI bats were tested in order to determine how the performance of an unaltered bat evolves with normal to extensive use. Finally, painted bats were investigated by comparing them to the bats they are trying to imitate.

The procedure for the Doctoring Study included purchasing 26 ASA certified softball bats and three popular bats that exceed the ASA performance standard. These 29 bats did not all have the same construction; 19 were multi-wall composite, eight were multi-wall aluminum, one was single wall aerospace grade aluminum, and one was a traditional wood bat. Herein, these bats will be referred to by a bat code of the form XY##; where X describes the construction style of the bat (S for single wall, M for multiple-wall), Y describes the material the bat is made of (A for aluminum, C for composite). The lone wood bat will be referred to as “wood.” One bat was chosen to be used as a standard bat to verify the consistency of the indirect performance measurements, it was a multiple-wall composite bat referred to as “std bat.” The std bat was tested intermittently for

barrel compression and vibration characteristics. Both modal analysis and barrel compression were found to be very repeatable with standard deviations of less than 1.5%. Data from the control bat can be found in Appendix 2. Table 3.1 is a list of all of the bats included in this study.

Table 3.1 – List of all bats included in the bat doctoring study.

Bat Code	Alteration method	Bat Code	Alteration method
MA01	Shaved	MC08	Shaved
MA02	Shaved	MC09	Shaved
MA03	Shaved	MC10	Rolled
MA04	Shaved	MC11	BCT
MA05	Weighted	MC12	ACT
MA06	Shaved	MC13	Viced
MA07	Shaved	MC14	Converted to Freak
MA08	NBI	MC15	Converted to Freak 98
MC01	Weighted	MC16	Converted to Velocite 2
MC02	Shaved	MC17	NBI
MC03	Shaved	MC18	NBI
MC04	Rolled	Std Bat	None
MC05	BCT	SA01	Weighted
MC06	ACT	Wood	Weighted
MC07	Viced		

Upon receipt of the bats, indirect performance measurements of each were made using modal analysis (to determine flexural and hoop frequencies) and barrel compression (to determine barrel stiffness). Next the performance of the bats was tested following a procedure similar to that which is outlined in ASTM F 2219. The performance testing procedure for the doctored bats differed in that three balls, instead of six, were used per bat. The balls used on each bat were organized such that each time the bats were tested the identical balls were used. In addition to controlling the balls used on each bat, the bats were oriented in a consistent manner in the test fixture to ensure that the identical bat locations were impacted during testing. After performance testing, indirect

performance tests were again performed and the bats were then divided into four groups; the structural group, weighted group, the NBI group, and the painted group.

The structural group included 18 bats (12 multi-wall composite and six multi-wall aluminum) and encompassed all of the bats that underwent wall shaving and ABI processes. Each of the bats was sent to one of 11 well known bat doctors to be modified. The bat doctors were chosen after numerous (no fewer than 16) well known doctors had been identified through clandestine research conducted on various internet softball websites and forums. The bat doctors were solicited for work without revealing that the modified bats were for research purposes to assure that the modified bats were representative of bats that could be obtained for use by an average player.

Four of the 12 composite bats were to be barrel shaved, while pairs of the remaining composite bats underwent the ABI processes Rolling, BCT, ACT, and Vising. After the bats had been modified, their indirect and direct performances were measured. Finally, after the bats were performance tested, their indirect performances were measured again. A flowchart depicting the process for the doctored bat group testing procedure can be found in Appendix 3.

The weighted bat group consisted of four bats; a wood bat, single wall aluminum bat, multiple-wall aluminum bat, and a multiple-wall composite bat. After initial testing, these bats were weighted such that their stock moment of inertia was increased 20%. This was accomplished by attaching lead tape and/or lead tire weights to the distal end of the bats.

The amount of weight necessary to increase the bats' moments of inertia 20% was calculated using a form of the parallel axis theorem,

$$W_a = \frac{\left(\frac{MOI_d}{MOI_i} \right)}{(d)^2}, \quad (3.1)$$

where W_a is the weight addition necessary to achieve the desired MOI, MOI_d is the desired MOI, MOI_i is the initial MOI, and d is the distance from the pivot point of the bat to the location of weight addition. The MOI of a bat with the weight attached was measured directly utilizing the MOI stand described in chapter two to verify the prediction and the ability to add the appropriate amount of weight to the bats. After the weight had been added, the BBS of each bat was determined; these measurements were followed by another set of indirect performance measurements which were conducted with the additional weight still attached to the bats.

The NBI group included three bats, two multiple-wall composite bats and one multiple-wall aluminum bat. After they were initially tested, the NBI bats were each hit 500 times with ASA certified .44 COR, 375 lb compression balls in an indoor batting cage. The bats were swung by mostly experienced softball and baseball players, and all of the pitches were of the slow-pitch variety.* Figure 3.1 shows the batting cage used for the NBI group of bats. After each bat had accumulated 500 impacts, the bats were tested using indirect performance tests and then direct performance tests. These tests were followed by 500 more hits on each bat and another round of indirect and direct performance measurements. This cycle was continued until each bat had been hit 2000 times. A flowchart depicting the NBI group test procedure can be found in Appendix 4.

The painted bats group included the three multiple-wall composite bats which exceeded the 2004 ASA performance limit. These bats were not ever tested for BBS as

* A slow-pitch style pitch describes a ball thrown underhand that follows an arc between 6 and 12 feet before crossing the plate in the batter's strike zone [3.1].

they are considerably more fragile than the other bats included in the study and often do not survive the direct performance test. As a result, the only tests conducted on the painted bats were visual inspections and indirect performance tests. The purpose of the visual inspections were to determine how accurate the painted bats were compared to actual bats. The purpose of conducting indirect performance measurements was to verify that the bats returned to us by the bat doctors were in fact the bats we had sent to them.

The following sections will discuss how the characteristics of each of these bats changed as a result of their modifications. Although indirect performance characteristics were measured at four different times during the life of most of the bats in the Bat Doctoring Study, most of the results are plotted showing only two of these data points as the bat characteristics before the first BBS scan and after the second BBS scan are superfluous in demonstrating the effect that the bat alterations have had. A table containing all of the data from the Bat Doctoring Study is provided in Appendix 5.



Figure 3.1 – Batting cage used for NBI bat group

3.2 Results

3.2.1 Structural group - shaved bats

All of the composite and aluminum bats that were shaved in this study showed measurable changes in barrel stiffness (as measured by barrel compression tests), hoop frequencies and performance (as measured by BBS). None of the shaved bats showed an appreciable change in flexural vibration, including the bats that had undergone handle shaving in addition to barrel shaving. Most of the bats' moments of inertia did not change significantly due to the work done by the bat doctors, although two did, MC03 and MC09, because one of the bat doctors endloaded the bats in addition to shaving them.

The average change in MOI of the shaved bats, excluding the two bats that had been endloaded (MC03 and MC09) was an increase of 2.3%. The slight increase in MOI is likely the result of bat doctors attempting to maintain a bat's original weight by adding weight to the end caps to make up for the weight loss resulting from the shaving process.

Figure 3.2 shows the MOI changes in all of the shaved bats.

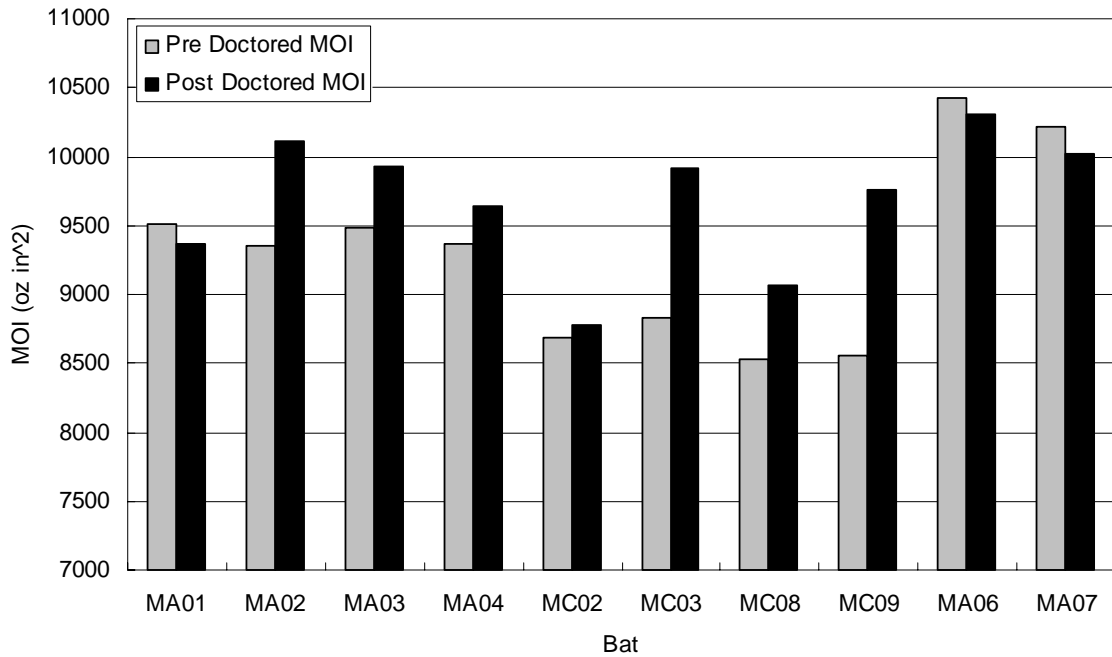


Figure 3.2 - MOI Changes due to Shaving

As mentioned before, the flexural vibration characteristics of the shaved bats did not change an appreciable amount, with even the largest change being less than 1.5%. Figure 3.3 shows the first resonant flexural frequency of the shaved bats before and after doctoring.

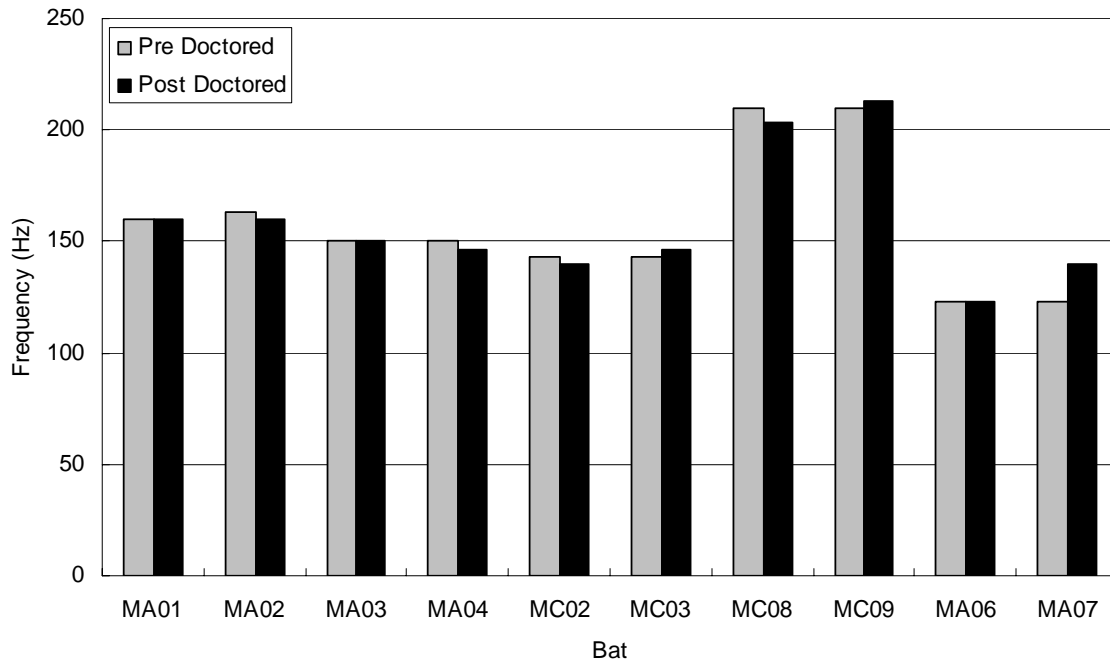


Figure 3.3 – Flexural Frequency Changes due to Shaving

The bats that were shaved showed an average decrease of 5% in their measured first natural hoop frequency between the time when they were sent to the doctor and when they were received from the doctor. The standard deviation of hoop frequency changes was 2%. Figure 3.4 shows how each shaved bat's hoop frequency changed as a result of the shaving process.

The shaved bats showed an average stiffness decrease (as measured by barrel compression) of 8% from the time when the bats were sent to doctors until they were returned. The standard deviation for barrel stiffness changes was 8%, which is comparatively higher than it was for hoop frequency. This suggests that tests for barrel stiffness using barrel compression methods may be more sensitive than stiffness tests using modal analysis. Figure 3.5 shows how the barrel stiffness of each shaved bat changed as a result of the doctoring process.

In discussing the performance changes due to wall shaving, it was useful to look at the composite and aluminum bats separately. The composite bats improved in BBS performance on average 6.4 mph (or 7%) with a standard deviation of 1.0 mph (or 1%), while the aluminum bats performance increased an average of 2.5 mph (or 3%) with a standard deviation of 1.0 mph (or 1%). Figure 3.6 shows the performance increase of each of the shaved bats.

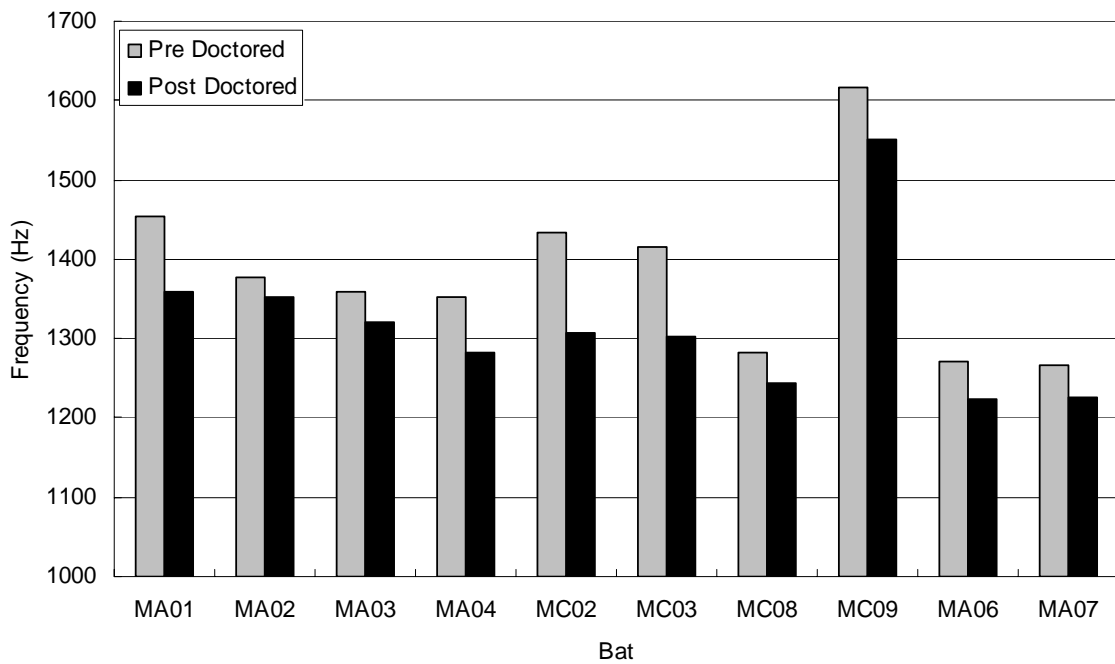


Figure 3.4 – First Resonant Hoop Frequency Changes due to Shaving

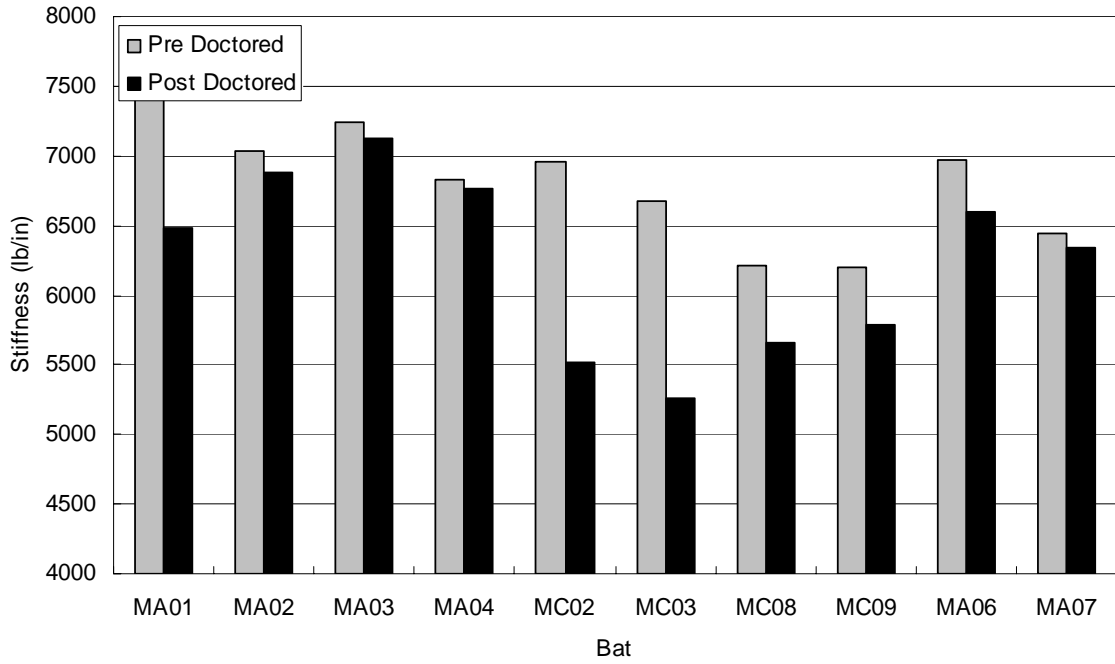


Figure 3.5 - Barrel Stiffness Changes due to Shaving

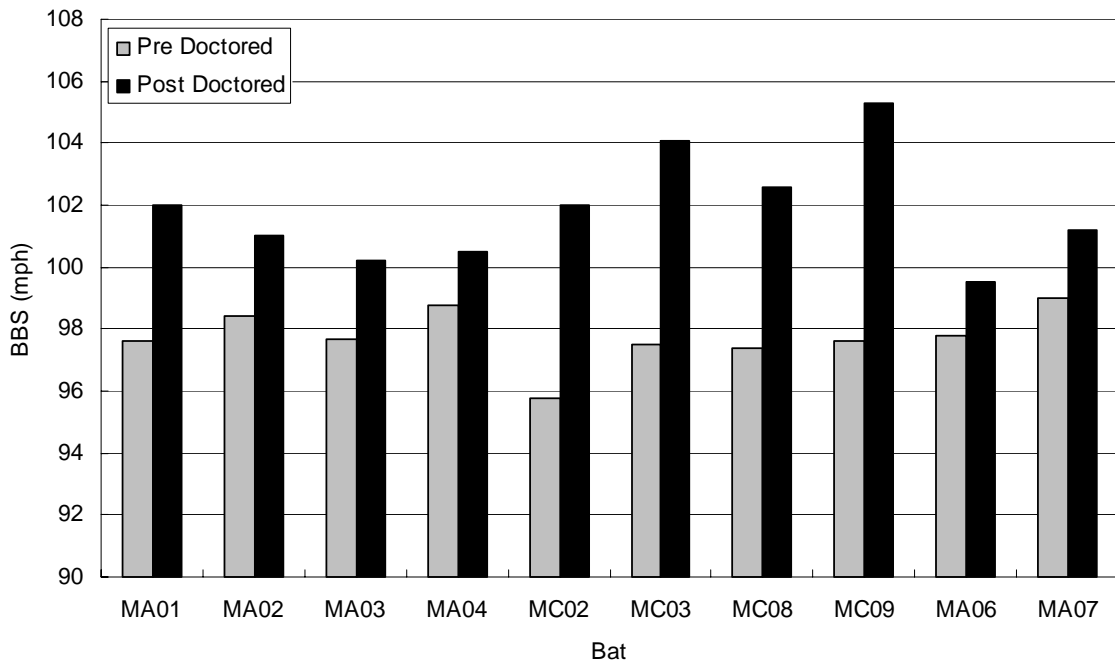


Figure 3.6 - Performance Changes due to Shaving

3.2.2 Structural group - ABI bats

Like the shaved bats, the eight bats that were sent out for ABI treatments did not experience significant changes in either MOI or flexural stiffnesses, in fact none of the first resonant flexural frequencies experienced measurable changes. Figures 3.7 and 3.8 show these trends. Bat MC13 showed an unexpected drop in MOI of 4.0%, and because its mass and balance points remained consistent, the error is attributed to experimental variation.

The first natural hoop frequencies of the ABI bats tended to decrease as a result of the ABI processes. The hoop frequency decreases ranged from essentially no change (0.5%) to 21.6%, and one bat's hoop frequency increased 11.9%. The changes in the hoop frequency of these bats due to ABI treatments are shown graphically in figure 3.9.

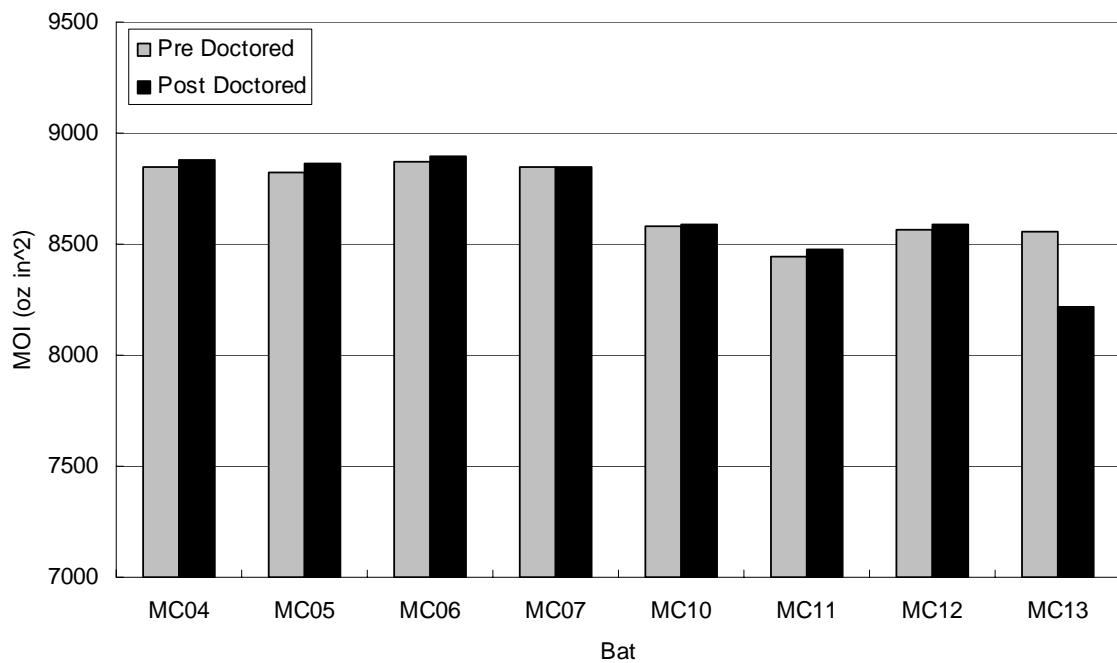


Figure 3.7 - MOI changes due to ABI processes

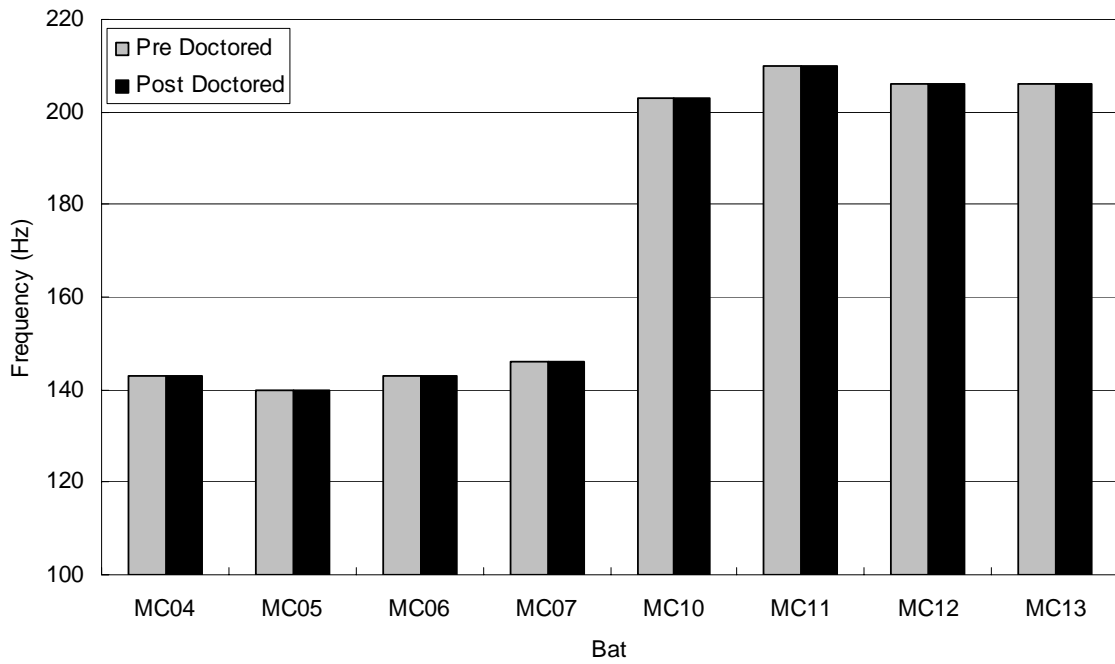


Figure 3.8 – Flexural Frequency Changes due to ABI Processes

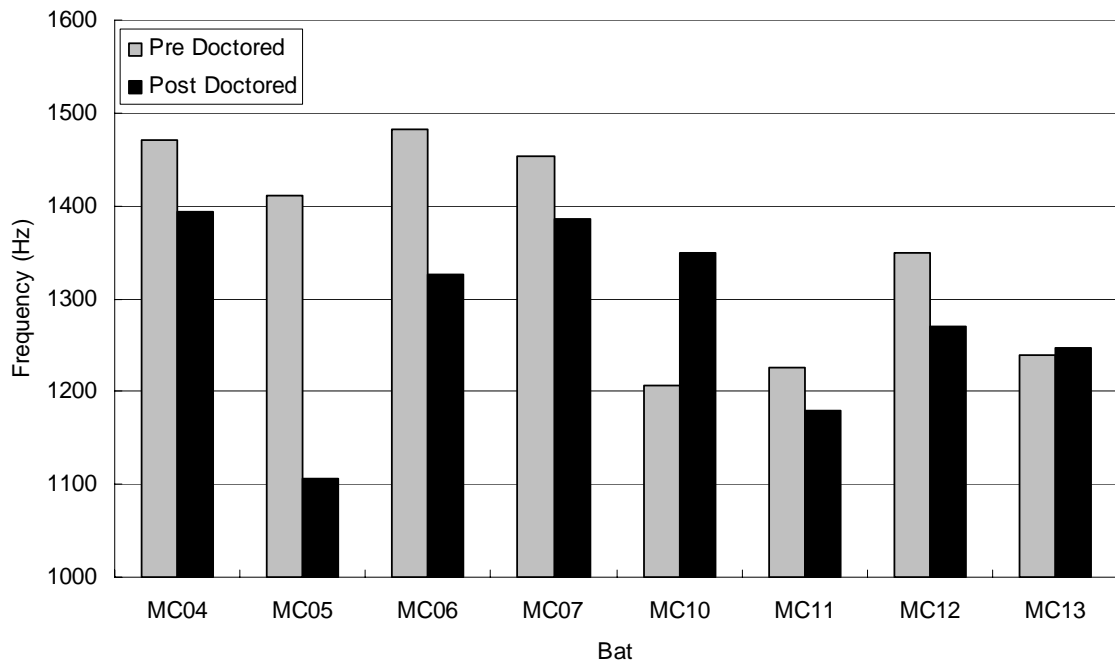


Figure 3.9 - First Resonant Hoop Frequency Changes due to ABI Processes

As expected, most of the ABI bats' barrel stiffnesses also decreased after the bats had been modified. The stiffnesses decreased from 1% to 54%, with three bats decreasing more than 18% and the other five bats decreasing less than 7%. The changes in barrel stiffness due to the ABI processes can be seen in figure 3.10.

Although the performance of all of the ABI bats increased, the magnitude of these gains varied a great deal. The performance increases ranged from 0.66 mph (or 0.66%) to 8.28 mph (or 8.53%) and seemed to be related to the severity of the process the bats underwent. For example, the bat whose performance increased the most had visible signs of damage as a result of the “proprietary” ABI technique, BCT. The performance increases in all ABI bats are shown in figure 3.11, and an example of a bat which shows significant damage due an ABI process (the BCT process) is shown in figure 3.12.

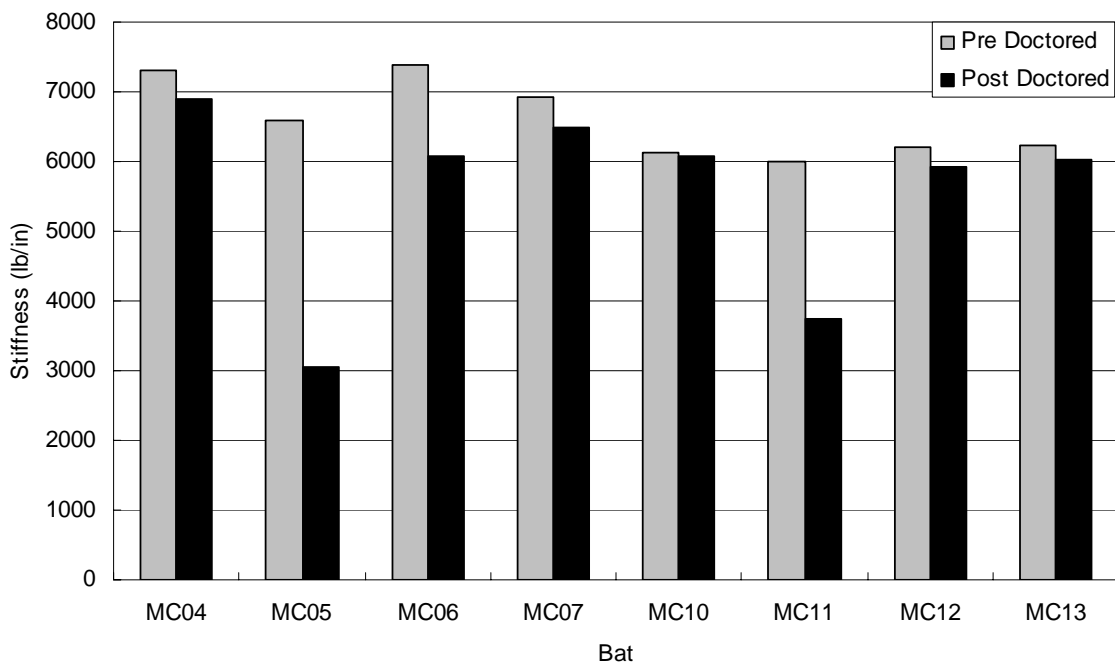


Figure 3.10 – Barrel Stiffness Changes due to ABI Processes

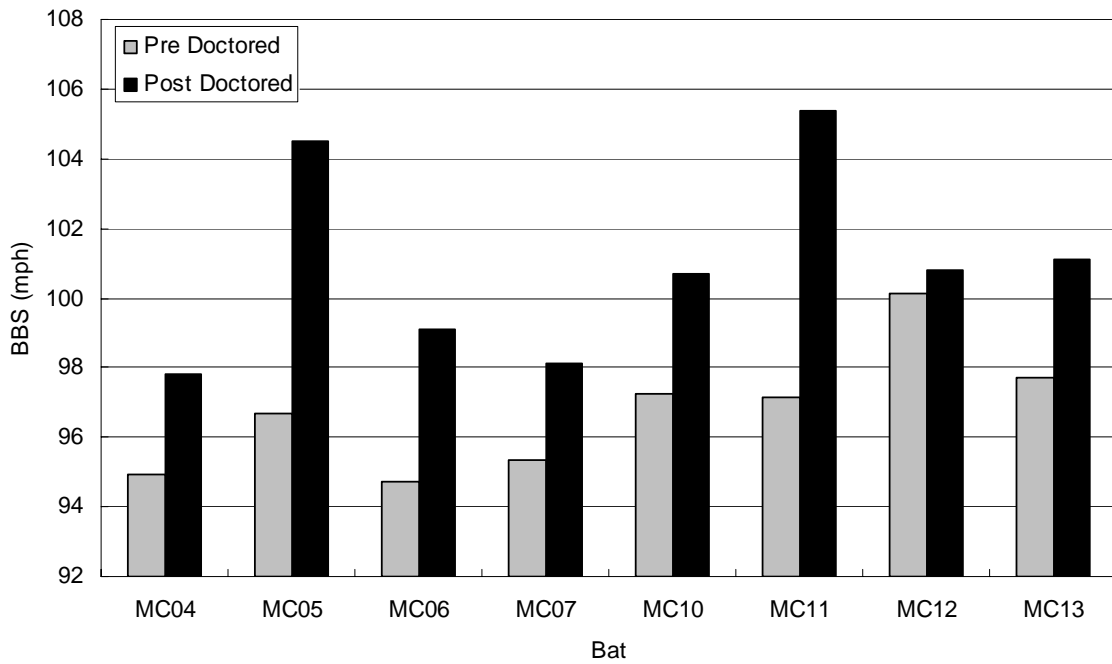


Figure 3.11 - Performance Changes due to ABI processes



Figure 3.12 - Visible Damage Resulting from BCT Treatment

The results from the structural bats group clearly shows that there are a number of bat alteration methods which can improve bat performance. It appears that shaving composite bats yields a greater performance advantage than shaving aluminum bats. This

may be due to the fact that stock aluminum bats are closer to their maximum performance/acceptable durability limit than stock composite bats. For example, more material cannot be removed from the aluminum bats because they would become too fragile. Furthermore, this would imply that the aluminum bats of today cannot be made to perform at levels as high as can be achieved with composite bats.

Experimental results also indicate that ABI processes have a wide range of effectiveness. Depending on the severity of the process, bat performance can change moderately or significantly. For example, vising bats past their axiomatic limits should result in larger performance gains than were seen in our study [3.1].

When comparing indirect performance measures, it becomes apparent that their values scale with improved performance, but not in an entirely predictable manner. For example, table 3.2 shows the errors that would arise if one attempted to rank the performance of the ABI bats based on either hoop frequency or barrel stiffness. A likely explanation for why bat performance cannot be predicted by either hoop frequency or barrel stiffness alone is that bat performance is a function of more than just barrel compliance. The other factors that affect performance will be discussed in Chapter 4.

Table 3.2 – Performance Rankings Based on Indirect and Direct Performance Measures

Performance Ranking Methods			
	<i>Hoop Frequency</i>	<i>Barrel Compression</i>	<i>BBS</i>
<i>Highest Performing</i>	MC05	MC05	MC11
	MC11	MC11	MC05
	MC13	MC12	MC13
	MC12	MC13	MC12
	MC06	MC10	MC10
	MC10	MC06	MC06
<i>Lowest Performing</i>	MC07	MC07	MC07
	MC04	MC04	MC04

3.2.3 Naturally Broken In Group

The NBI bats exhibited distinct trends in both direct and indirect performance measures as a result of their break in procedure. The performance of all of the bats in the study increased significantly after 500 impacts and essentially maintained that same elevated performance level through the 2000 impacts in the study. It should be noted that none of the bats in the study developed any visible signs of damage such as cracking or denting due to the repeated impacts.

The indirect performance trends were found to be dependent on the material of which the bat was made. Because there were only three bats tested in the study, it is impossible to determine if the observed trends would apply to a much larger sampling of bats. One trend observed in all bats was that flexural frequencies remained constant through the study – this trend can be observed in figure 3.13.

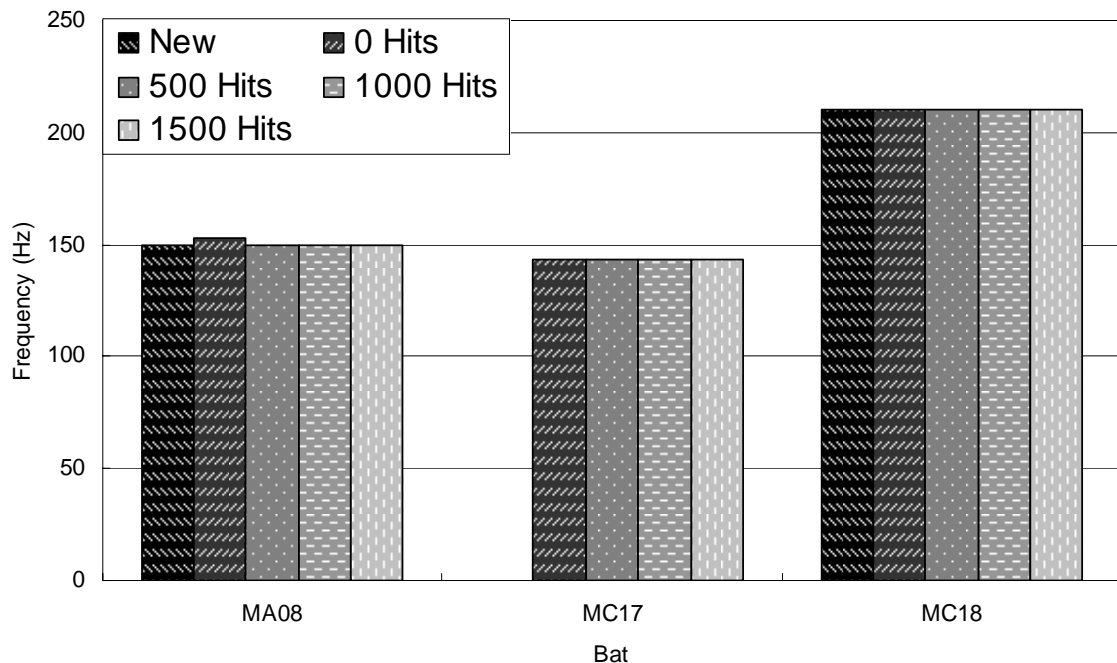


Figure 3.13 – Flexural frequency trends due to natural break in methods

The MOIs of the NBI bats were only measured prior to initial performance testing because no weight was added to or removed from the bats. As a result, the same MOI values were used in the BBS calculations for each round of performance tests. This allowed for the truest assessment of performance change as it prevented the experimental variation in measured MOI from introducing error into the BBS calculations.

Figure 3.14 shows how the performance of the NBI bats evolved during the study. After the first 500 impacts each bat improved an average of 2.90 mph (or 3.02%). Additional impacts were not observed to have a significant effect on further performance changes.

The composite bats' barrel stiffnesses were found to decrease with increased hits, seemingly converging to some nominal, bat-dependent value. The multiple-wall bat's barrel stiffness followed a low order exponential increase, which also seemed to approach a bat-dependent nominal value. These trends are shown in figure 3.15.

The hoop frequencies of the composite bats decreased with increased hits, seemingly converging to a bat-dependent value. The multiple-wall aluminum bat's hoop frequency also decreased with increasing impacts, although the decrease followed a much shallower slope than the composite bats. The aluminum bat's hoop frequency also seemed to converge to a specific value. The trends in hoop frequency are shown in figure 3.16.

Due to the fact that the NBI bats' MOI's remained constant through the study, it is assumed that any observed performance increase was a result of a dramatic decrease in barrel stiffness – which would enhance performance by improving the trampoline effect. In this case, the indirect performance measures, which often scale with the trampoline effect, would not be an accurate performance predictor for the bat, as the barrel

compression and hoop frequency behaved in inconsistent manners. The two indirect performance measures of the composite bats followed the expected trends.

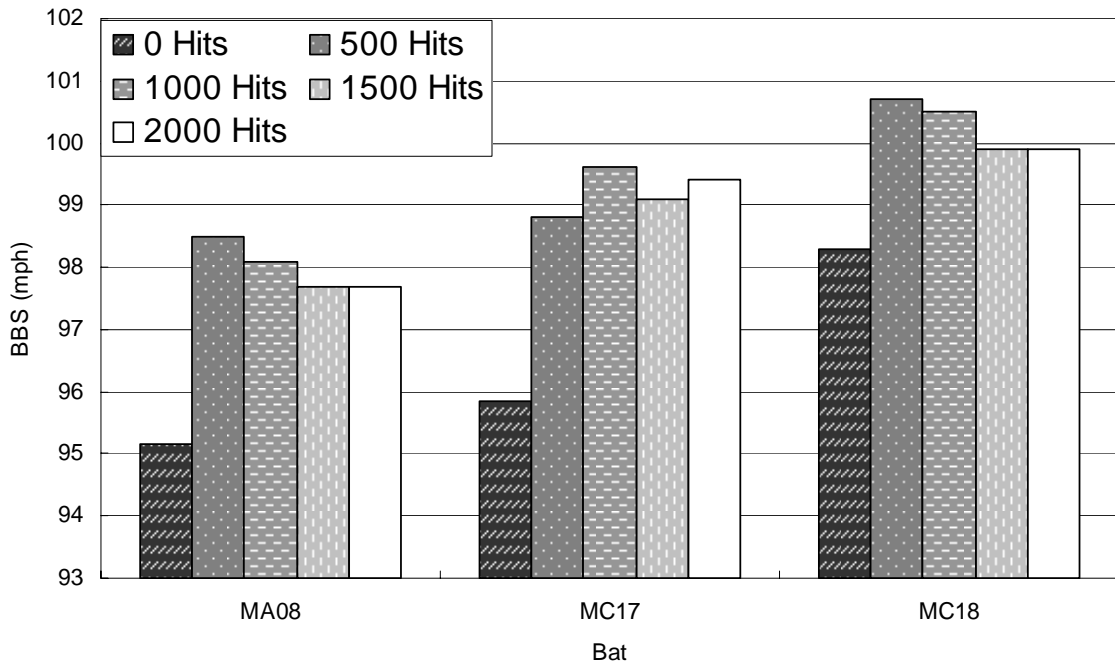


Figure 3.14 – BBS trends due to natural break in methods

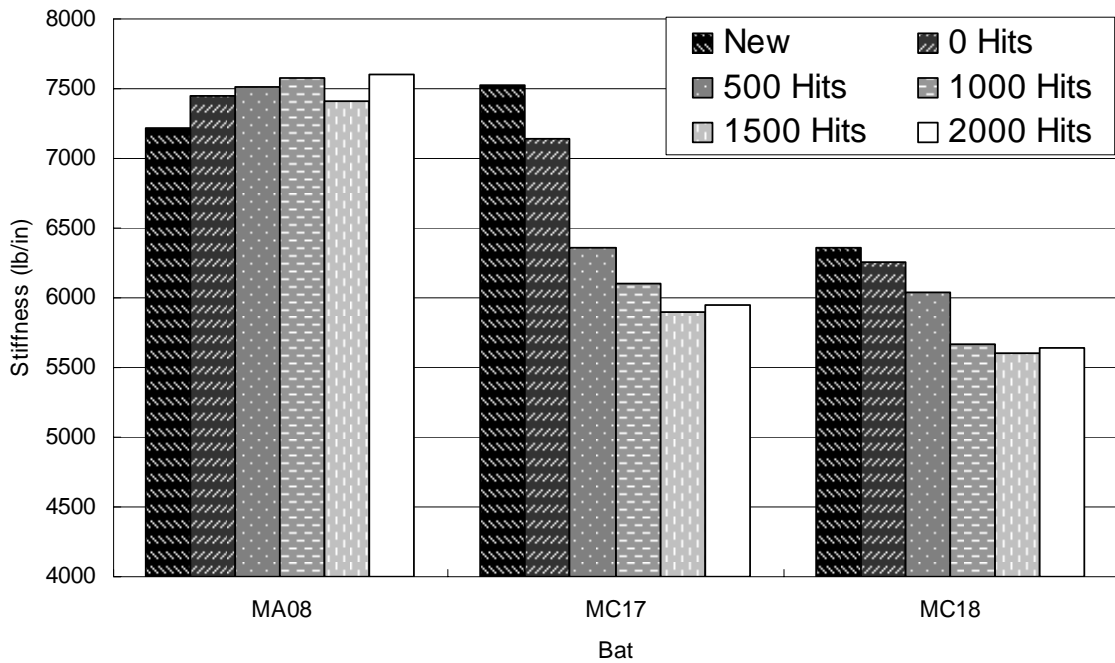


Figure 3.15 – Barrel stiffness trends due to natural break in methods

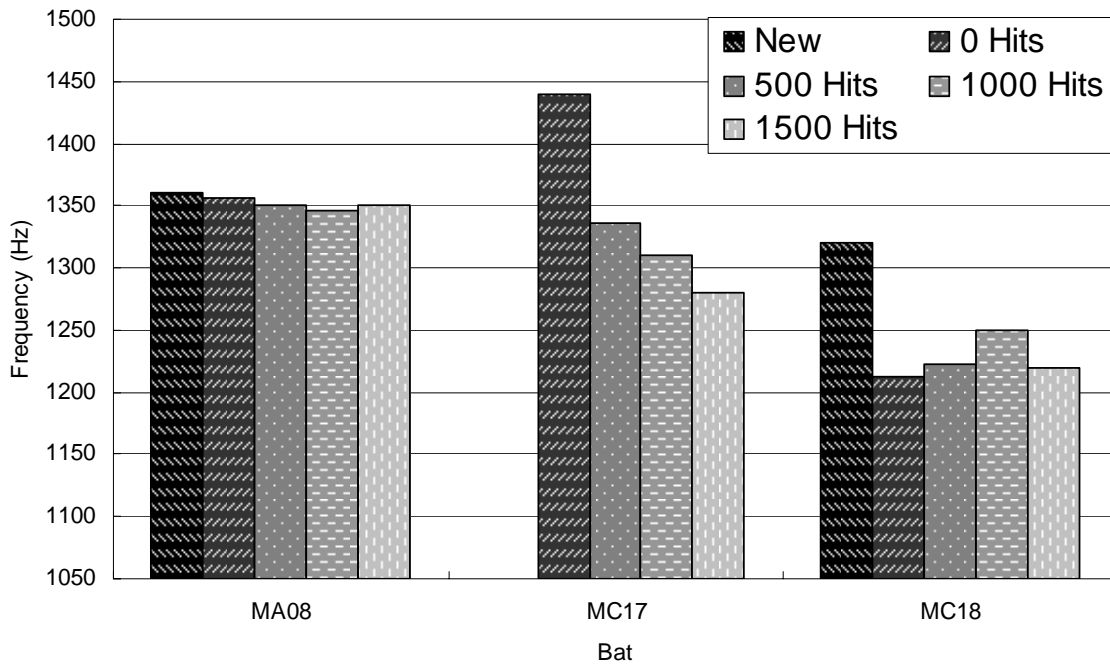


Figure 3.16 – Hoop frequency trends due to natural break in methods

3.2.4 Weighting group

The bats chosen for the weighting group represent the four most common bats currently in use; multiple-wall composite, multiple-wall aluminum, single-wall aluminum, and solid wood. These bats’ direct and indirect performance levels were tested before and after their stock MOI’s were increased by 20%.* The MOI was increased by adding weight to the distal end of each bat, in an attempt to simulate loading strategies used by the popular bat doctors. Figure 3.17 shows how weight was added to the bats. The actual amount of weight added to each bat can be found in Appendix 6.

* A 20% increase in MOI was chosen because in a previous study a bat whose MOI had increased nearly 20% experienced significant performance gains.



Figure 3.17 - Method of Increasing MOI of Weight Group

As expected, neither the barrel stiffness or hoop frequency changed in any of the bats as a result of the increased MOI. Vibrational data for the flexural frequencies of the bats proved inconclusive; the effect of various loading strategies on flexural frequencies will be examined in more detail in Chapters 4 and 5.

The performance of all the bats increased an average of 2.72 mph (or 2.95%) and can be seen in figure 3.18. Possible causes for the performance increases and changes in dynamic properties will be discussed in Chapter 4, when the effects of added weight on performance and bat characteristics will be investigated in more detail.

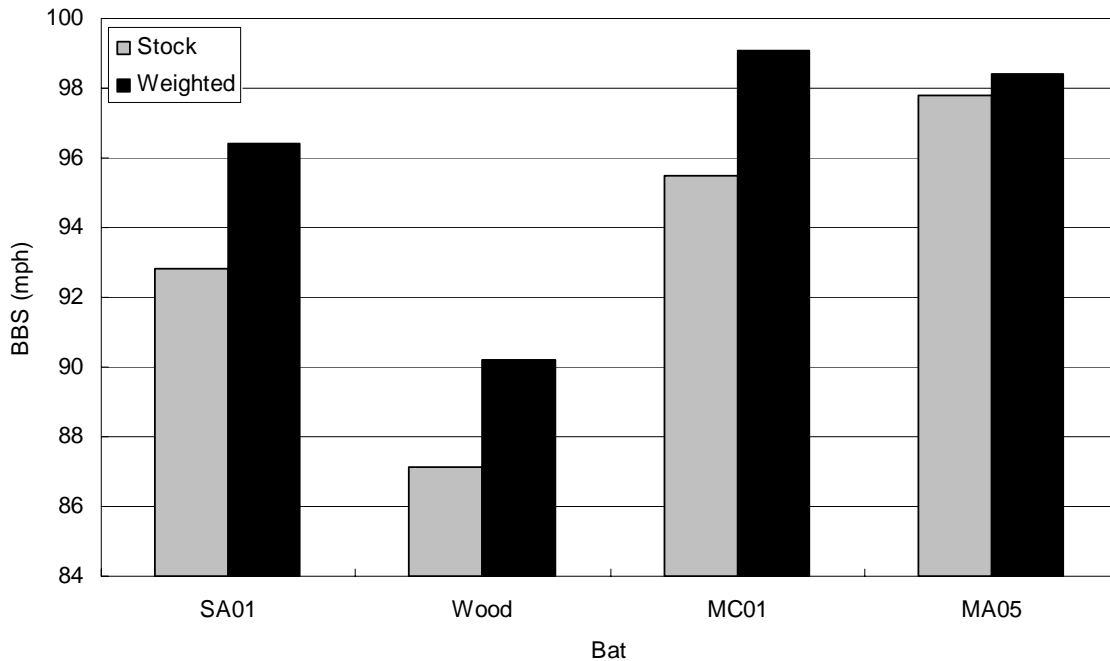


Figure 3.18 - Performance Changes due to End Loading

3.2.5 Painted group

While the visual inspection of the painted bats is a subjective process, figures 3.19-3.27 demonstrate that bat doctors can convert bats with enough skill to fool, at the very least, most casual observers. The pictures compare the stock bats, painted bats, and the imitated bats. In addition, the end caps and knobs of each bat are compared. In the case of most of the bats, the decals used for the most prominent graphics on the bat look nearly identical to the graphics used on the real bats. Often, converted bats can stand out because these graphics have been poorly applied and their edges appear to be raised off of the surface of the bat, or because the text fonts and resolutions are not a perfect match. Occasionally, the diameter of painted bats will exceed their allowable limit of 2.25

inches, thus allowing them to be identified by the ASA Ring Test.* Because the main focus of investigating painted bats was to determine how accurate the imitations could be, these bats were not performance tested.

Barrel compression testing was performed on two of the bats. Figure 3.28 shows the barrel stiffness values of two of the painted bats before and after painting, neither bat's stiffness values changed more than 3%. Such a result is evidence that the bats that were sent out to be painted were in fact returned to us. If that had not been the case the barrel stiffnesses probably would have been inconsistent.

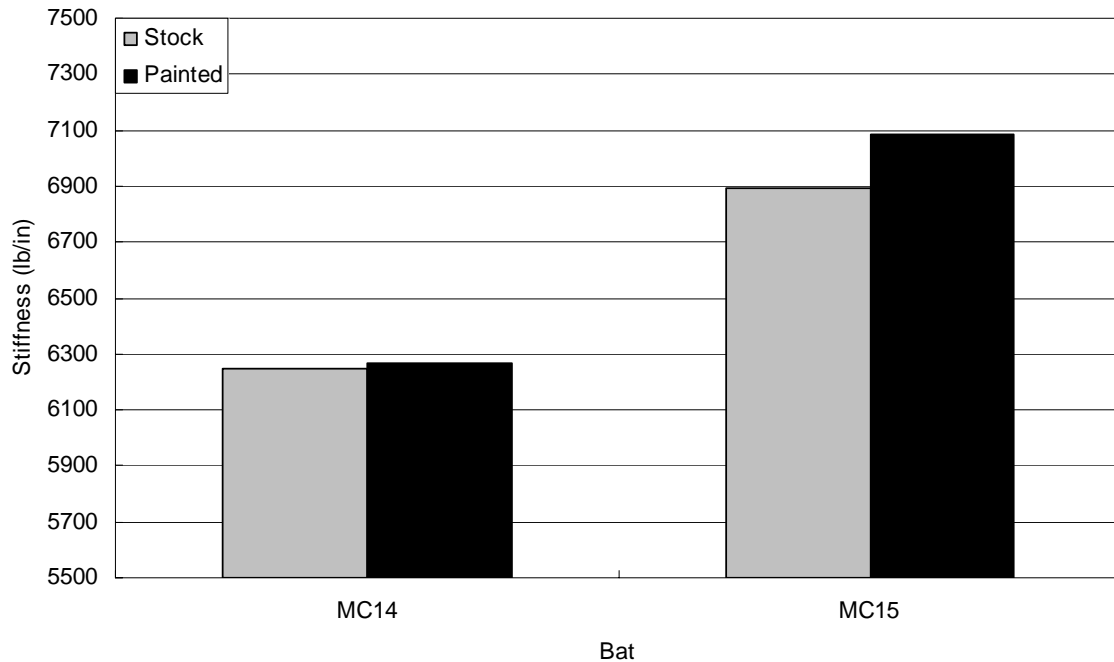


Figure 3.28 – Barrel Stiffness Comparison Before and After Painting

* The ASA Ring Test is a test that is in place to identify bats that have dented past allowable limits. The test involves sliding a ring with diameter 2.375 inches over the barrel of the bat. If the ring does not freely slide over the bat, the bat is not acceptable for use in play.



Figure 3.20 - Ultra Converted to Velocit-e II



Figure 3.21 - Ultra Converted to Velocit-e II (knobs)



Figure 3.22 - Ultra converted to Velocit-e II (end caps)



Figure 3.23 - Ultra II Converted to Freak



Figure 3.24 - Ultra II Converted to Freak (knobs)



Figure 3.25 - Ultra II converted to Freak (end caps)



Stock Miken
Ultra II

Converted to
Miken Freak 98

Stock Miken
Freak 98

Figure 3.26 - Ultra II Converted to Freak 98



Figure 3.27 - Ultra II Converted to Freak 98 (knobs)



Figure 3.28 - Ultra II converted to Freak 98 (end caps)

3.3 Discussion

Testing has verified that there are many effective methods of doctoring some of today's most popular bats. Shaving composite bats resulted in the highest average performance increase followed by ABI methods, NBI methods, end-loading, and then shaving aluminum bats. Figure 3.29 shows these rankings graphically. It is unclear how these bat modifications interact, but it is reasonable to assume that the performance increases due to some of the methods should be additive. For example, a shaved composite bat that was endloaded should have a performance increase of nearly 10%.

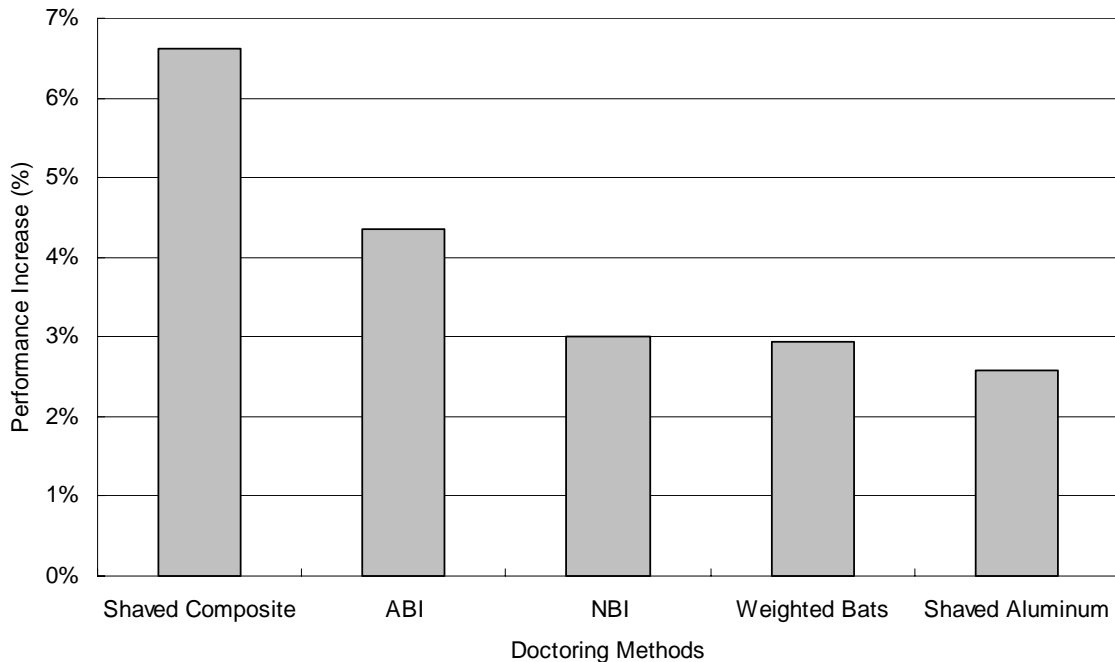


Figure 3.29 - Effectiveness of Various Doctoring Methods

ABI methods resulted in the widest ranges of performance changes, with increases from 0.66 mph (or 0.66%) to 8.28 mph (or 8.53%). The performance increases due to these methods seem to be dependent on the severity of the process.

Testing showed that regular use of some of the most popular bats today can result in performance increases comparable to some ABI treatments. This poses potential

problems for regulating agencies as it would be very difficult to tell the difference between an altered bat and a naturally broken in bat. Furthermore, comparing the NBI and ABI bats, it becomes clear that in terms of indirect performance characteristics and BBS values, three ABI processes (rolling, ACT, and vising) are equivalent to naturally breaking a bat in.

Testing has shown that a BBS scan usually does not improve performance levels in the same way natural break-in does. In addition, natural break-in causes greater changes in bats' indirect performance measures. These results imply that if regulating agencies want to test bats that have already reached their maximum naturally attainable performance level, it would not be sufficient to simply increase the number of impacts used in a certified BBS scan by a small amount.

It has also been shown that indirect performance measurements follow general trends with bat increasing performance. These trends, however, contain a considerable amount of scatter. Figures 3.30 and 3.31 show how hoop frequencies and barrel stiffnesses of the doctored bats scaled with performance.

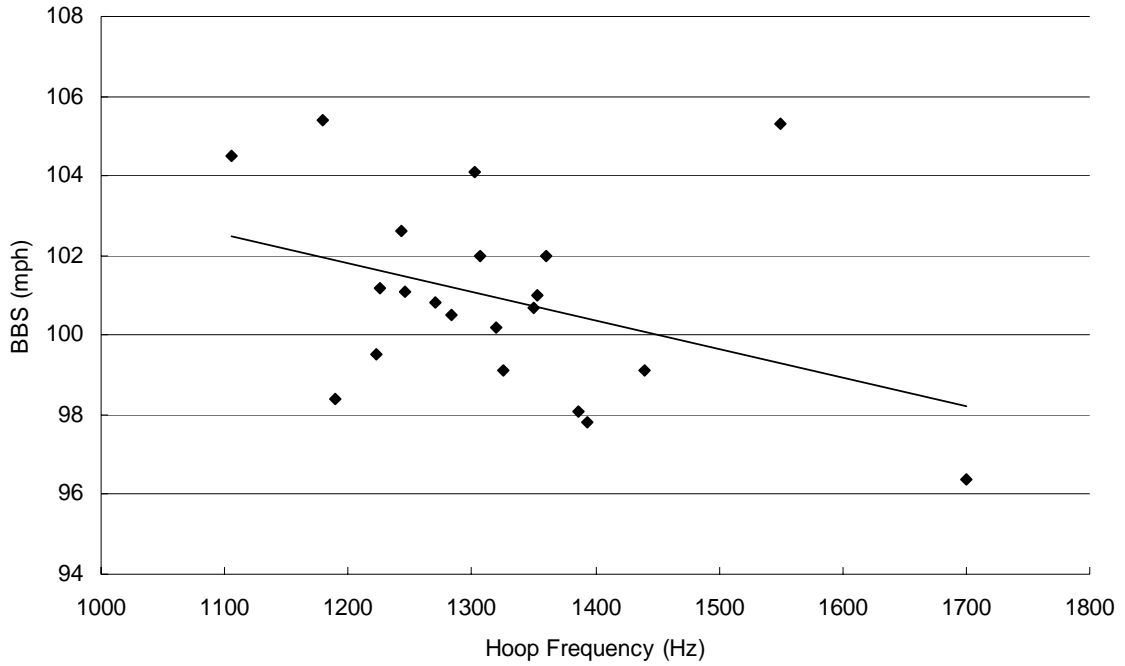


Figure 3.30 – Hoop frequencies plotted against bat performance

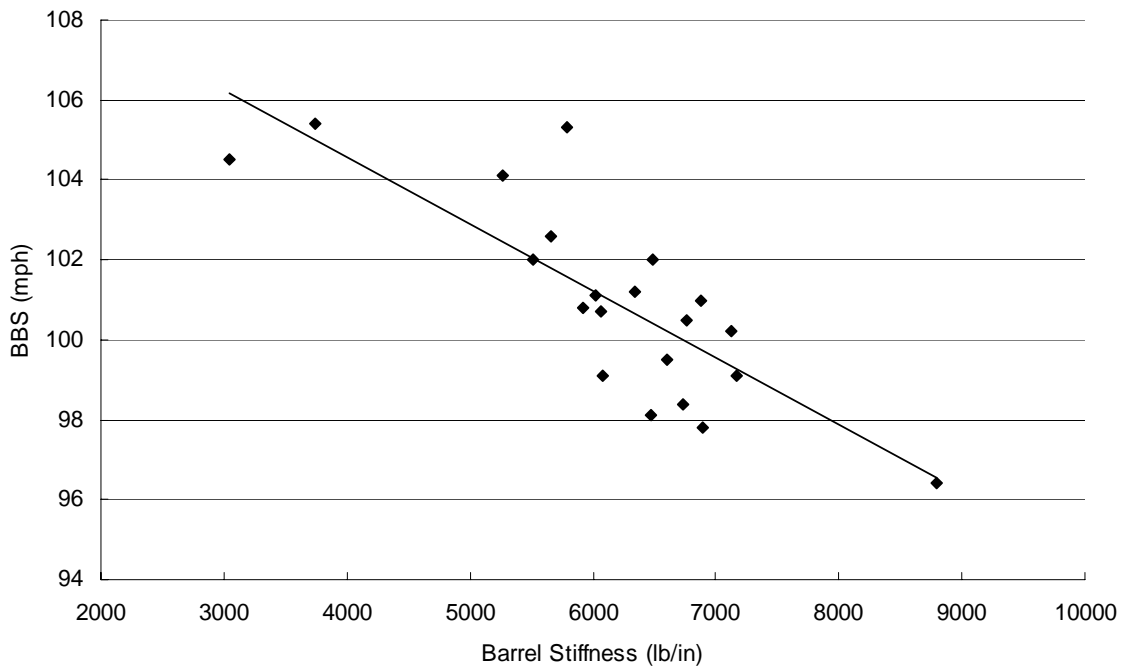


Figure 3.31 – Barrel stiffnesses plotted against bat performance

The following chapter will investigate the topic of added weight/increased MOI in greater detail. In doing so, a clearer understanding of the bat-ball collision will be realized.

REFERENCES

- 3.1 Jones, John. Pioneer of the vising method. *Private communication*. September 8, 2005
- 3.2 Official rules of softball – umpire edition. 2004 edition. Oklahoma City, OK: Amateur Softball Association of America, 2004.

CHAPTER FOUR

- BAT WEIGHT DISTRIBUTIONS -

4.1 – Weighting Study

Results from the weighted bats group in the Doctored Bat Study showed that adding weight to the distal end of bats of all construction types improved performance.

Consideration of the compliance of the impacting bodies suggests that the contribution of weight distributions is non-trivial. Few publications have investigated this phenomenon, although several studies pertaining to the contact time of the bat-ball collision have been completed. Nathan [4.1] and Adair [4.2] both concluded that the bat-ball collision was so short in duration (between 0.6 and 1.0 ms) that the ball rebound could not be affected by the boundary conditions of the bat knob.

One may assume, therefore, that weight added sufficiently distant from the impact location will not affect a bat's hitting performance (except for the way in which an increased MOI slows swing speed). In order to further investigate the effect of increased MOI/weight on performance, the Weighting Study was devised.

The Weighting study involved adding weight to initially un-weighted bats at 12 different locations. The amount of weight that was added varied with each location, but was governed by the requirement that the weight addition was to increase the bat's original MOI by 10%. A 10% increase was chosen because the 20% increase used in the weighted bat group from the bat doctoring study would have required adding unreasonable amounts of weight to the bat (over 3.5 pounds).

Each time the bat was re-weighted, the test protocol again followed ASTM 2219, where the BBCOR was measured before and after each weight amount was applied.

Unweighted tests were conducted to quantify how the performance of the bats was evolving due to the repeated impacts. Four bats were chosen for the Weighting study; a solid wood bat, single wall aluminum bat, multiple-wall aluminum bat, and a multiple-wall composite bat. The wood bat was tested at 110 *mph*, while the remaining bats were tested at 90 *mph* in order to avoid denting or cracking during the 100+ impacts required in the study.

Figure 4.1 is a schematic showing the approximate locations where the bat was impacted, Q , and where weight was added to it, d . The additional weight, in the form of adhesive-backed lead tire weights, was attached to the bat using reinforced adhesive.

Figures 4.2-4.6 show specific examples of how the weight was actually fixed to the bats.

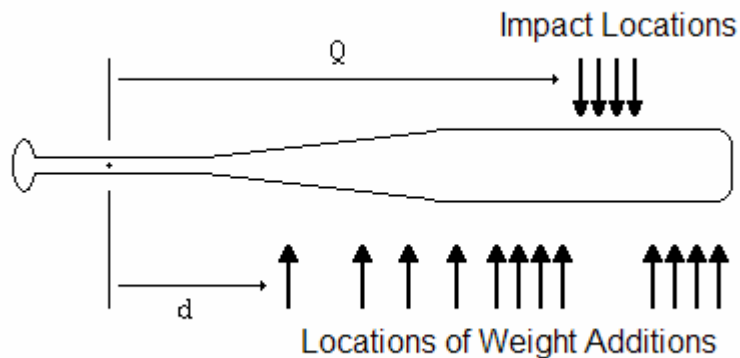


Figure 4.1 - Schematic of bat impact and weight addition locations

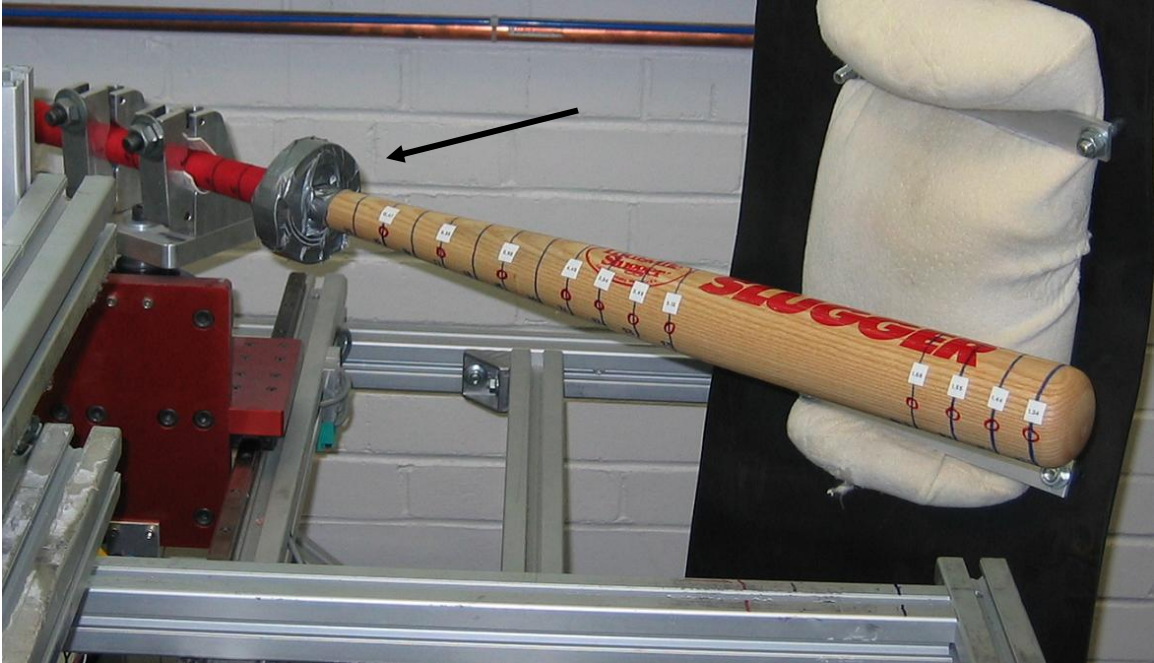


Figure 4.2 - MOI Study weight addition example 1



Figure 4.3 - MOI Study weight addition example 2



Figure 4.4 - MOI Study weight addition example 3

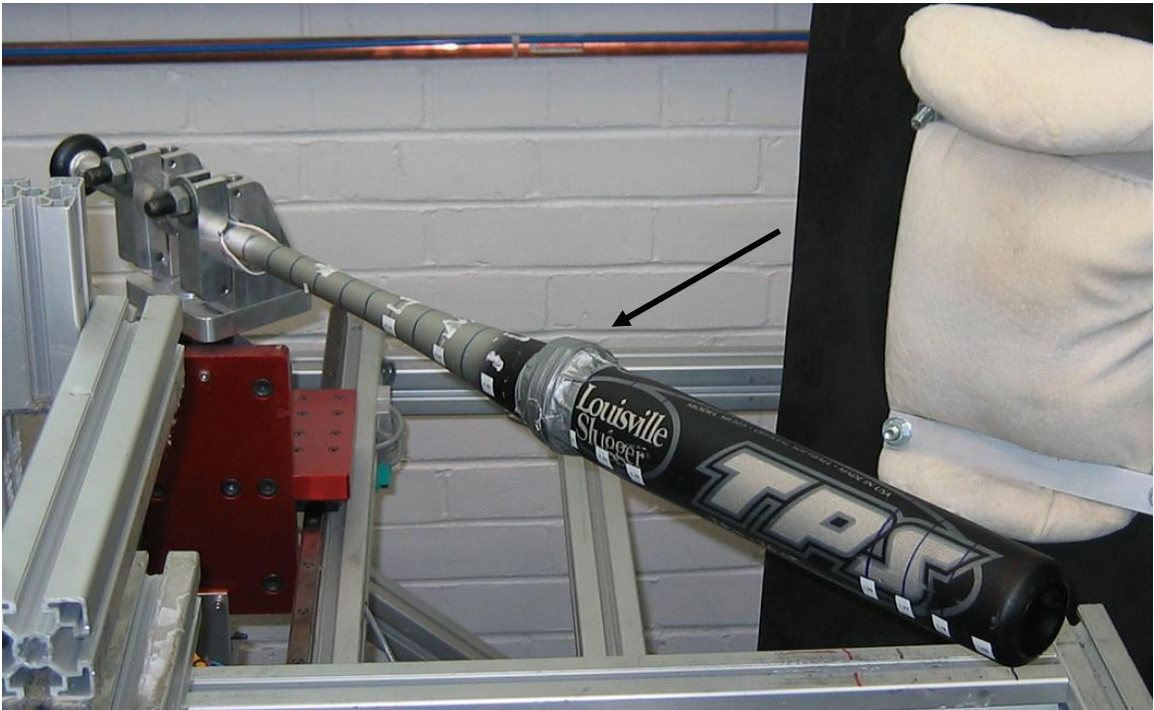


Figure 4.5 - MOI Study weight addition example 4



Figure 4.6 - MOI Study weight addition example 5

The amount of weight necessary to increase each bat's MOI 10% was found using the parallel axis theorem. Appendix 7 compares the target and actual weight additions for each weight location. The 10% MOI increase of all weight locations was verified by measuring the MOI of bat at several weight locations. In all cases its MOI was observed to be within 1% of the target values.

Modal analysis was performed on the bats with and without weight attached to determine how the mode shapes and node locations were affected by the added weight.

4.2 – Results

In Chapter 3 BBS was used as the performance metric because it provided the most accurate method for comparing how different bats would perform relative to one another when swung by players. In this chapter, BBCOR will be used so that performance changes can be compared, independent of the bats' MOI.

Recall the formulation of BBCOR, given as

$$e_{BB} = \frac{v_r}{v_i} + \frac{mQ^2}{v_i I_p} (v_i + v_r). \quad (2.10)$$

Applied to the Weighting Study, the terms, v_i , m , and I_p were constant. This implies that any BBCOR increase, for a given impact location ($Q=\text{constant}$), must be a result of an increased rebound speed, v_r .

4.2.1 – Wood bat

Figure 4.7 shows the BBCOR as a function of weight location for the three impact locations. The plot also shows a baseline performance level which is the BBCOR value with no weight attached to the bat. This baseline measurement was taken to verify that bat performance did not change as a result of the repeated impacts. The shaded column on the plot identifies the region in which the bat was impacted. The plot reveals multiple trends in the bat-ball collision. First, the impact location that produces the highest BBCOR changes with the location of weight addition, and second, there seems to be a finite distance from the impact location at which the addition of weight has no effect on the bat-ball collision.

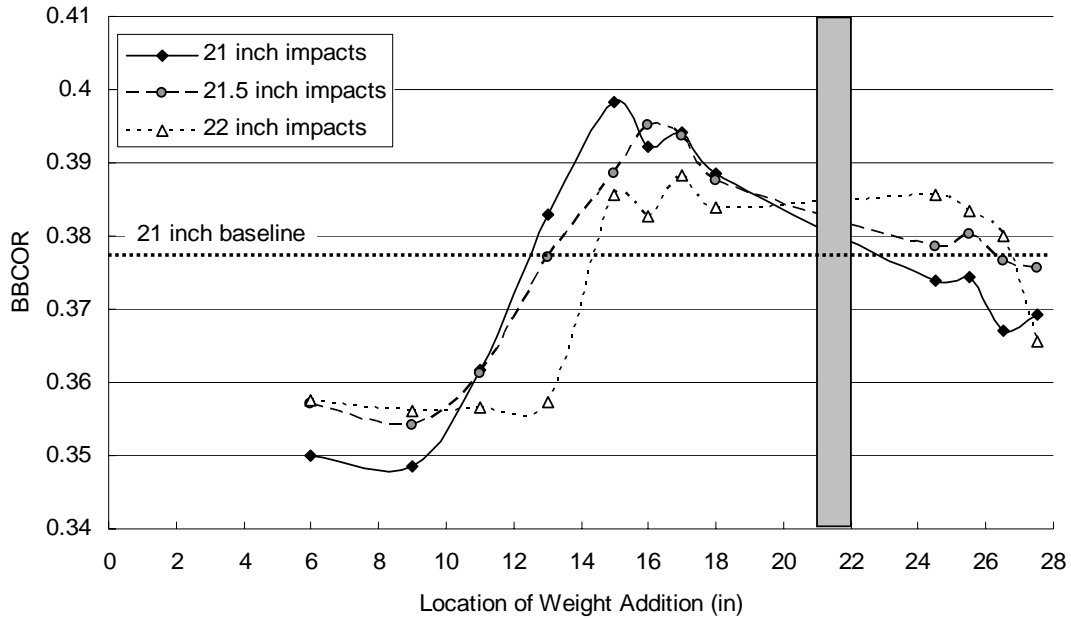


Figure 4.7 – BBCOR as a function of weight location – wood bat

The BBCOR of the wood bat reached a maximum value when weight was added 5-6 inches inside (toward the knob end of the bat) of the impact location. The distance (from the weight to the impact location) at which the added weight had no effect on BBCOR values was beyond about 9 inches.

4.2.2 – Single wall aluminum bat

The single wall aluminum bat, whose trends are shown in figure 4.8, yielded similar results to the wood bat.

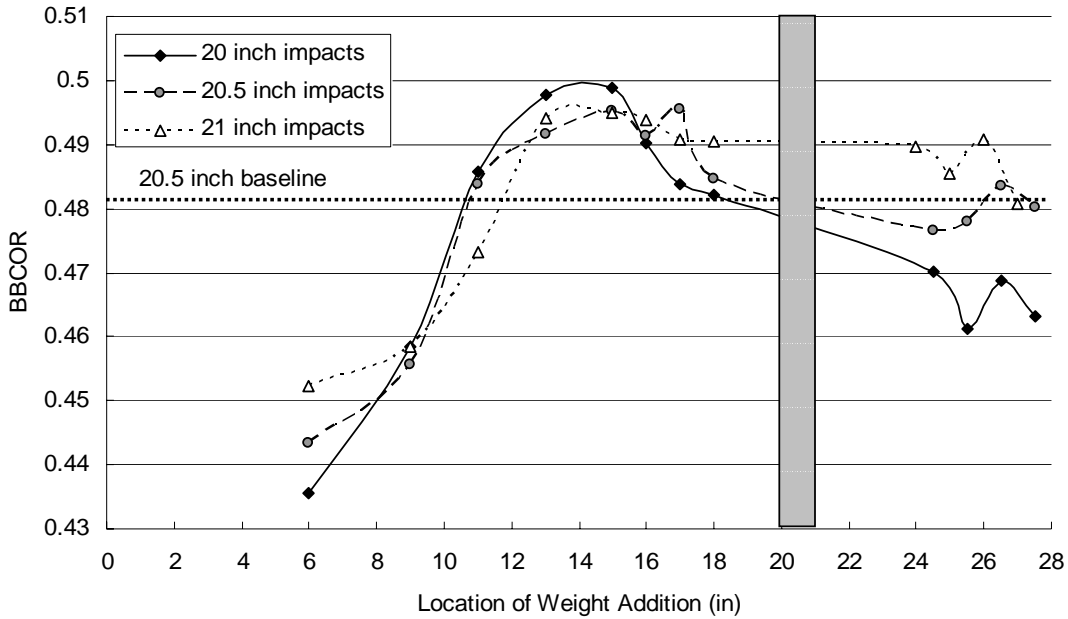


Figure 4.8 - BBCOR as a function of weight location – single wall aluminum bat

In this case the distance at which weight additions had no effect on BBCOR values was beyond about 12 inches, and the distance at which BBCOR was optimized was between 5-6 inches inside the impact location.

4.2.3 – Multiple-wall aluminum bat

As shown in figure 4.9, the high speed testing data collected from the multiple-wall aluminum bat exhibited more scatter than the wood, single wall aluminum, or the soon to be discussed multiple-wall composite bats.

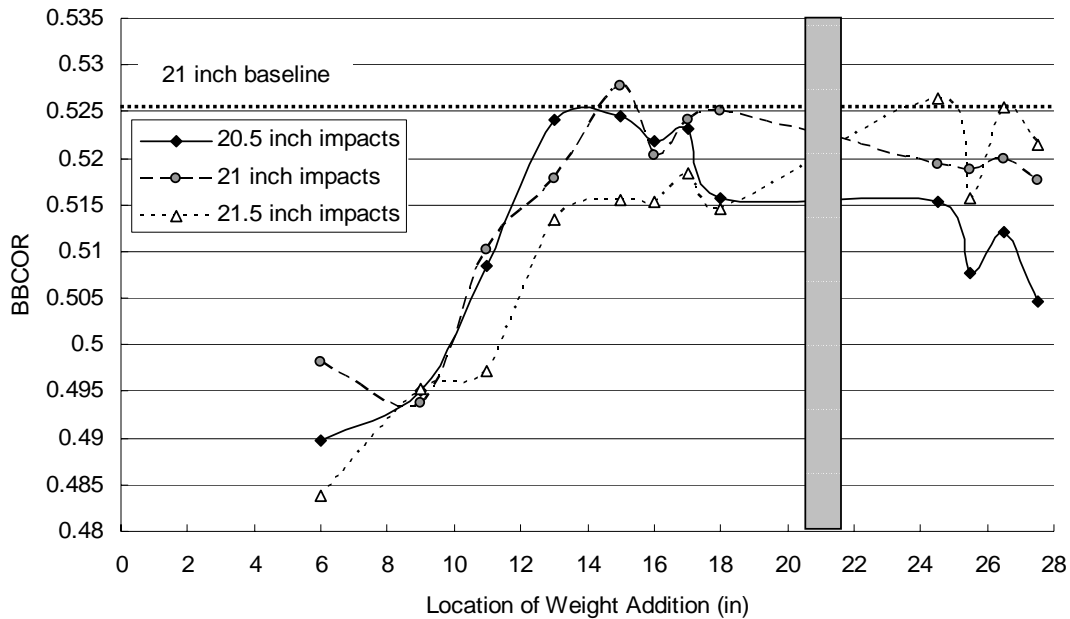


Figure 4.9 – BBCOR as a function of weight location – multiple-wall aluminum bat

The data nevertheless indicates that the bat-ball impact involving a multiple-wall aluminum bat is not affected by weight added further than about 11 inches inside the impact location. BBCOR seems to reach a maximum when weight is located between 6-3 inches inside the impact location.

Test data for the previously mentioned bats in this study showed that the location of maximum BBCOR was influenced by the location of weight addition. The multiple-wall aluminum bat did seem to follow this same trend, but not as distinctly or consistently.

4.2.4 – Multiple-wall composite bat

The results from the composite bat had less scatter than those for the multiple-wall aluminum bat. As shown in figure 4.10, it was found that the bat ball collision was unaffected by the weight addition when it was further than about 12 inches from the impact location. The optimum location for weight addition was found to be between 5-7

inches from impact location. The composite bat also demonstrated the trend that the impact location providing the maximum BBCOR was dependent on the location of the weight addition.

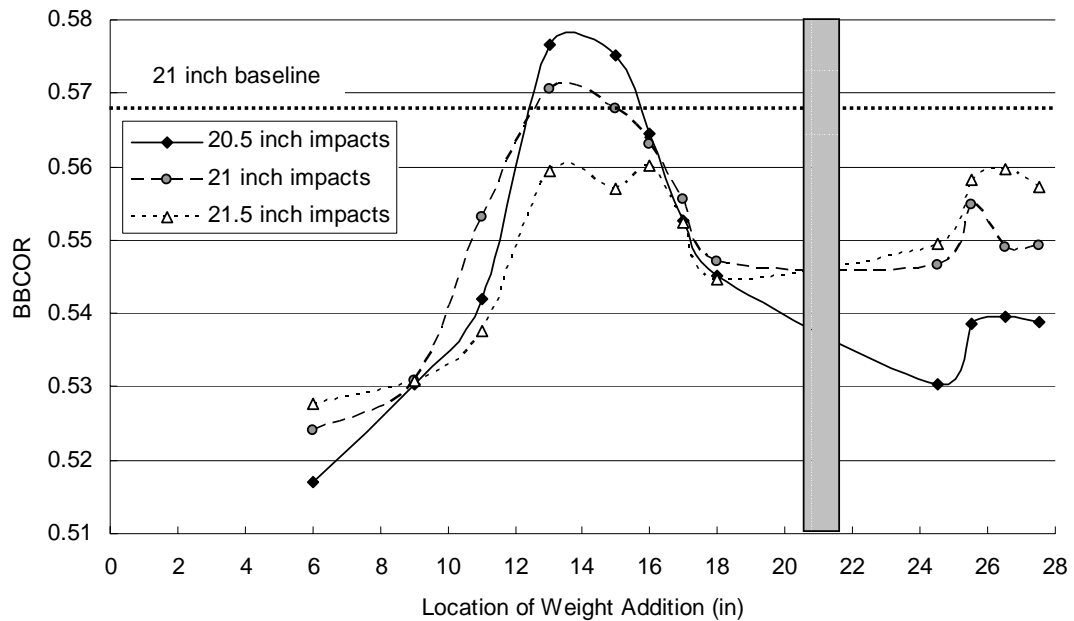


Figure 4.10 – BBCOR as a function of weight location – multiple-wall composite bat

4.3 – Discussion

Testing shows that the location at which weight is added to a bat does have a direct effect on performance. The performance of each bat reached a maximum when the weight was located at a specific distance from the impact location. This location was unique for each bat, although it followed the same trend in all bats.

The fact that BBCOR changed as a function of the weight location on all of the bats, including the wood bat, implies that the change in performance was a related to the bats’ flexural responses.

Modal analysis was used as a means of comparing the bats' flexural responses. A full modal analysis was performed on the single wall aluminum and multiple-wall composite bats* with and without weight attached to the location which provided the maximum BBCOR value. This analysis was done in order to determine if the flexural properties of the bats, such as bending frequencies or node locations, changed as a result of weight addition.

Figures 4.11-4.14 are waterfall plots showing the first two flexural mode shapes of the aluminum and composite bats and their relative magnitudes. The node locations of each mode (the location at which the plot crosses zero on the amplitude axis) can also be seen in each of the plots. It should be noted that on the plots of the weighted bats, the location on the bat where weight was added can be seen by a localized spike in the mode shape.

* The wood bat could not be analyzed because it fractured after performance testing. The multiple wall aluminum bat data had large scatter and was difficult to interpret.

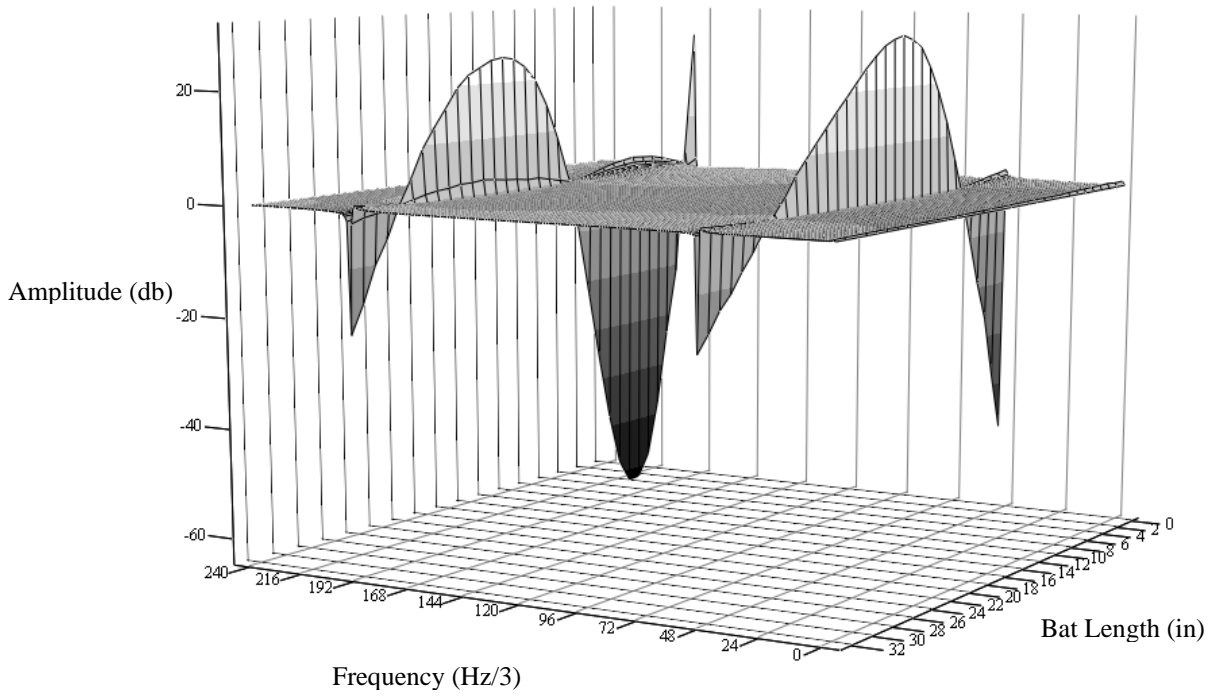


Figure 4.11 - Waterfall plot of single wall aluminum: no weight

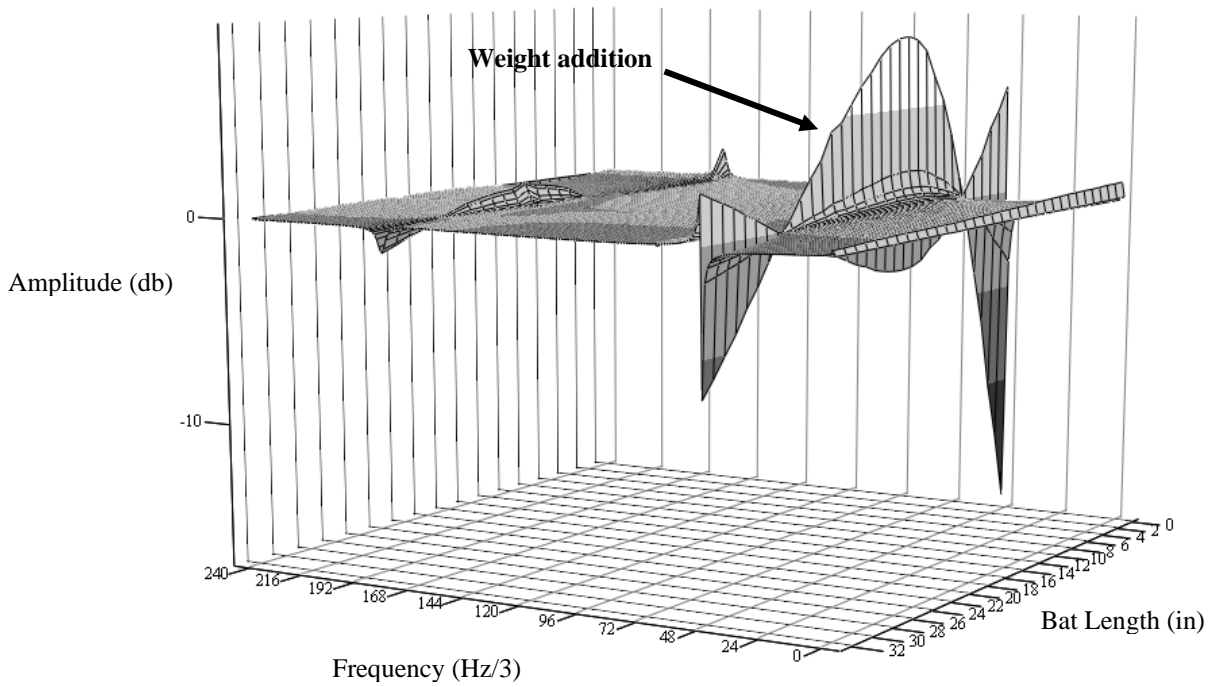


Figure 4.12 - Waterfall plot of single wall aluminum: weight at 17'' location

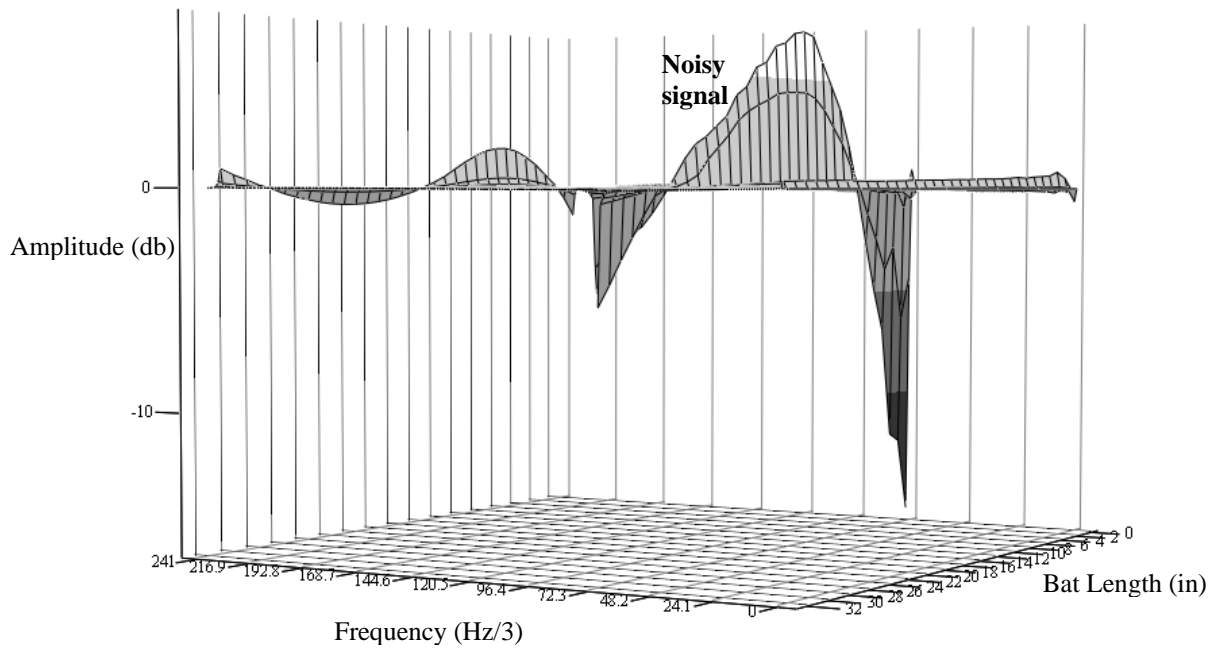


Figure 4.13 - Waterfall plot of multiple-wall composite: no weight

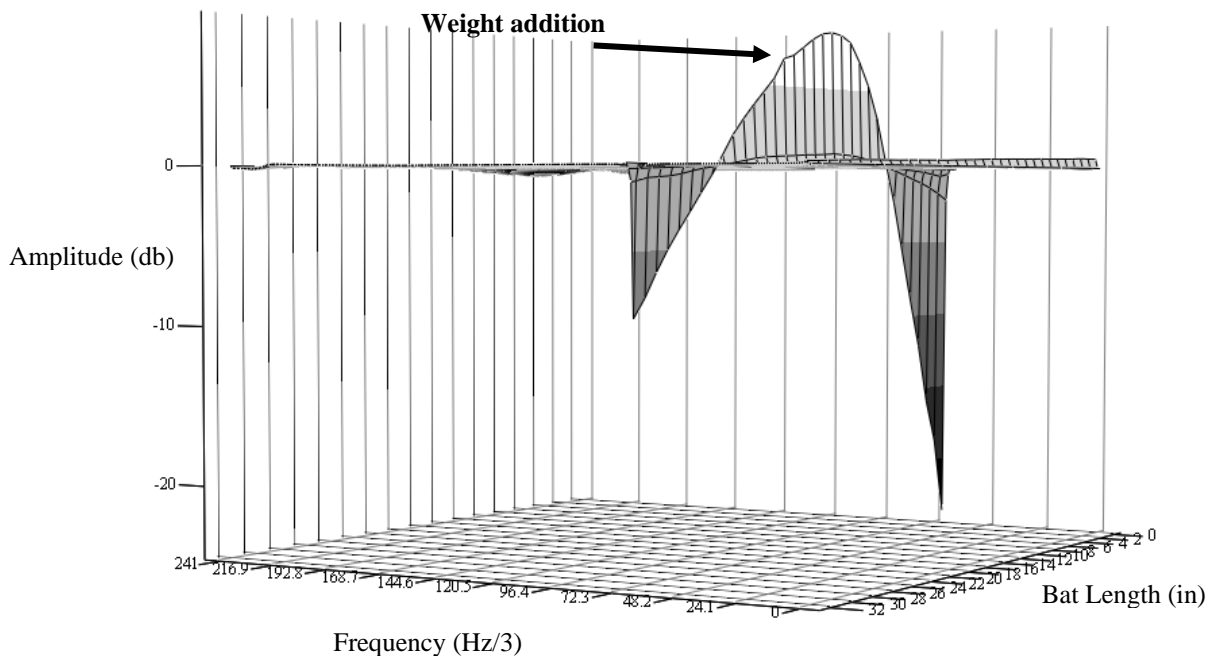


Figure 4.2 - Waterfall plot of multiple-wall composite: weight at 17'' location

The added weight seemed to have one consistent effect on flexural frequencies in that each decreased less than 10%, except for the second flexural mode of the composite bat, which increased less than 5%. None of the node locations for any of the bats changed more than one inch. The nodes that did move generally shifted toward the knob end of the bat. The remaining trend shown in the plots is that the addition of weight seemed to attenuate the second flexural bending modes. It is unclear whether the apparent attenuation was a result of the small node location shift or an actual decrease in vibration amplitude. The results of modal testing have been insufficient in determining whether the performance trends were a result of the bats' vibrational characteristics.

The most significant performance trend observed in the Weighting Study was that the impact location providing the maximum BBCOR was a function of the weight location. In addition there does appear to be a region of the bat where added weight did not affect the bat-ball collision.

Due to the fact that the wood bat showed performance increase it is reasonable to conclude that the performance increases observed in this study are not (at least entirely) a result of an improved trampoline effect. One explanation for why various loading conditions improve performance can be derived from the fact that the ball COR measured off of a rigid wall is higher than it is off of a recoiling wall [4.3]. This idea can be converted to the bat-ball impact by closely examining the impact. As the ball impacts a bat, the bat deflects a small amount during the time in which they are in contact. In addition to this global deflection (bending) that occurs and is shown in figure 4.15, a

hollow bat also compresses circumferentially. For a given net impact speed and impact location, each bat will bend and might compress a set amount.

Before further analysis, it is helpful to avoid thinking of a bat in a traditional, global sense. Instead it can be useful to think of a bat as the sum of many small pieces all of which can have an individual weight and inertia, figure 4.16 shows such a bat. It is important to note that the sum of each of these pieces' weights and inertias will remain constant. Just as in the Weighting Study where the weight distribution was altered while maintaining a constant MOI. If the weight, and therefore inertia, of a small piece of the bat near the impact location is increased, the local inertia will hinder the bat's global tendency to bend. If the bat is hollow, the added inertia will also resist the barrel compression due to the impact.

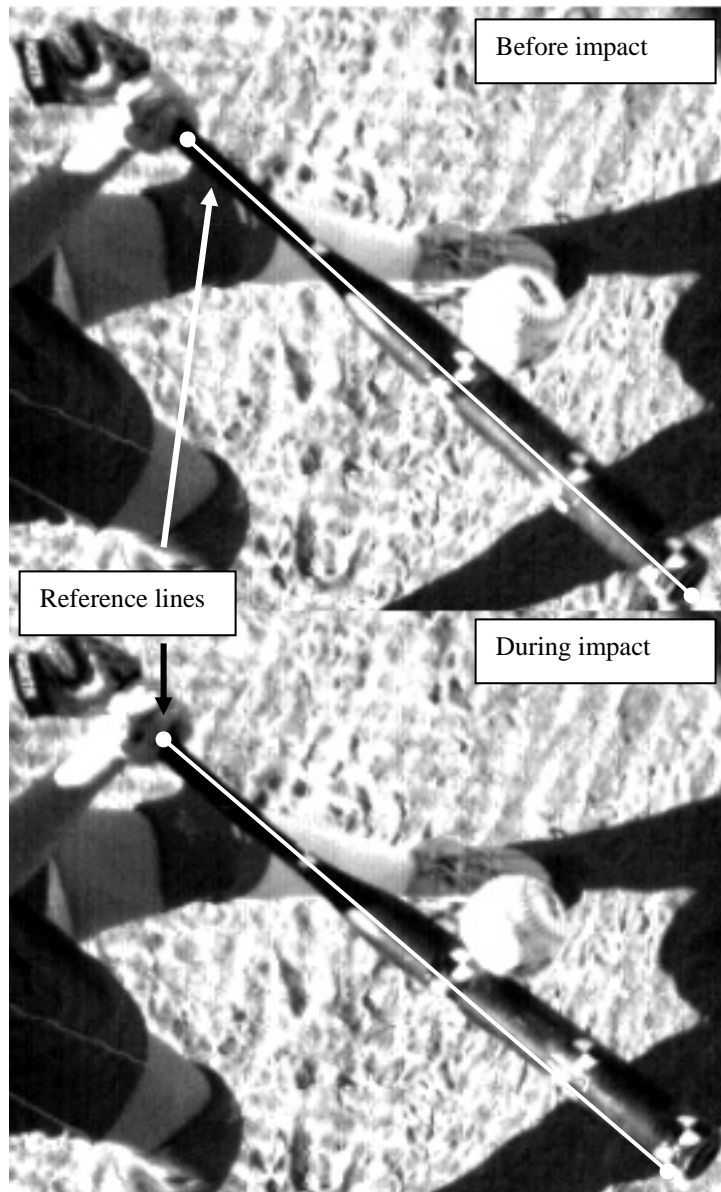


Figure 4.15 – High speed video capture of bat-ball impact

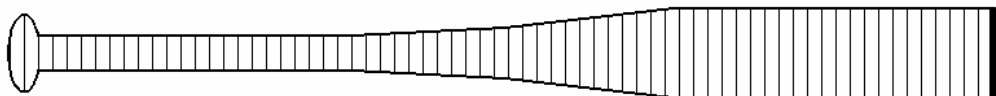


Figure 4.16 – Discretized softball bat

The effect of the reduced bending in the bat makes more energy available to be returned to the ball. This can account for the performance increase observed in wood bats as well as the other bats involved in the study. The fact that the hollow bats' performances decreased as weight was added closer to the impact location supports the idea that the local increase in inertia resisting the bat's tendency to compress reduces the efficiency of the trampoline effect. This would imply that a solid bat's performance should continue to increase as weight is added closer and closer to the impact location, but this has not been confirmed in this small scale study.

REFERENCES

- 4.1 Nathan, A. *Bat performance metrics*. Presentation at Bat-Ball 102 symposium. Pullman, WA. 2004.
- 4.2 Adair, R. The Physics of Baseball. Third Edition. Perennial: New York. 2002. ISBN:0060084367.
- 4.3 Experimental and numerical characterization of softballs. Duris, J. Unpublished Master's Thesis. December 2004.

CHAPTER FIVE
- COMPUTER MODELING -

5.1 – Modeling Methods

In this work, finite element modeling was used to verify the results of physical characteristics (MOI, balance point, etc) and modal analysis testing. The finite element software package used was LS-DYNA, double-precision version 970 (Livermore Software Technology Corporation).

A complete discussion regarding the fundamentals of finite element methods is beyond the scope of this research. The following discussion of finite element methods will be limited to the methods used in this study. The reader is referred to [5.1], [5.2], [5.3] for further information on general finite element theory.

A dynamic finite element analysis can be performed using two different calculation methods, explicit and implicit time integration. The explicit method calculates the nodal displacement matrix $\{D\}$ using the general difference method

$$\{D\}_{n+1} = f(\{D\}_n, \{\dot{D}\}_n, \{\ddot{D}\}_n, \{D\}_{n-1}, \dots), \quad 5.1$$

combined with the equation of motion evaluated at time step n . The result is a $\{D\}$ matrix that is based solely on historical information [5.1].

The implicit method calculates the nodal displacement matrix using the general difference method

$$\{D\}_{n+1} = f(\{\dot{D}\}_{n+1}, \{\ddot{D}\}_{n+1}, \{D\}_n, \{\dot{D}\}_n, \{\ddot{D}\}_n, \dots) \quad 5.2$$

which is combined with the equation of motion at time step $n + 1$. The equation of motion at time step $n + 1$ is written as

$$[M]\{\ddot{D}\}_{n+1} + [C]\{\dot{D}\}_{n+1} + [K]\{D\}_{n+1} = \{R\}_{n+1}. \quad 5.3$$

The major difference between the formulation of the explicit and implicit methods is that the former is based entirely on historical data and the latter is only partially based on historical data. As a result of their unique formulations, each of these methods exhibit distinctive characteristics.

The explicit method is conditionally stable – which means that the numerical process will be stable unless a model dependent critical time step is exceeded. A benefit of this method is that the numerical process is greatly simplified for each time step because the coefficient matrix of $\{D\}$ (the equivalent stiffness matrix) can be diagonalized. As a result, each time step requires relatively small computational power. The drawback to the explicit method is that acceptable time step sizes are so small that the solution time can be large due to the high number of equations that must be solved.

The implicit method is unconditionally stable – which means that the numerical process is stable regardless of the time step size. One benefit of this method is that fewer time steps are necessary during an analysis, although if time steps become too large accuracy can suffer. The drawback to the implicit method is that the coefficient matrix of $\{D\}$ cannot be diagonalized, the result of this is a relatively large amount of computing power is necessary to solve the equations at each time step.

As a result of their distinct characteristics, these methods should not be used interchangeably when a high degree of computing efficiency is desired. Generally, the explicit method is used when the simulated event occurs on a short time scale so that the benefit of faster computation time is not negated by the number of time steps necessary to describe the event. Impacts and explosions are examples of events that the explicit method is well suited for. The implicit method is most often used for simulations of

events occurring on much larger time scales, such as earthquakes or slow ramp loads.

Modal analysis problems are also candidates for the implicit solution method.

In a simplified modal analysis problem (neglecting damping effects), the equation for free vibration

$$([K] - \omega^2 [M])\{\bar{D}\} = \{0\} \quad 5.4$$

must be solved [5.1]. Equation (5.4) is an eigenvalue problem, where $[K]$ is the global stiffness matrix, ω^2 is an eigenvalue whose natural frequency is ω , $[M]$ is the global mass matrix, and $\{\bar{D}\}$ is the displacement matrix which is associated with nodal displacements and accelerations by

$$\{D\} = \{\bar{D}\} \sin \omega t \quad 5.5$$

and

$$\{\ddot{D}\} = -\omega^2 \{\bar{D}\} \sin \omega t . \quad 5.6$$

The LS-DYNA software suite offers many element options. In this work, 8-node solid brick elements were used. The brick elements employed selective reduced integration without rotational degrees of freedom (LS-DYNA solid element formulation 2). These elements were fully integrated over the deviatoric stress field and had one integration point in the pressure field. Solution time would have been reduced by using shell elements. They were not used, however, since the preprocessor only supported constant thickness shell elements. Thick shell elements were considered because they are not a constant thickness element. The thick shell elements were not implemented because they were not compatible with LS-DYNA's implicit eigenvalue analysis.

In the following sections, the results of a convergence study are presented. Frequency and mode shapes from experimental modal analysis are compared to numerical predictions for a wood bat and a single and multiple-wall aluminum bat.

5.2 – Convergence study

When modeling a hollow baseball or softball bat, there are three methods for altering the mesh density in the model. One method involves changing the number of elements along the length of the bat (longitudinal elements); another involves changing the number of elements around the circumference of the bat (circumferential elements); finally, the number of elements through the thickness of the bat walls can be manipulated.

The effect that each of these parameters had on solution accuracy and solution time were studied to find the most accurate and efficient method for modeling a bat. The profile used during the convergence study was a simplified single wall aluminum bat which did not include an end cap or knob. The results were normalized using the finest mesh density

Figures 5.1 and 5.2 show how the normalized flexural and hoop frequencies converge as the number of elements along the length of the bat increase. In these simulations, the number of elements through the wall thickness and around the circumference of the bat were held constant at 1 and 72 respectively.

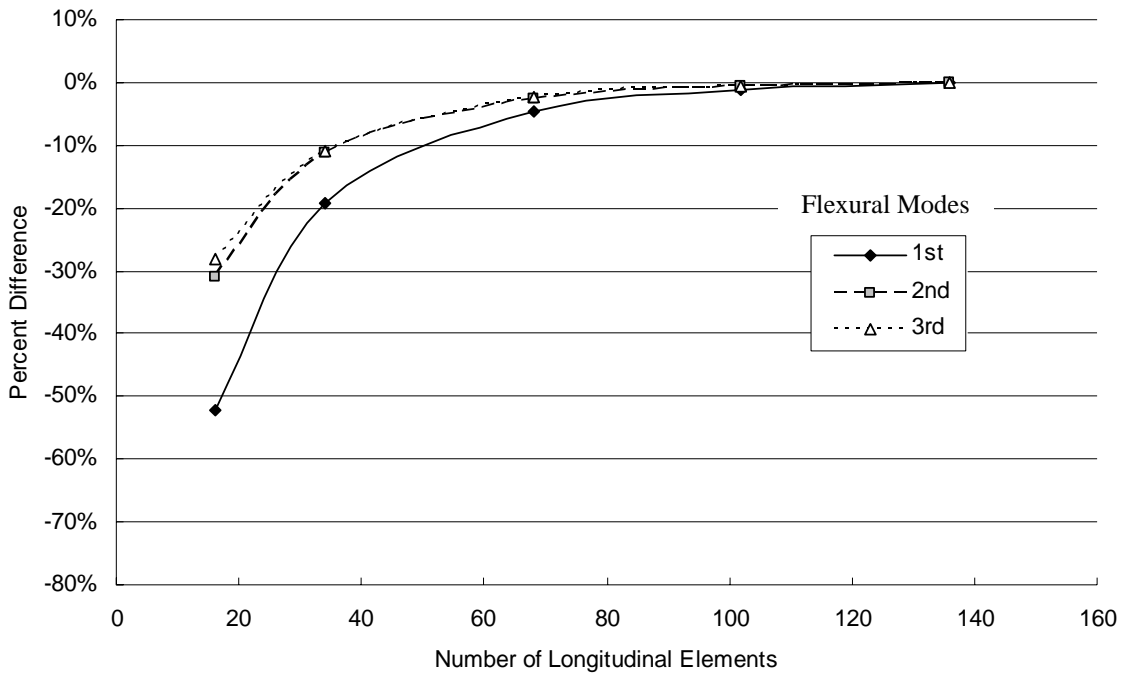


Figure 5.1 – Flexural frequency convergence due to longitudinal element variations

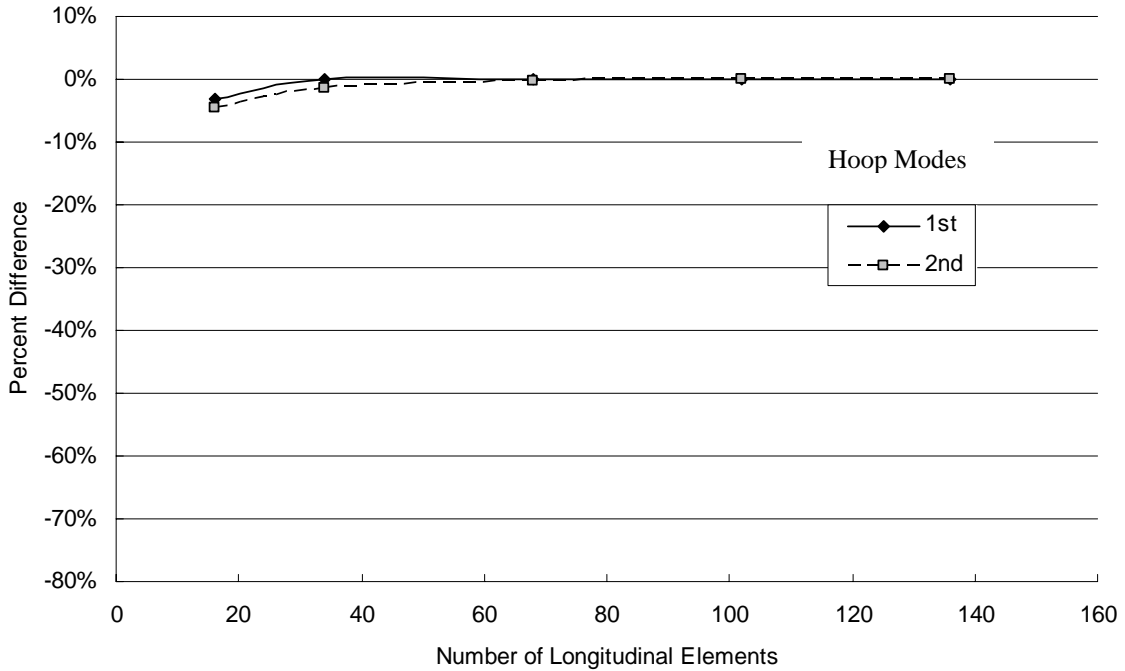


Figure 5.2 – Hoop frequency convergence due to longitudinal element variations

The plots depicting the convergence due to increasing the number of longitudinal elements imply that too few elements result in an overly stiff model. This would be expected as larger elements provide a poor representation of bending.

Figures 5.3 and 5.4 show how the flexural and hoop frequencies are affected by changing the number of elements around the circumference of the bat. In these simulations the number of elements along the length of the bat and through the thickness were held constant at 34 and 1 respectively.

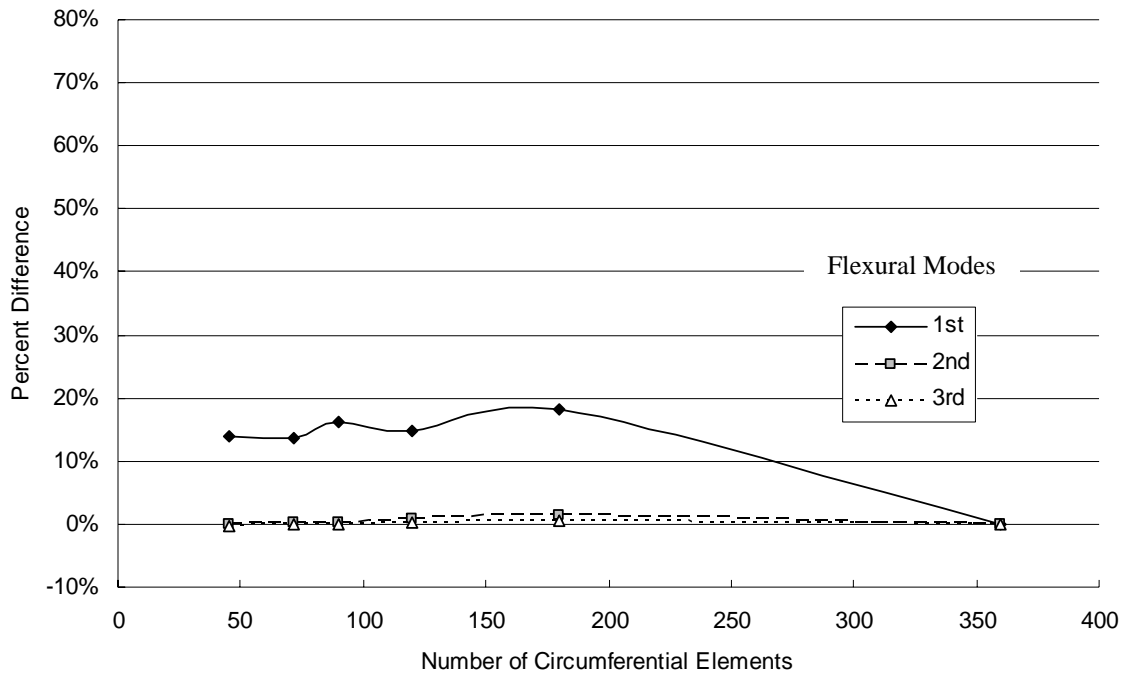


Figure 5.3 - Flexural frequency convergence due to circumferential element variations

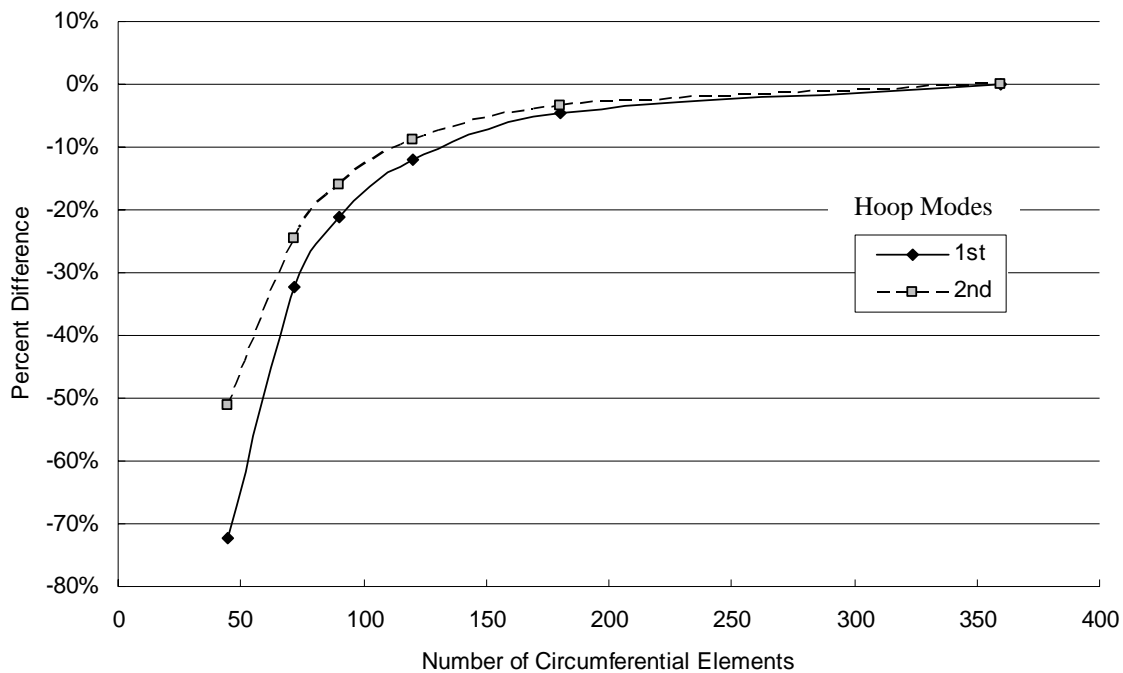


Figure 5.4 – Hoop frequency convergence due to circumferential element variations

The flexural frequency convergence due to increasing elements around the bat circumference did not follow the same trends observed in other cases. In figure 5.3 the percent difference does not seem to converge to any value. One possible reason for this result is that a very high aspect ratio of 51:1 occurs in the finest mesh density. Convergence of the hoop frequencies does follow the expected trend in that as the number of elements increase, the model becomes better suited to describe bending motion.

The effects of altering the number of elements through the wall thickness are shown in figures 5.5 and 5.6. In these simulations the number of elements along the length of the bat and around its circumference were held constant at 102 and 120 respectively.

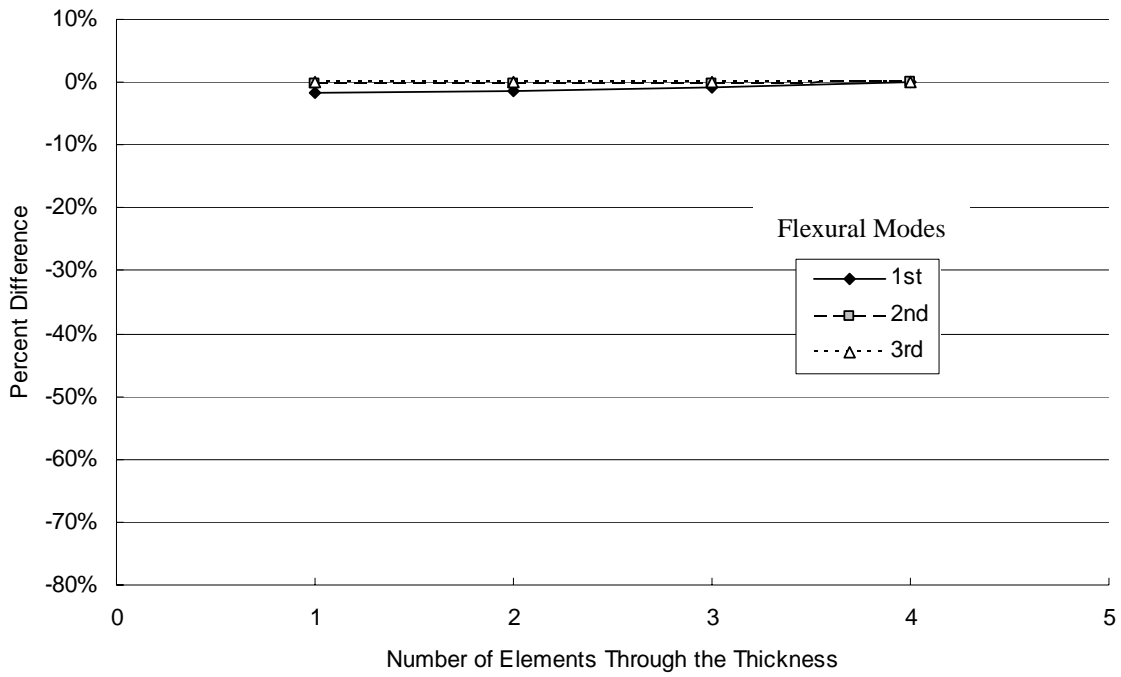


Figure 5.5 – Flexural frequency convergence due to through the thickness element variations

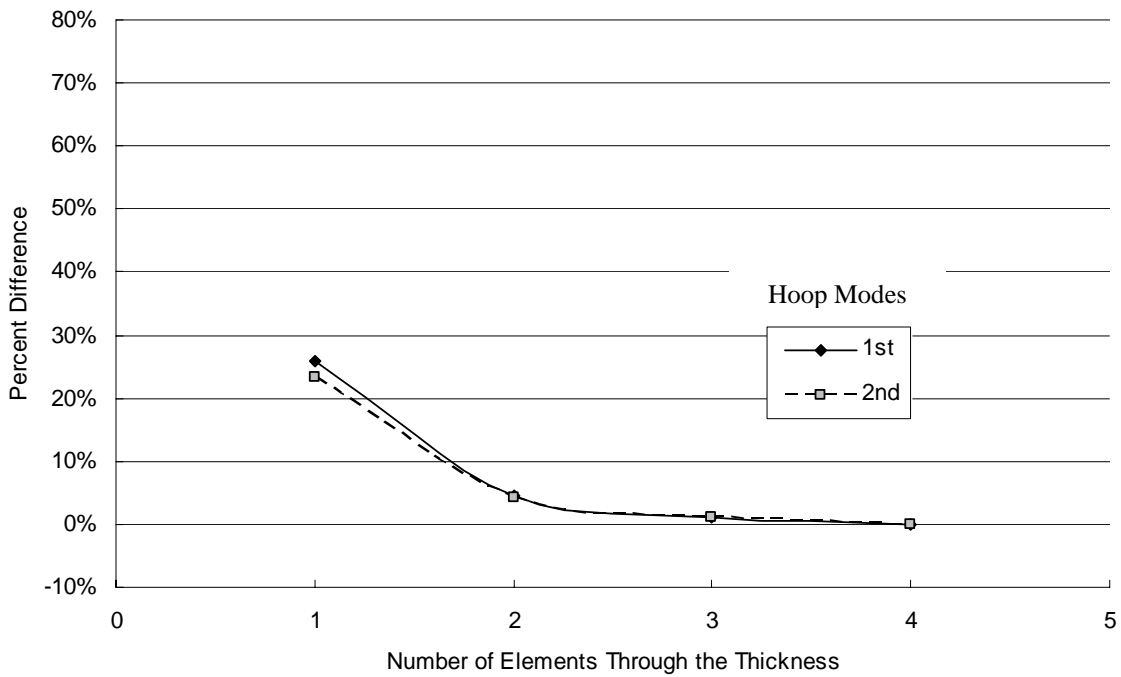


Figure 5.6 - Hoop frequency convergence due to through the thickness element variations

The convergence plots demonstrate that, in general, increasing mesh density reduces the model's stiffness. Figures 5.3 and 5.6 stand out because their stiffnesses increase as more elements are added to the model. Investigation into the details of the brick elements used in the convergence study revealed they were linear elements, which do not incorporate incompatible modes. Such elements tend to show increased stiffness as aspect ratios increase due to element locking, which helps explain the observed trends.

The convergence study showed that flexural response of the model is dominated by the number of longitudinal elements, while hoop response is dominated by the number of circumferential elements and elements through the thickness.

While the highest mesh densities provided the most accurate results when modeling bats, the solution time for the higher mesh densities were large (on the order of 7 hours). A compromise between solution convergence and solution time was made using a 95% convergence threshold. Accordingly, the mesh density for all bat models was 102 elements along the length of the bat, 180 elements around its circumference, and 2 elements through the thickness. The largest aspect ratio using this configuration was relatively large at 30:1, but still provided results that were consistent with measured values.

5.3.1 – Bat models

Three bats have been modeled in this study, a wood bat, a single wall aluminum bat, and a multiple-wall aluminum bat. The profiles of the hollow bats were found by dissecting a sample bat and measuring wall thicknesses with calipers. It was assumed that neither the knob nor end cap of the bats were critical to the response of the hollow bats. They were included in the model using simplified geometries. The properties for

each material used in the bat models were defined according to actual material properties (Appendices F and G include the bat profiles and material definitions used to model the bats) [5.4]. The densities of the end cap and knob were manipulated so that the mass, mass center, and MOI of the models matched the measured values of the modeled bats.

Figures 5.7-5.14 are examples of all of the modeled bats.

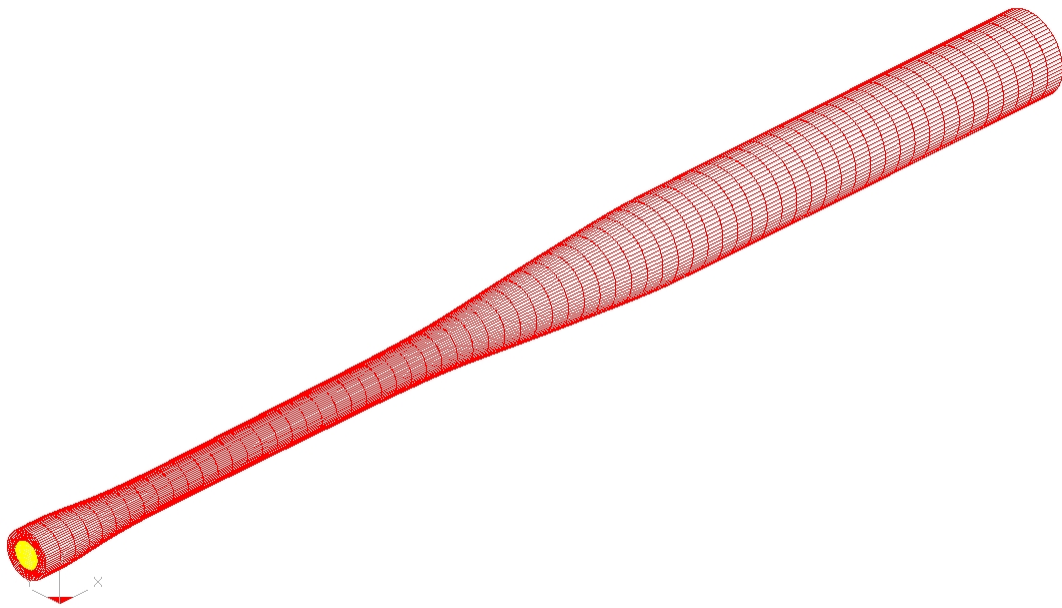


Figure 5.7 – Wood bat model

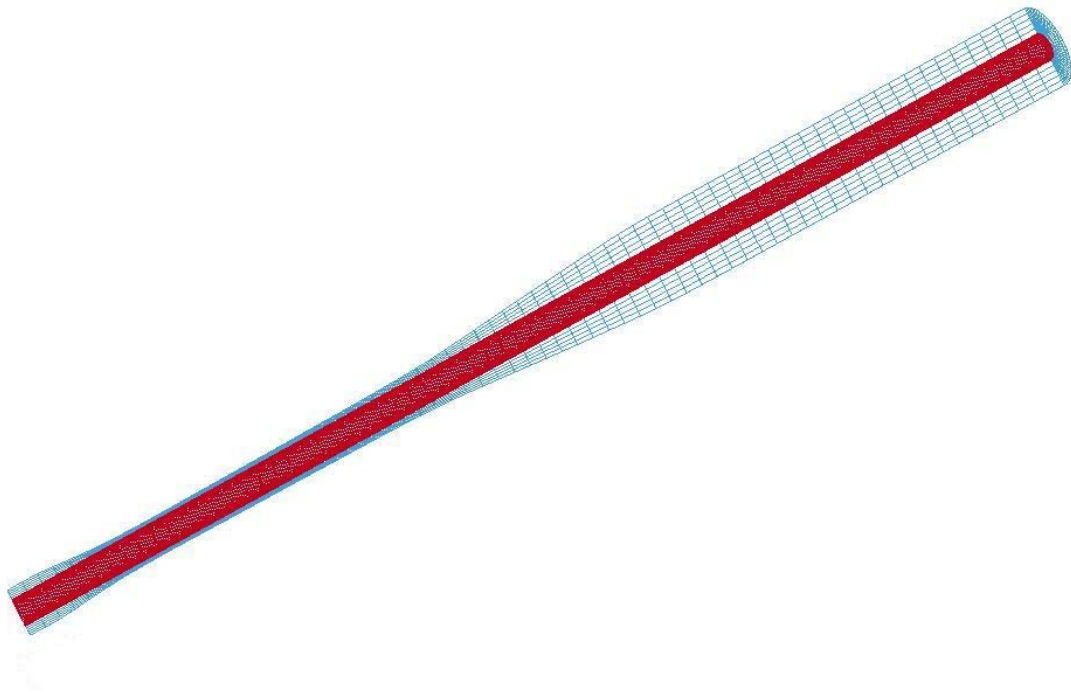


Figure 5.8 – Sectioned view of wood bat model

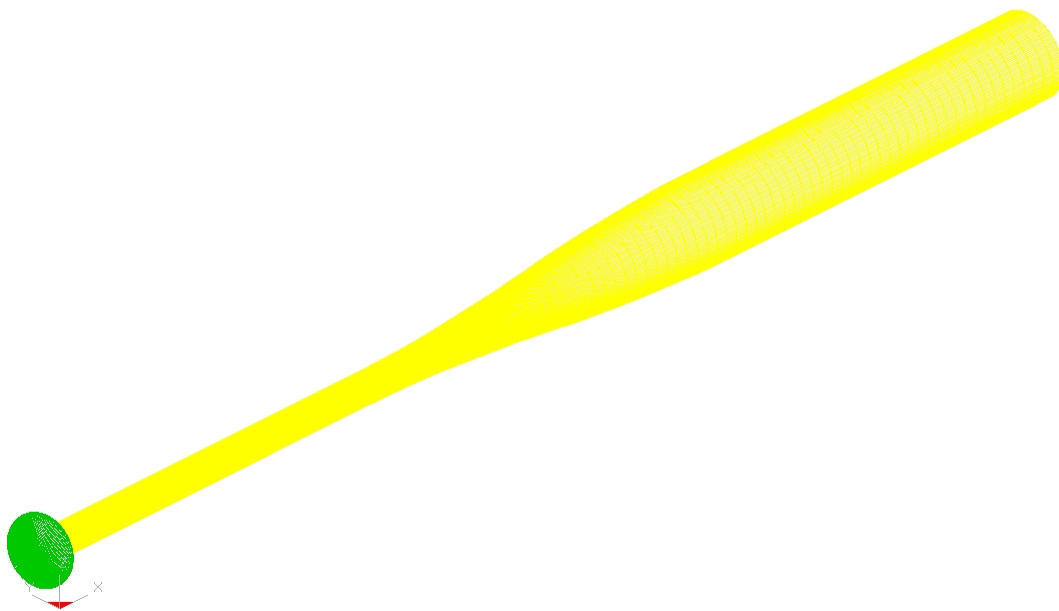


Figure 5.9 – Single wall aluminum bat model



Figure 5.10 – Sectioned view of single wall aluminum bat model

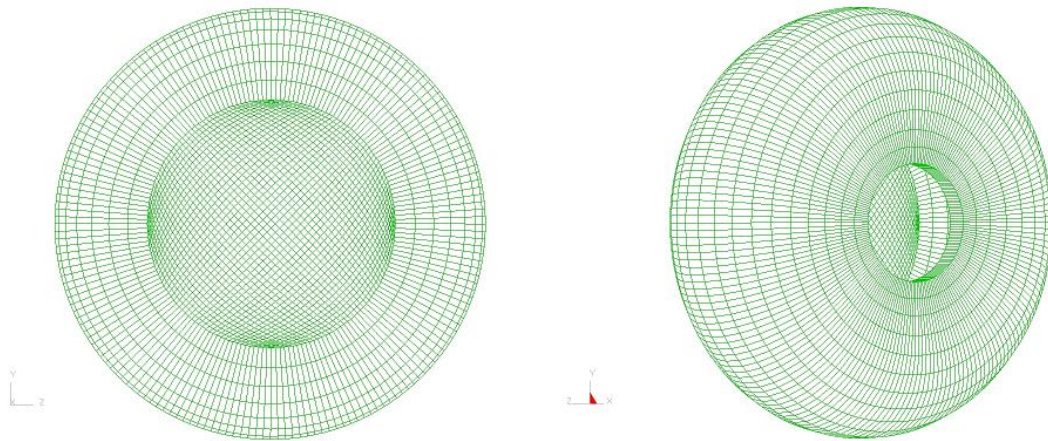


Figure 5.11 – Views of knob used on aluminum bat models

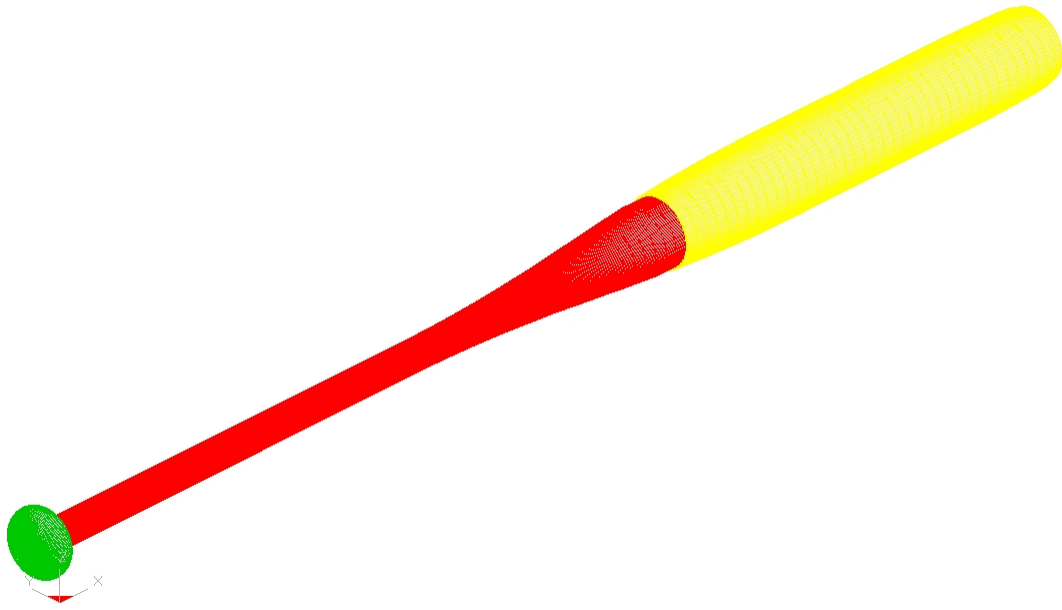


Figure 5.12 – Multiple-wall aluminum bat model

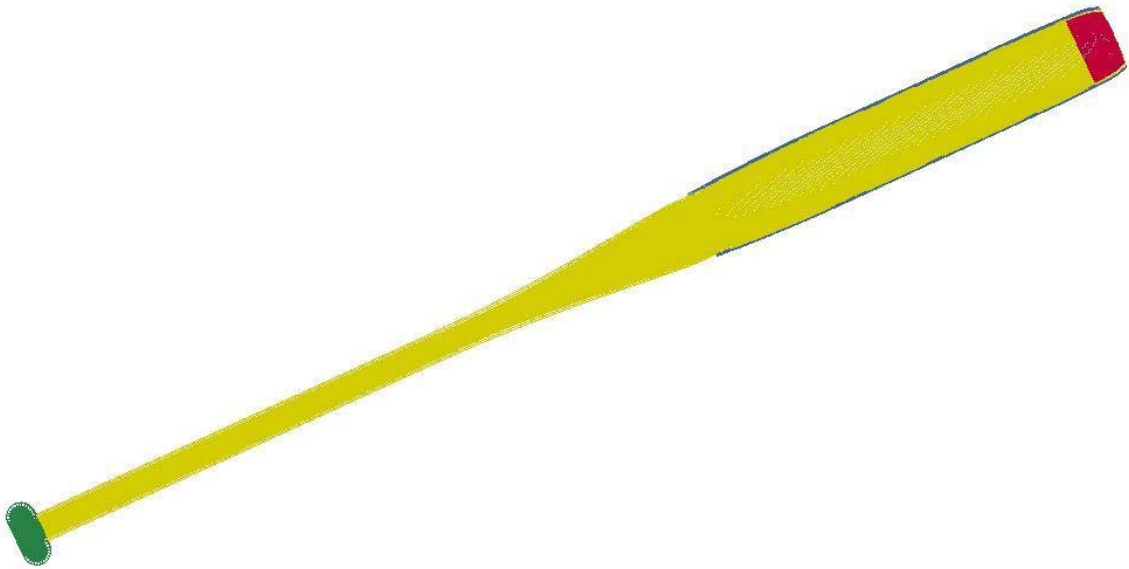


Figure 5.13 – Sectioned view of multiple-wall aluminum bat model

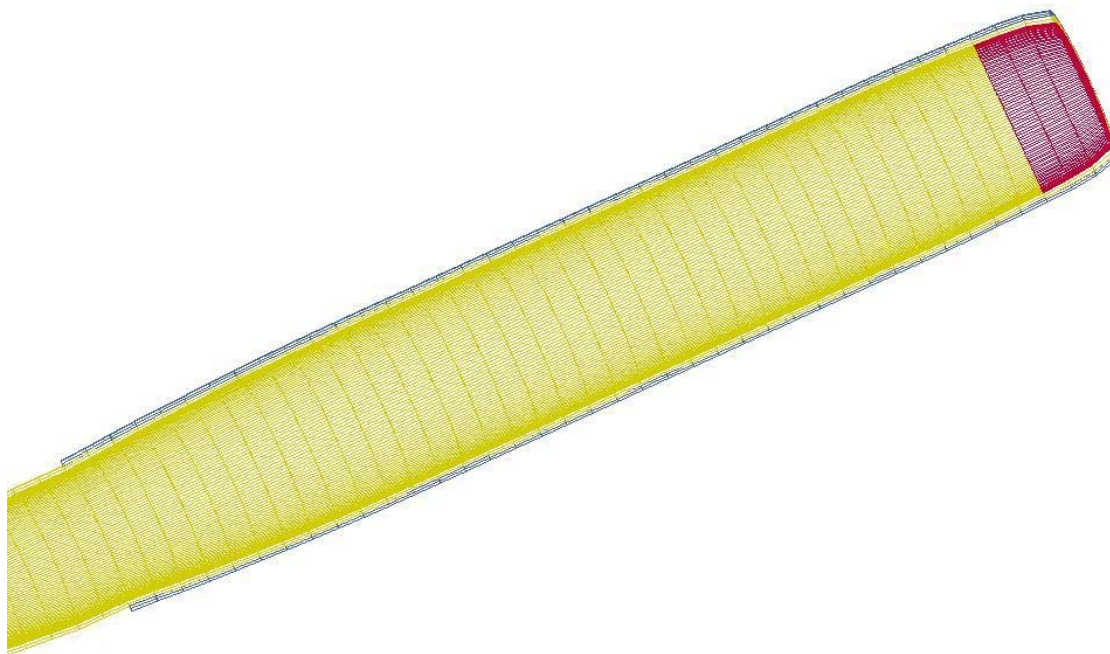


Figure 5.14 – Close-up of sectioned view of multiple-wall aluminum bat model

5.3.2 – Solid wood bat

As shown in figure 5.8, the wood bat was meshed in two separate pieces and then combined into one. This was done to prevent the use of inconsistently shaped elements. Since the wood bat response was not of primary interest for this study, it was modeled without a knob and as an isotropic material. This shifted the balance point of the bat toward the knob end of the bat and reduced the overall weight of the bat less than 2%.

Modeling the solid wood bat resulted in flexural frequencies that were very similar to measured values. In addition to the model's accurate representation of vibrational characteristics, the bat's physical properties including its center of mass and moment of inertia were well represented by the model. Tables 5.1 and 5.2 compare the numerical and measured vibrational and physical characteristics of the wood bat. The first two

flexural frequencies deviated less than 4% from measured values. The center of mass of the numerical model was nearly 1% further from the knob than the actual bat, and the MOI was less than 1% from its measured value.

Table 5.1 - Measured and simulated vibrational characteristics of a solid wood bat

	Numerical Results	Measured values	% error
1st flexural mode (Hz)	149	153	2.6%
2nd flexural mode (Hz)	552	536	-3.0%

Table 5.2 - Measured and simulated physical characteristics of a solid wood bat

	Numerical Results	Measured Values	% error
Mass (oz)	33.86	34.25	-1.1%
Center of Mass (in)	22.32	22.11	0.9%
MOI (oz in ²)	11437	11534	-0.8%

The wood bat model was also used to examine how adding weight to the distal end of the bat (as discussed in Chapter 3) affected its vibrational characteristics. In the model, weight was added to the distal end of the wood bat by adding a set of shell elements around the circumference of the last half inch of the bat. These elements were merged to the existing solid elements. The modulus of these elements were 0.1% of the wood so they would not affect the bat's flexural response. The comparison with experimental measurements was generally favorable, as shown in tables 5.3 and 5.4.

Table 5.3 - Measured and simulated vibrational characteristics of a weighted solid wood bat

	Numerical Results	Measured values	% error
1st flexural mode (Hz)	151	158	4.4%
2nd flexural mode (Hz)	561	542	-3.5%

Table 5.4 - Measured and simulated physical characteristics of a weighted solid wood bat

	Numerical Results	Measured Values	% error
Mass (oz)	37.15	37.35	-0.5%
Center of Mass (in)	23.33	23.10	1.0%
MOI (oz in ²)	13971	13962	0.1%

5.3.3 – Single wall aluminum

Modeling the single wall aluminum bat resulted in flexural and hoop frequencies that were very similar to measured values. In addition to the model’s accurate representation of vibrational characteristics, the bat’s physical properties, including its center of mass and moment of inertia, were well represented by the model. Tables 5.5 and 5.6 compare the vibrational and physical characteristics of the bat to the characteristics predicted by the numerical model. The first two flexural frequencies deviated less than 5% from measured values, and the first hoop frequency deviated less than 1% from measured value. The center of mass of the numerical model was less than 1% further from the knob than the dissected bat, and the MOI was less than 1% from its measured value.

Table 5.5 – Measured and simulated vibrational characteristics of a single wall aluminum bat

	Numerical Results	Measured values	% error
1st flexural mode (Hz)	185	180	2.8%
2nd flexural mode (Hz)	685	653	4.9%
1st hoop mode (Hz)	2009	2030	1.0%

Table 5.6 - Measured and simulated physical characteristics of a single wall aluminum bat

	Numerical Results	Measured Values	% error
Mass (oz)	27.64	27.65	0.0%
Center of Mass (in)	19.39	19.26	0.7%
MOI (oz in ²)	7579	7530	0.7%

The model was also used to examine how adding weight to various locations on the bat affected its vibrational characteristics. In the model, weight was added to the distal end of the bat by increasing the density of the end cap material. The model was

successful in predicting the vibrational characteristics and physical properties of the weighted bats, although the first flexural mode did increase more than expected. This outcome could have resulted from flawed experimental measurements due to the non-ideal weight attachment (in comparison to the computer model) used during experimental testing. Tables 5.7 and 5.8 compare the measured properties of the weighted bat to the simulated properties.

A study was also completed in which the effect of the end cap's modulus of elasticity was investigated. It was found that varying the end cap's modulus from 500 – 10,000,000 psi had no effect on the bat's first fundamental hoop frequency.

Table 5.7 - Measured and simulated vibrational characteristics of a weighted single wall aluminum bat

	Numerical Results	Measured values	% error
1st flexural mode (Hz)	204	185	10.3%
2nd flexural mode (Hz)	654	633	3.3%
1st hoop mode (Hz)	2009	2040	1.5%

Table 5.8 - Measured and simulated physical characteristics of a weighted single wall aluminum bat

	Numerical Results	Measured Values	% error
Mass (oz)	30.53	30.87	-1.1%
Center of Mass (in)	20.70	20.78	-0.4%
MOI (oz in ²)	9713	9920	-2.1%

5.3.4 – Multiple-wall aluminum

The success of this model describing the contact interface between the interior and exterior shells in a multiple-wall bat was not a trivial task, and the details of this particular model can be found in Appendix 8. In addition to details of the multiple-wall bat, Appendix 8 also contains information pertaining to the other models, such as number and type of elements used and shape profiles.

Modeling the multiple-wall aluminum bat resulted in flexural and hoop frequencies that were very similar to measured values. In addition to the model's accurate representation of vibrational characteristics, the bat's physical properties including its center of mass and moment of inertia were well represented by the model. Tables 5.9 and 5.10 compare the vibrational and physical characteristics of the dissected bat to the characteristics predicted by the numerical model. The first two flexural frequencies deviated less than 4% from measured values, and the first hoop frequency deviated less than 1% from measured values. The center of mass of the numerical model was less than one half of one percent closer to the knob than the dissected bat, and the MOI was barely 1% lower than its measured value.

Table 5.9 – Measured and simulated vibrational characteristics of a multiple-wall aluminum bat

	Numerical Results	Measured values	% error
1st flexural mode (Hz)	138	133	3.8%
2nd flexural mode (Hz)	550	533	3.2%
1st hoop mode (Hz)	1469	1466	0.2%

Table 5.10 – Measured and simulated physical characteristics of a multiple-wall aluminum bat

	Numerical Results	Measured Values	% error
Mass (oz)	28.00	28.18	-0.6%
Center of Mass (in)	20.33	20.37	-0.2%
MOI (oz in ²)	9141	9237	-1.0%

5.4 – Summary

The numerical model used in this research has accurately described the vibrational and physical characteristics of a wood bat and a single and multiple wall aluminum bat. In addition, the model has verified the vibrational response of wood and aluminum bats whose weight distributions have been altered.

Further research is necessary to determine if using the current model will be sufficient for use in bat-ball impact simulations. The excessive number of elements required when using solid brick elements may prove to be unreasonable in an impact simulation. As a result, different elements should be considered during future work.

REFERENCES

- 5.1 Cook, R., D. Malkus, M. Plesha, R. Witt. Concepts and applications of finite element analysis. Fourth edition. John Wiley and Sons. New York, NY. ISBN: 0471356050
- 5.2 Reddy, J. N. An introduction to the finite element method. Second edition. McGraw Hill. New York, NY. ISBN: 0070513554
- 5.3 *LS-DYNA keyword user's manual*. Version 970. Livermore Software Technology Corporation. April 2003.
- 5.4 Chauvin, Dewey. Easton Sports. *Private communication*. March, 2005.

CHAPTER SIX

- SUMMARY -

6.1 – Review

This study has considered how bat modifications and repeated use affect direct and indirect performance measurements change as a bat experiences repeated use, and if the effect of these changes could be reproduced in a numerical model.

6.2 – Bat modifications

The Doctored Bat Study has shown that bat modifications can have significant effects on bat performance. All of the methods proved capable of producing bats whose performance exceeds the ASA 2004 certification standard. Of the three most common doctoring methods, the act of barrel shaving composite bats produced the largest average performance increase of 6.6%.

The NBI bats also showed significant performance increases due to repeated impacts. After 2000 hits, the bats' performance levels had improved an average of 4.2%, which resulted in two of the three bats exceeding the ASA 2004 certification standard.

The issue of detecting bats that have been altered or whose performance levels are in excess of certification standards has been investigated using modal analysis and barrel compression techniques. Both of these indirect performance methods increased with bat performance. The correlation of these measures with performance had large scatter, however, making them unsuitable as individual detection tools.

6.3 – Weighting study

One bat alteration method that increases performance while remaining undetectable by either modal analysis or barrel compression techniques is altering weight and/or its

distribution. These alterations are best detected by measuring a bat's MOI and balance point. The Weighting Study demonstrated that the maximum BBCOR location on a bat is a function of the bat's weight distribution. The study showed that each bat had an optimum weight location which produced the maximum BBCOR value.

6.4 – Computer modeling

Using the LS-DYNA finite element software suite, three bats of different construction methods have been successfully modeled. The modeling of a stock solid wood bat and single wall aluminum bat has resulted in simulated physical and vibrational characteristics that are consistent with measured values. Additionally, the computer simulations of the wood bat and single wall aluminum bat have proved reasonable for predicting the physical and vibrational effects that various weighting strategies have on the bats.

The model of the multiple-wall aluminum bat succeeded in predicting the physical and vibrational characteristics of the actual bat. The weight distribution of the model was not manipulated as it was for the wood and single wall aluminum bats, as the main focus of modeling the multiple-wall bat was to verify that current, readily-available, finite element software packages were capable of modeling the contact interface between the bat's interior and exterior shells.

6.5 – Future work

The results of this body of research have answered many questions pertaining to the performance of softball bats. At the same time, it has also uncovered many more softball bat related topics deserving of further investigation.

If the indirect performance methods described herein are to be used to identify modified bats, the effect that temperature has on both should both first be investigated. It would also be useful to determine the effect that loading rates have on the barrel compression technique. It is reasonable to expect manufacturers to attempt to design bats with rate dependent barrel stiffnesses optimized for the bat-ball collision.

Another area of research with many possibilities is computer modeling. LS-DYNA has proved successful in modeling various bat constructions, but no modeling of the bat-ball impact has been performed.

Additionally, finite element modeling would be an ideal technique for verifying the results seen in the weighting study of this research. In such a model a more accurate or justifiable explanation for why performance increases as a function of weight distribution could be obtained.

APPENDIX ONE

Apparatus - Ball Cannon

In order to test the properties of a softball bat, it is necessary to propel the ball toward the bat in an accurate, repeatable manner. There a number of methods which could potentially satisfy these requirements. One of these methods is a standard pitching machine, however, the variability in pitch speed, impact location, and spin of the ball pose multiple problems. To address these issues, an air cannon was designed that is capable of firing balls up to 150 mph accurately and without spin. A picture of the cannon used for this work is shown in figure A1.1.

To fire a ball out of the cannon, a ball is placed in a sabot, and the ball/sabot combination is loaded into the breach end of the cannon, as shown in figure A1.2 (the sabot functions to assure consistent aiming and to prevent the ball from spinning as it travels down the barrel). Once the breach end plate has sealed the barrel shut, the valves on the air accumulator tank are opened and the sabot and softball ride down the barrel until the sabot impacts the arrestor plate. The arrestor plate functions to stop the sabot and allow the ball to continue traveling unobstructed towards a target.

Once the ball leaves the cannon, a series of three light curtains measure the speed of the ball before and after impact with the target. A picture of the arrestor plate, light curtains, and a bat positioned for impact is shown in figure A1.3. The desired pitch speed is achieved by adjusting the pressure in the accumulator tank. The tank is fed by a large air compressor that allows a wide range of pressures to be maintained. LabView version 7.1 (National instruments, Austin, TX) was used to control the accumulator tank pressure and impact location of the ball.

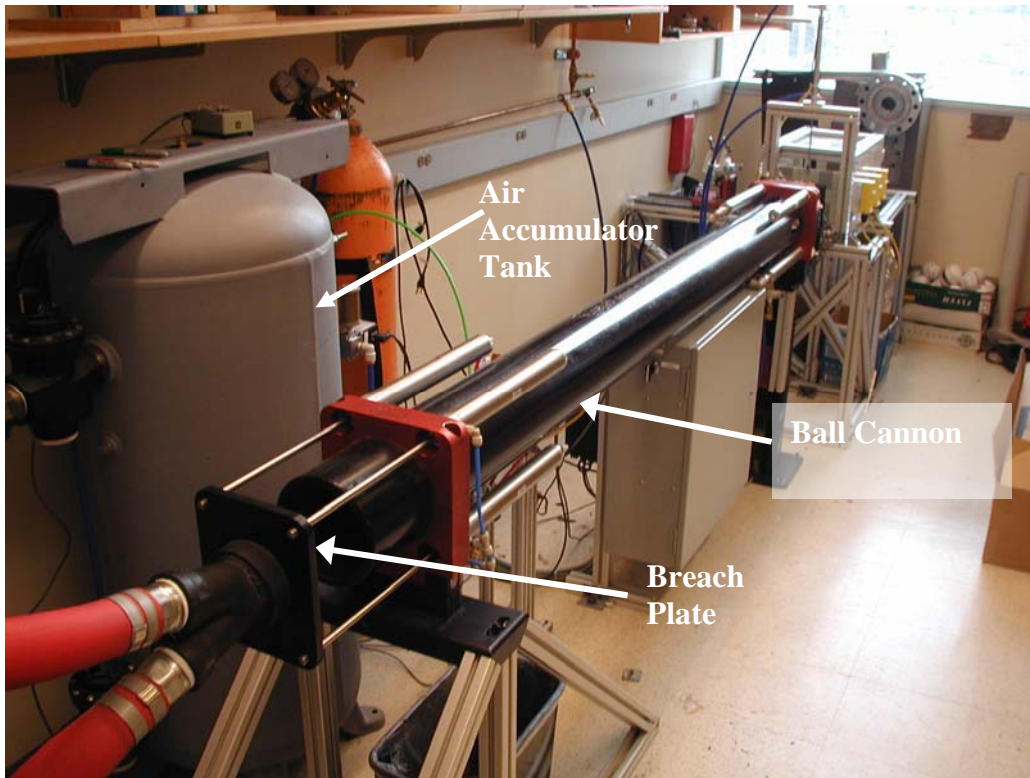


Figure A1.1 – Ball cannon, Breach plate, and Air tank accumulator

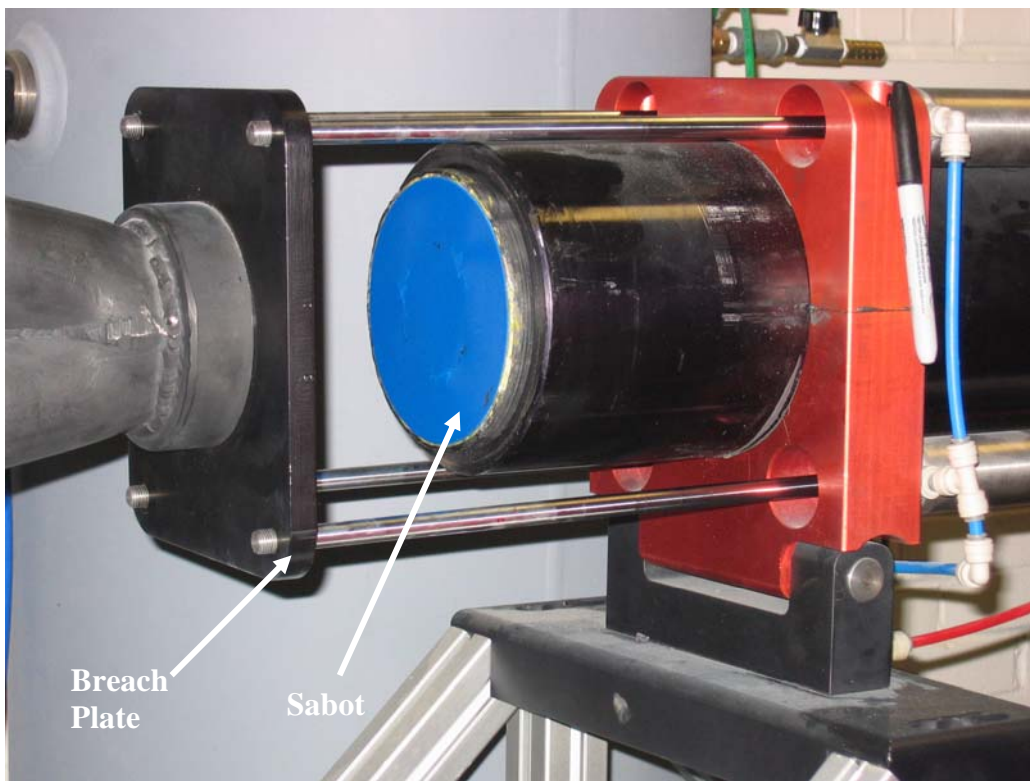


Figure A1.2 – Ball cannon loading procedure

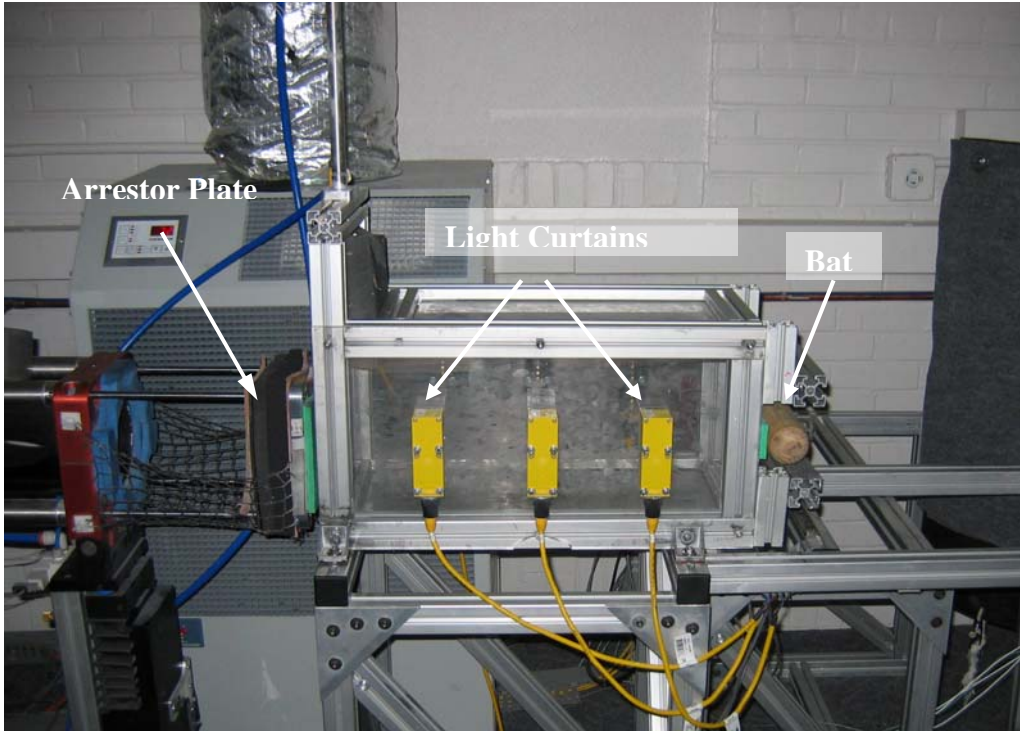


Figure A1.3 – Arrestor plate, Light curtains, and bat in position for impact

APPENDIX TWO

Standard Bat Data and Plots

Table A2.1 – Standard bat barrel compression and modal analysis data

Date	Barrel Compression (lb/in)	1st Flexural Mode (Hz)	1st Hoop Mode (Hz)
10/9/2004	7323	190	1456
10/27/2004	7323	190	1453
11/2/2004	7198	190	1453
11/8/2004	7351	186	1453
11/22/2004	7250	190	1456
12/21/2004	7453	186	1456
<i>standard deviation</i>	1%	1%	0%

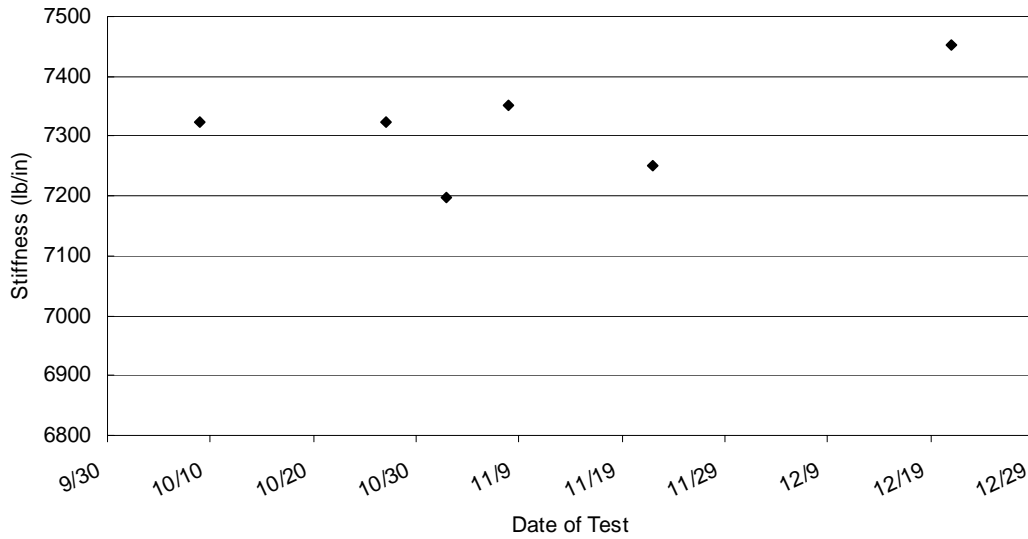


Figure A2.1 - Standard bat barrel compression trend

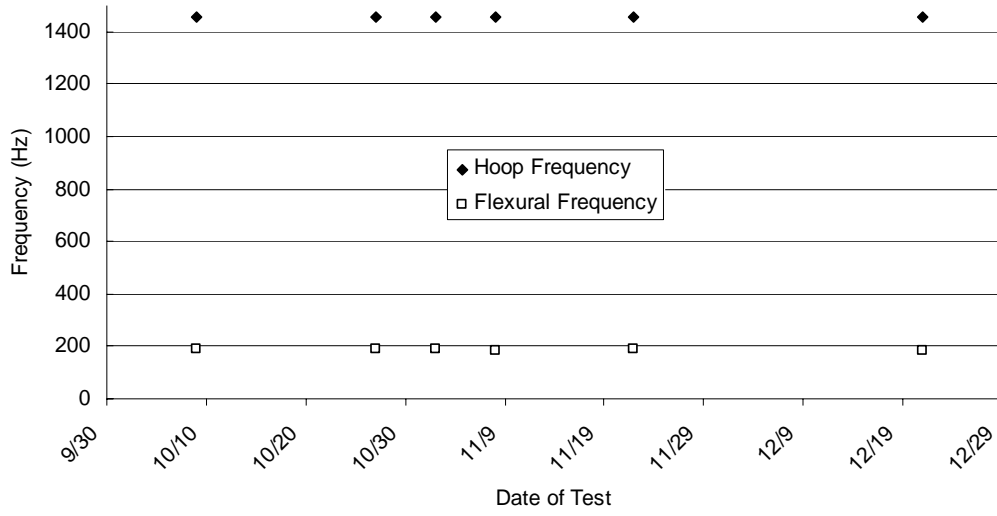
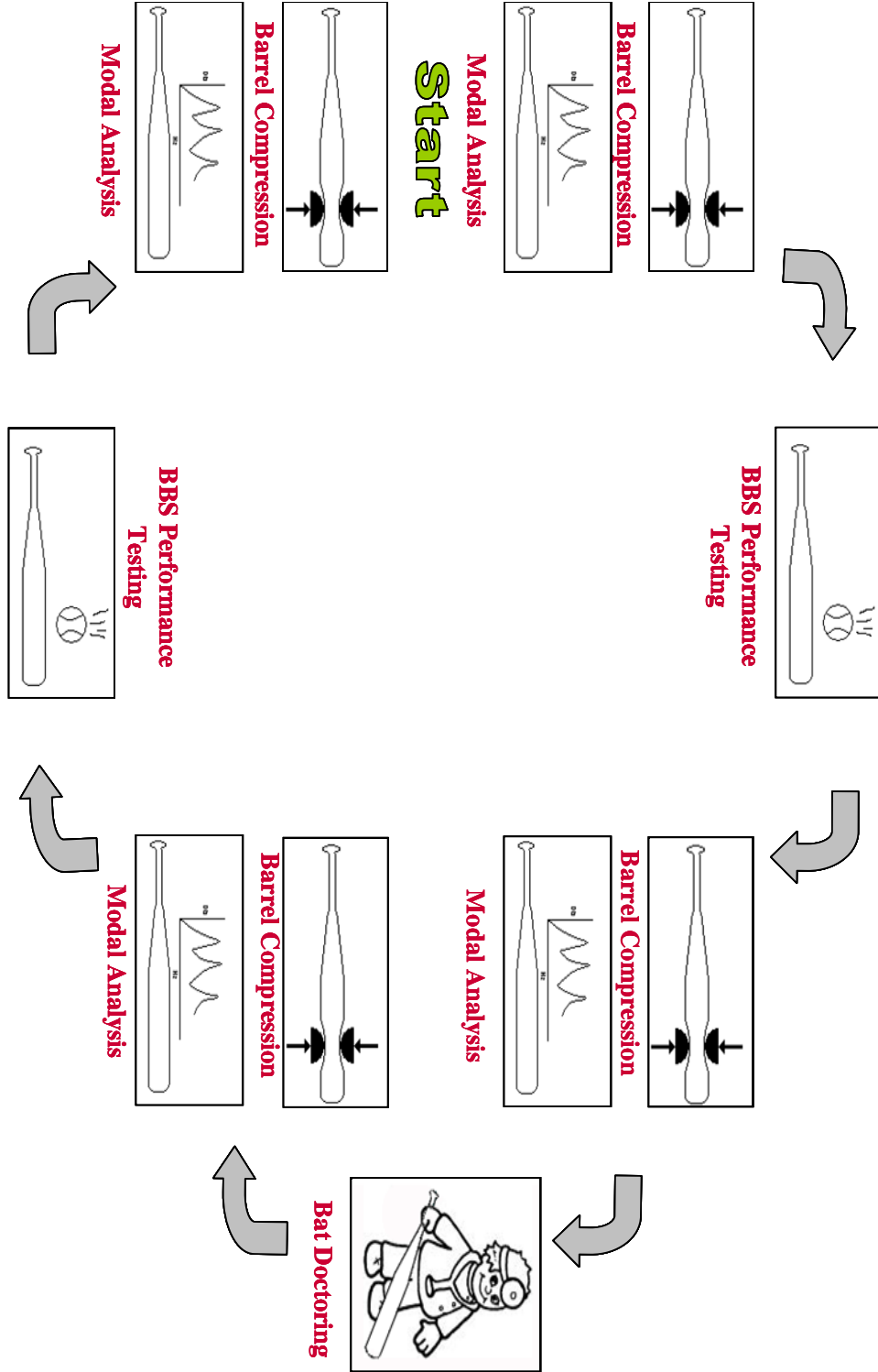


Figure A2.2 - Standard bat modal analysis trends

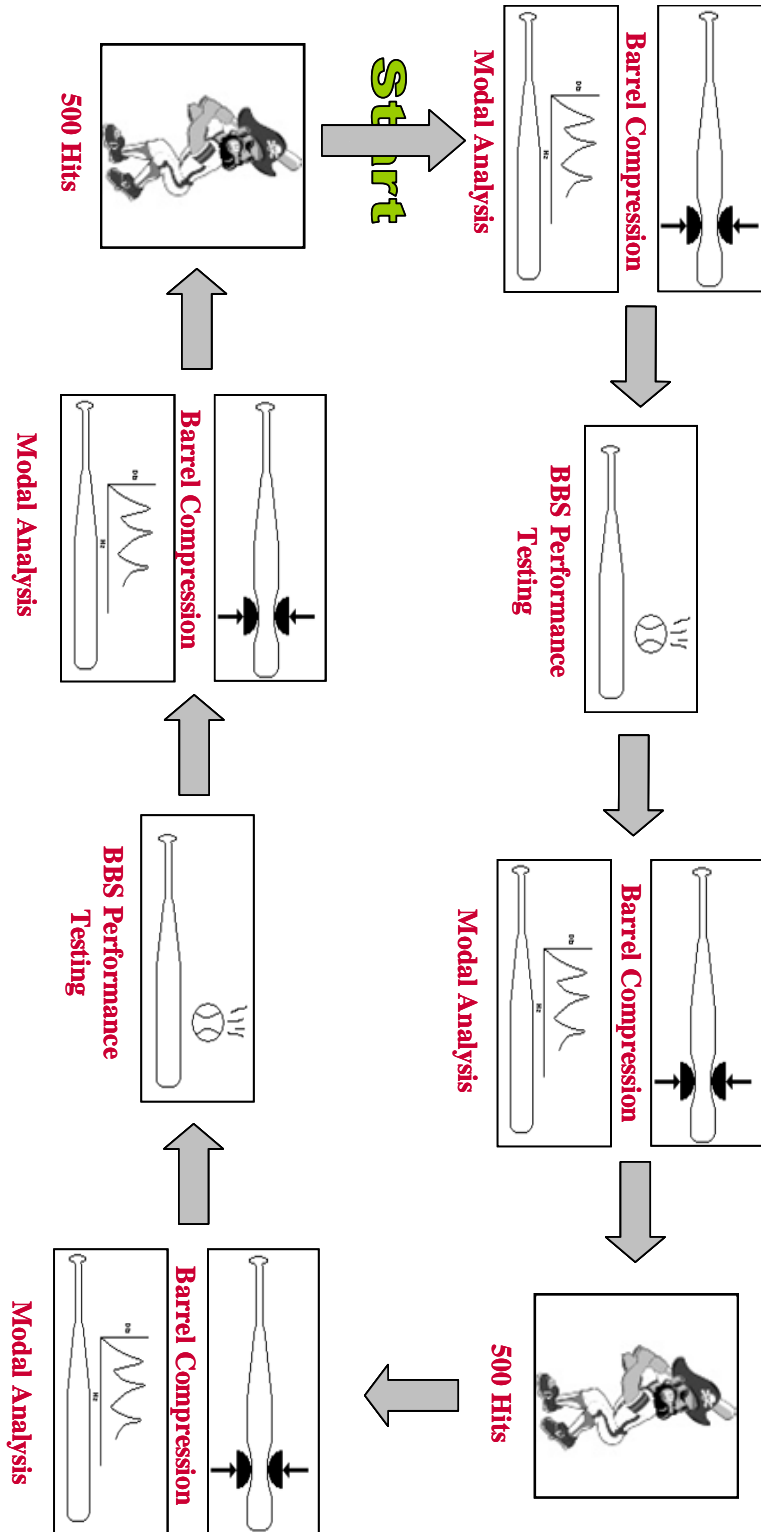
APPENDIX THREE

Flowchart describing doctored bat testing procedure



APPENDIX FOUR

Flowchart describing NBI bat testing procedure



APPENDIX FIVE

Doctoring Study Data

Bat Code	Work Performed	MOI (oz in ²)		Flexural Frequency (Hz)			
		New	After modification	New	BBS 1	After modification	BBS 2
MA01	Shaved	9511	9361	160	160	160	160
MA02	Shaved	9353	10107	163	163	160	160
MA03	Shaved	9479	9925	150	150	150	150
MA04	Shaved	9368	9642	150	150	146	146
MA05	Weighted	10058	12576	120	120	N/A	116
MA06	Shaved	10429	10313	123	123	123	123
MA07	Shaved	10221	10018	123	123	140	140
MA08	NBI	See NBI results section		See NBI results section			
MC01	Weighted	8877	10670	143	143	N/A	136
MC02	Shaved	8685	8775	143	143	140	143
MC03	Shaved	8836	9912	143	143	146	143
MC04	Rolled	8844	8875	143	143	143	143
MC05	BCT	8822	8863	140	140	140	140
MC06	ACT	8874	8896	143	143	143	143
MC07	Viced	8845	8843	146	146	146	146
MC08	Shaved	8532	9067	206	210	203	206
MC09	Shaved	8549	9752	206	210	213	193
MC10	Rolled	8577	8588	203	203	203	203
MC11	BCT	8444	8477	206	210	210	210
MC12	ACT	8568	8588	206	206	206	206
MC13	Viced	8557	8218	206	206	206	206
MC14	Coverted to Freak	8396	N/A	170	N/A	N/A	N/A
MC15	Coverted to Freak 98	8483	N/A	166	N/A	N/A	N/A
MC16	Coverted to Velocite 2	N/A	9607	153	N/A	N/A	N/A
MC17	NBI	See NBI results section		See NBI results section			
MC18	NBI	See NBI results section		See NBI results section			
Std Bat	None	8312	N/A	See Appendix X			
SA01	Weighted	7937	9655	176	176	N/A	170
Wood	Weighted	11533	13962	153	N/A	158	N/A

Bat Code	Work Performed	Hoop Frequency (Hz)				BC (lb/in)			
		New	BBS 1	After modification	BBS 2	New	BBS 1	After modification	BBS 2
MA01	Shaved	1466	1453	1360	1360	7463	7532	6484	6478
MA02	Shaved	1386	1376	1353	1346	6873	7041	6882	6763
MA03	Shaved	1360	1360	1320	1303	7385	7244	7126	7164
MA04	Shaved	1363	1353	1283	1283	6689	6833	6764	6766
MA05	Weighted	1193	1193	N/A	1190	6945	6713	N/A	6730
MA06	Shaved	1283	1270	1223	1223	7126	6973	6597	6551
MA07	Shaved	1293	1266	1226	1233	6800	6438	6345	6345
MA08	NBI	See NBI results section				See NBI results section			
MC01	Weighted	1493	1493	N/A	1440	7556	7353	N/A	7167
MC02	Shaved	1476	1433	1306	1300	7241	6959	5518	5598
MC03	Shaved	1456	1416	1303	1416	7035	6673	5264	5388
MC04	Rolled	1493	1470	1393	1386	7599	7297	6892	6816
MC05	BCT	1443	1410	1106	1020	6922	6594	3042	2759
MC06	ACT	1493	1483	1326	1313	7612	7383	6086	6010
MC07	Viced	1493	1453	1386	1380	7400	6932	6477	6424
MC08	Shaved	1686	1283	1243	1230	6863	6215	5657	5603
MC09	Shaved	1926	1616	1550	1313	7188	6201	5787	5453
MC10	Rolled	1220	1206	1350	1316	6145	6119	6066	5960
MC11	BCT	1330	1226	1180	1113	6325	6006	3745	3598
MC12	ACT	1410	1350	1270	1283	6338	6195	5920	5940
MC13	Viced	1573	1240	1246	1236	6467	6239	6026	6309
MC14	Coverted to Freak	1470	N/A	N/A	N/A	6245	6269	N/A	N/A
MC15	Coverted to Freak 98	1783	N/A	N/A	N/A	6892	7087	N/A	N/A
MC16	Coverted to Velocite 2	1070	N/A	N/A	N/A	2968	2689	N/A	N/A
MC17	NBI	See NBI results section				See NBI results section			
MC18	NBI	See NBI results section				See NBI results section			
Std Bat	None	See Appendix X				See Appendix X			
SA01	Weighted	1700	1696	N/A	1700	7023	8705	N/A	8796
Wood	Weighted	N/A	N/A	N/A	N/A	N/A	N/A	N/A	N/A

<i>Bat Code</i>	<i>Work Performed</i>	Performance (mph)	
		<i>BBS1</i>	<i>BBS2</i>
MA01	Shaved	97.6	102.0
MA02	Shaved	98.4	101.0
MA03	Shaved	97.7	100.2
MA04	Shaved	98.8	100.5
MA05	Weighted	97.8	98.4
MA06	Shaved	97.8	99.5
MA07	Shaved	99.0	101.2
MA08	NBI	See NBI results section	
MC01	Weighted	95.5	99.1
MC02	Shaved	95.8	102.0
MC03	Shaved	97.5	104.1
MC04	Rolled	94.9	97.8
MC05	BCT	96.7	104.5
MC06	ACT	94.7	99.1
MC07	Viced	95.4	98.1
MC08	Shaved	97.4	102.6
MC09	Shaved	97.6	105.3
MC10	Rolled	97.3	100.7
MC11	BCT	97.1	105.4
MC12	ACT	100.1	100.8
MC13	Viced	97.7	101.1
MC14	Coverted to Freak	N/A	N/A
MC15	Coverted to Freak 98	N/A	N/A
MC16	Coverted to Velocite 2	N/A	N/A
MC17	NBI	See NBI results section	
MC18	NBI	See NBI results section	
Std Bat	None	N/A	N/A
SA01	Weighted	92.8	96.4
Wood	Weighted	87.1	90.2

APPENDIX SIX

Doctoring Study: Weighted bat data

Wood	
Initial bat weight (oz)	34.25
Initial bat inertia (oz)	11534
Desired bat inertia (oz in ²)	13840
Location of weight addition (in)	27.5
Weight added (oz)	3.1
Final bat weight (oz)	37.35
Final bat inertia (oz in ²)	13962

SA01	
Initial bat weight (oz)	26.91
Initial bat inertia (oz)	7937
Desired bat inertia (oz in ²)	9524
Location of weight addition (in)	27.5
Weight added (oz)	2.28
Final bat weight (oz)	29.19
Final bat inertia (oz in ²)	9655

MA05	
Initial bat weight (oz)	28.82
Initial bat inertia (oz)	10058
Desired bat inertia (oz in ²)	12070
Location of weight addition (in)	27.5
Weight added (oz)	3.29
Final bat weight (oz)	32.11
Final bat inertia (oz in ²)	12576

Wood	
Initial bat weight (oz)	34.25
Initial bat inertia (oz)	11534
Desired bat inertia (oz in ²)	13840
Location of weight addition (in)	27.5
Weight added (oz)	3.1
Final bat weight (oz)	37.35
Final bat inertia (oz in ²)	13962

APPENDIX SEVEN

Weighting Study Data

Solid wood bat

Initial Weight (oz)	28.50
Initial MOI (oz in²)	10098.00
Desired MOI (oz in²)	11108.00

Distance from pivot (in)	Necessary weight addition (oz)	Actual Weight Added (oz)	Final Bat	
			Weight (oz)	Actual MOI
6	28.050	28.015	56.52	11106.54
9	12.467	12.500	41.00	11110.50
11	8.345	8.280	36.78	11099.88
13	5.975	6.000	34.50	11112.00
15	4.488	4.520	33.02	11115.00
16	3.945	4.000	32.50	11122.00
17	3.494	3.505	32.01	11110.95
18	3.117	3.140	31.64	11115.36
24.5	1.682	1.685	30.19	11109.42
25.5	1.553	1.555	30.06	11109.14
26.5	1.438	1.450	29.95	11116.26
27.5	1.335	1.345	29.85	11115.16
			std deviation:	5.58

Single wall aluminum bat

Initial Weight (oz)	23.54
Initial MOI (oz in²)	7241.00
Desired MOI (oz in²)	7965.00

Distance from pivot (in)	Necessary weight addition (oz)	Actual Weight Added (oz)	Final Bat	
			Weight (oz)	Actual MOI
6	20.114	20.095	43.63	7964.42
9	8.940	8.940	32.48	7965.14
11	5.984	5.980	29.52	7964.58
13	4.285	4.280	27.82	7964.32
15	3.218	3.220	26.76	7965.50
16	2.829	2.845	26.38	7969.32
17	2.506	2.515	26.05	7967.84
18	2.235	2.230	25.77	7963.52
24	1.257	1.260	24.80	7966.76
25	1.159	1.170	24.71	7972.25
26	1.071	1.070	24.61	7964.32
27	0.993	0.990	24.53	7962.71
			std deviation:	2.73

Multiple-wall aluminum bat

Initial Weight (oz)	25.86
Initial MOI (oz in²)	8279.00
Desired MOI (oz in²)	9107.00

Distance from pivot (in)	Necessary weight addition (oz)	Actual Weight Added (oz)	Final Bat Weight (oz)	Actual MOI
6	22.997	22.990	48.85	9106.64
9	10.221	10.215	36.08	9106.42
11	6.842	6.840	32.70	9106.64
13	4.899	4.900	30.76	9107.10
15	3.680	3.680	29.54	9107.00
16	3.234	3.235	29.10	9107.16
17	2.865	2.865	28.73	9106.99
18	2.555	2.560	28.42	9108.44
24.5	1.379	1.385	27.25	9110.35
25.5	1.273	1.265	27.13	9101.57
26.5	1.179	1.185	27.05	9111.17
27.5	1.095	1.085	26.95	9099.53
std deviation:				3.23

Multiple-wall composite bat

Initial Weight (oz)	25.53
Initial MOI (oz in²)	8373.00
Desired MOI (oz in²)	9210.00

Distance from pivot (in)	Necessary weight addition (oz)	Actual Weight Added (oz)	Final Bat Weight (oz)	Actual MOI
6	23.258	23.255	48.79	9210.18
9	10.337	10.340	35.87	9210.54
11	6.920	6.920	32.45	9210.32
13	4.954	4.955	30.49	9210.40
15	3.721	3.725	29.26	9211.13
16	3.271	3.270	28.80	9210.12
17	2.897	2.895	28.43	9209.66
18	2.584	2.580	28.11	9208.92
24.5	1.395	1.390	26.92	9207.35
25.5	1.288	1.290	26.82	9211.82
26.5	1.192	1.190	26.72	9208.68
27.5	1.107	1.110	26.64	9212.44
std deviation:				1.38

APPENDIX EIGHT

Bat Profiles (all profiles in inches) used for numerical modeling

Solid wood bat

Location	Diameter
1	1.310
2	1.155
3	1.030
4	0.980
5	0.975
6	0.990
7	1.000
8	1.015
9	1.025
10	1.045
11	1.055
12	1.075
13	1.120
14	1.200
15	1.345
16	1.515
17	1.680
18	1.835
19	1.980
20	2.120
21	2.215
22	2.235
23	2.250
24	2.250
25	2.250
26	2.260
27	2.260
28	2.260
29	2.260
30	2.260
31	2.260
32	2.260
33	2.260
34	2.260

Single wall aluminum bat

Location	Wall Thickness	Bat Diameter	Location	Wall Thickness	Bat Diameter
0.0			17.0	0.126	1.515
0.5			17.5	0.121	1.634
1.0	0.147	0.81	18.0	0.119	1.75
1.5	0.147	0.81	18.5	0.107	1.822
2.0	0.147	0.81	19.0	0.103	1.917
2.5	0.15	0.81	19.5	0.102	1.99
3.0	0.15	0.81	20.0	0.098	2.05
3.5	0.15	0.81	20.5	0.095	2.105
4.0	0.15	0.809	21.0	0.093	2.15
4.5	0.15	0.809	21.5	0.09	2.205
5.0	0.15	0.808	22.0	0.09	2.24
5.5	0.15	0.807	22.5	0.09	2.245
6.0	0.15	0.806	23.0	0.09	2.245
6.5	0.15	0.805	23.5	0.09	2.246
7.0	0.15	0.805	24.0	0.09	2.247
7.5	0.15	0.805	24.5	0.09	2.247
8.0	0.15	0.805	25.0	0.09	2.248
8.5	0.15	0.805	25.5	0.09	2.248
9.0	0.15	0.804	26.0	0.09	2.248
9.5	0.152	0.803	26.5	0.09	2.248
10.0	0.154	0.803	27.0	0.09	2.248
10.5	0.154	0.803	27.5	0.09	2.249
11.0	0.155	0.804	28.0	0.09	2.249
11.5	0.155	0.812	28.5	0.09	2.249
12.0	0.16	0.83	29.0	0.09	2.249
12.5	0.173	0.848	29.5	0.09	2.25
13.0	0.19	0.885	30.0	0.09	2.25
13.5	0.208	0.925	30.5	0.09	2.25
14.0	0.208	1.002	31.0	0.09	2.25
14.5	0.183	1.073	31.5	0.09	2.25
15.0	0.171	1.155	32.0	0.09	2.25
15.5	0.157	1.23	32.5	0.09	2.248
16.0	0.145	1.307	33.0	0.065	2.247
16.5	0.136	1.415	33.5	0.087	2.247

Multiple wall aluminum bat

Location	Inner Shell		Outer Shell		Location	Inner Shell		Outer Shell	
	Diameter	Thickness	Diameter	Thickness		Diameter	Thickness	Diameter	Thickness
0.00	N/A	N/A	N/A	N/A	18.50	1.41	0.085	N/A	N/A
0.50	N/A	N/A	N/A	N/A	19.00	1.5	0.085	N/A	N/A
0.66	0.82	0.095	N/A	N/A	19.50	1.6	0.075	N/A	N/A
1.00	0.82	0.09	N/A	N/A	20.00	1.7	0.072	N/A	N/A
1.50	0.82	0.09	N/A	N/A	20.50	1.775	0.065	N/A	N/A
2.00	0.82	0.09	N/A	N/A	20.75	1.825	0.065	N/A	N/A
2.50	0.82	0.09	N/A	N/A	21.00	1.86	0.065	N/A	N/A
3.00	0.825	0.09	N/A	N/A	21.25	1.795	0.065	1.92	0.057
3.50	0.825	0.09	N/A	N/A	21.50	1.835	0.065	1.955	0.062
4.00	0.825	0.09	N/A	N/A	21.75	1.865	0.065	1.99	0.06
4.50	0.825	0.09	N/A	N/A	22.00	1.905	0.065	2.025	0.06
5.00	0.825	0.09	N/A	N/A	22.50	1.97	0.06	2.09	0.06
5.50	0.825	0.09	N/A	N/A	23.00	2.02	0.06	2.135	0.055
6.00	0.825	0.09	N/A	N/A	23.50	2.065	0.057	2.17	0.055
6.50	0.825	0.09	N/A	N/A	24.00	2.095	0.057	2.205	0.055
7.00	0.825	0.09	N/A	N/A	24.50	2.12	0.057	2.225	0.055
7.50	0.825	0.09	N/A	N/A	25.00	2.125	0.057	2.235	0.055
8.00	0.82	0.09	N/A	N/A	25.50	2.13	0.057	2.24	0.055
8.50	0.82	0.09	N/A	N/A	26.00	2.125	0.057	2.24	0.055
9.00	0.82	0.09	N/A	N/A	26.50	2.125	0.057	2.24	0.055
9.50	0.82	0.09	N/A	N/A	27.00	2.125	0.057	2.24	0.055
10.00	0.82	0.09	N/A	N/A	27.50	2.125	0.057	2.24	0.055
10.50	0.82	0.09	N/A	N/A	28.00	2.12	0.057	2.235	0.055
11.00	0.82	0.09	N/A	N/A	28.50	2.12	0.057	2.23	0.055
11.50	0.82	0.09	N/A	N/A	29.00	2.12	0.057	2.23	0.055
12.00	0.82	0.09	N/A	N/A	29.50	2.12	0.057	2.23	0.055
12.50	0.82	0.09	N/A	N/A	30.00	2.12	0.057	2.23	0.055
13.00	0.82	0.095	N/A	N/A	30.50	2.12	0.057	2.23	0.055
13.50	0.825	0.1	N/A	N/A	31.00	2.12	0.057	2.23	0.055
14.00	0.84	0.11	N/A	N/A	31.50	2.12	0.057	2.23	0.055
14.50	0.87	0.115	N/A	N/A	32.00	2.12	0.057	2.23	0.055
15.00	0.905	0.125	N/A	N/A	32.50	2.1	0.057	2.215	0.055
15.50	0.95	0.12	N/A	N/A	33.00	2.07	0.057	2.185	0.055
16.00	1.005	0.115	N/A	N/A	33.50	2.04	0.065	2.155	0.055
16.50	1.075	0.11	N/A	N/A	34.00	1.95	0.075	2.075	0.055
17.00	1.147	0.105	N/A	N/A	34.25	1.8	0.09	1.9	0.055
17.50	1.215	0.1	N/A	N/A					
18.00	1.312	0.095	N/A	N/A					

Model information used in numerical simulations

Material	Modulus of Elasticity (msi)	Mass Density (lbm/in ³)	Poisson's ratio
Aluminum	10.3	0.000259	0.3
Wood	1.8	0.00006708	0.3
Plastic*	0.5	0.00007	0.3

* The plastic material was used for the endcaps of the aluminum bats.

Model	Element type	Total number of elements
Wood	Solid	46512
Single wall aluminum	Solid	46035
Multiple-wall aluminum	Solid	61920

Detailed information used for multiple-wall aluminum bat model

```

$-----1-----2-----3-----4-----5-----6-----7-----8
$
$                                CONTROL CARD                                $
$
$-----1-----2-----3-----4-----5-----6-----7-----8
*CONTROL_TERMINATION
$   ENDTIM      ENDCYC      DTMIN      ENDENG      ENDMAS
0.00000030      0          0.0        0.0        0.0
*CONTROL_IMPLICIT_GENERAL
$   IMFLAG      DT0         IMFORM      NSBS        IGS         CNSTN      FORM
          10.00000015      2          1          2          0          0
*CONTROL_IMPLICIT_EIGENVALUE
$   NEIG        CENTER      LFLAG      LFTEND      RFLAG      RHTEND      EIGMTH      SHFSCL
          10          0.0          0          0          0          2          0.0
$-----1-----2-----3-----4-----5-----6-----7-----8
$
$                                PART CARDS                                $
$
$-----1-----2-----3-----4-----5-----6-----7-----8
*PART
Knob
$   PID         SECID        MID         EOSID        HGID         GRAV        ADPOPT        TMID
          3           1           3           0           0           0           0           0
*PART
Shell-1
$   PID         SECID        MID         EOSID        HGID         GRAV        ADPOPT        TMID
          4           1           1           0           0           0           0           0
*PART
End Cap
$   PID         SECID        MID         EOSID        HGID         GRAV        ADPOPT        TMID
          6           1           2           0           0           0           0           0
*PART
outer shell
$   PID         SECID        MID         EOSID        HGID         GRAV        ADPOPT        TMID
          7           1           1           0           0           0           0           0
$-----1-----2-----3-----4-----5-----6-----7-----8
$
$                                SECTION CARDS                                $
$
$-----1-----2-----3-----4-----5-----6-----7-----8
*SECTION_SOLID_TITLE
P-1
$   SECID      ELFORM      AET
          1         2          0
$-----1-----2-----3-----4-----5-----6-----7-----8
$
$                                MATERIAL CARDS                                $
$
$-----1-----2-----3-----4-----5-----6-----7-----8
*MAT_ELASTIC_TITLE
M-1
$   MID        RO          E          PR          DA          DB
          1  0.0002591.0300E+07      0.30      0.0      0.0
*MAT_ELASTIC_TITLE
M-2
$   MID        RO          E          PR          DA          DB
          2  0.000007  500000.0      0.30      0.0      0.0
*MAT_ELASTIC_TITLE
M-3
$   MID        RO          E          PR          DA          DB
          3  0.000801.0300E+07      0.30      0.0      0.0
$-----1-----2-----3-----4-----5-----6-----7-----8
$
$                                BOUNDARY SPC CARDS                                $
$

```

```

$
$-----1-----2-----3-----4-----5-----6-----7-----8
*BOUNDARY_SPC_SET_ID
$
  ID
  1
$
  NSID      CID      DOFX      DOFY      DOFZ      DOFRX      DOFRY      DOFRZ
  1          0          0          0          1          0          0          0
$-----1-----2-----3-----4-----5-----6-----7-----8
$
$
$
$
$
$
$
$
$
$
$-----1-----2-----3-----4-----5-----6-----7-----8
*CONTACT_SURFACE_TO_SURFACE
$^CONTACT1
$
  SSID      MSID      SSTYP      MSTYP      SBOXID      MBOXID      SPR      MPR
  7          4          3          3          0          0          0          0
$
  FS         FD         DC         VC         VDC         PENCHK      BT         DT
  0.0        0.0        0.0        0.0        0.0        01.0000E-101.0000E+20
$
  SFS        SFM        SST        MST        SFST        SFMT        FSF        VSF
  1.0        1.0        0.0        0.0        1.0        1.0        1.0        1.0
$
  SOFT       SOFSCL    LCIDAB    MAXPAR    SBOPT     DEPTH      BSORT     FRCFRQ
  0          0.10     0          1.025    0.0       2.0        0         1
$
  PENMAX     THKOPT    SHLTHK    SNLOG     ISYM      I2D3D     SLDTHK    SLDSTF
  0.0        0         0          0         0         0         0.0       0.0
$
  IGAP       IGNORE
  2          0

```

Certain flags are critical when running modal analysis in LS DYNA, and additional flags are essential for running the multiple wall aluminum bat model successfully. To run a standard modal analysis the implicit solution method must first be set, and the appropriate time steps must be set. The number of eigenvalues of interest must also be set. These settings are controlled by the following cards:

Control_Termination – endtim: must be non-zero

Control_Implicit_General – imflag: 1

dt0: must be non-zero

Control_Implicit_Eigenvalue – Neig: must be non-zero

When running a multiple wall model the contact between the walls must be properly defined. A standard surface to surface contact definition is sufficient, but the birth time must be smaller than the time step defined in the implicit analysis. This setting should be:

Contact_Surface_to_Surface – BT: < implicit time step